A review of Solid Oxide Fuel Cell cathode materials with respect to their resistance to the effects of chromium poisoning

Harrison, Christopher; Slater, Peter; Steinberger-Wilckens, Robert

DOI:
10.1016/j.ssi.2020.115410

Document Version
Peer reviewed version

Citation for published version (Harvard):
Harrison, C, Slater, P & Steinberger-Wilckens, R 2020, 'A review of Solid Oxide Fuel Cell cathode materials with respect to their resistance to the effects of chromium poisoning', *Solid State Ionics*, vol. 354, 115410. https://doi.org/10.1016/j.ssi.2020.115410

Accepted by Solid State Ionics, 15 June 2020, manuscript no. SSI_2020_282

A review of Solid Oxide Fuel Cell cathode materials with respect to their resistance to the effects of chromium poisoning

C.M. Harrison[1 $], P.R. Slater[2], R Steinberger-Wilckens[1]

Affiliation/Address: [1] Centre for Fuel Cell and Hydrogen Research, School of Chemical Engineering,

[2] School of Chemistry,

University of Birmingham, Birmingham, B15 2TT U.K.

[$]Corresponding author: CMH725@bham.ac.uk

Abstract: Solid Oxide Fuel Cell (SOFC) cathode materials have been shown to be susceptible to a 'chromium poisoning' phenomenon that can significantly deteriorate cell output during operation. Chromium-containing species, released from stack and system materials, migrate to the SOFC cathode where they are able to form new phases through reaction with the cathode material. Such phases have been shown to diminish the catalytic and conductive performance of the electrodes and even block the pathways through which oxygen must diffuse. To date, there has been a significant body of research afforded to this subject area. Efforts have been made towards understanding the chromium poisoning effect, whilst also considering how it may be mitigated. In this review, we discuss the effects of chromium-containing phases on both conventional and non-conventional cathode materials. This is in order to understand the most successful approaches towards developing chromium-tolerant cathode materials. The influences of environmental parameters such as temperature and humidity are also discussed. This is to explore how degradation rates may be affected by the operating conditions themselves and the extent to which the phenomenon can be mitigated by suitable control of such factors. In the most part, these environmental effects are studied in relation to the most common cathode materials, $La_{1-x}Sr_xCo_{1-y}Fe_yO_3$ and $La_{1-x}Sr_xMnO_3$, where there has been the largest body of work conducted.

Keywords: SOFC, Chromium Poisoning, Cathode Materials

Funding: This work was supported by the EPSRC via the Centre for Doctoral Training on Fuel Cells and their Fuels, grant reference EP/L015749/1, and the JUICED Hub Grant ref EP/R023662/1

1 Introduction

Rising concerns relating to climate change are driving a global interest in low-carbon technologies that offer clean and reliable power to a growing population. One technology that may yet play a key role in future energy systems is the Solid Oxide Fuel Cell (SOFC), which has the ability to utilise a wide variety of fuels to generate electrical power and heat at high efficiencies. Ferritic stainless steel (FSS) "interconnects" are used in SOFC stacks to connect the single cells and separate the fuel gas from the oxidant. FSS are equipped to resist the harsh operating conditions in an SOFC by alloying 17 to 22% of chromium into the steel. Such alloys have been acknowledged as having the potential to offer a number of cost benefits in comparison with ceramic materials [**1–4**]. Alternatives to FSS include chromium-based alloys (commonly denoted CFY) which contain up to 95% chromium **[5].** As a side effect of utilising chromium-alloyed metallic interconnects, however, conventional cathode materials have been shown to suffer from a chromium-related poisoning phenomenon that deteriorates the performance of the SOFC. Studies of this subject have remained an area of intense research which, in itself, has resulted in several review articles [**6–8**]. In general, these studies have concentrated heavily on the common SOFC cathode materials LSM and LSCF with only a relatively minor consideration of the various other materials which have been researched. In this review, we aim to provide a comprehensive and up-to-date consideration on the various approaches and materials which have been studied in relation to chromium poisoning.

Highlighting the importance of studies in this area, Arregui et al. [**9**] analysed a number of operational and manufacturing parameters for a small sub-section of SOFC cathode materials and concluded that the most influential factor, with respect to performance degradation, was the introduction of a chromium source. The US Department of Energy have also commented on the need to mitigate the effects of chromium poisoning [**10**]**,** labelling the phenomenon a "*major contributor to performance degradation and reduced system reliability*". In Japan, the New Energy and Industrial Technology Development Organization (NEDO) have highlighted this issue as one of the main factors in the degradation of SOFC stacks [**11**]**.** Importantly, however, there is an indication that a careful selection of appropriate parameters and materials allows extended lifetime of SOFC stacks up to ten years [**12**]**.**

One approach to eradicating the problem of chromium poisoning could be to remove the chromium from the alloy altogether. However, in reality this is not a viable option. The use of chromium in ferritic stainless steels enables the formation of a protective chromia (Cr_2O_3) surface-layer; this layer provides the alloy's resistance to the degradative effects of corrosion. Since other metals are capable of forming a similar protective layer (e.g. the formation of Al_2O_3 on alumina-forming steel alloys),

there may remain a question as to why chromium-containing alloys specifically are the preferred material. The answer to this is related to the all-important electrical conductivity of the oxide species [**13,14**], the adherence of the oxide scale to the bulk material, and the slow growth of the oxide scale. It is with these considerations that chromium-containing metallic alloys have been identified as the most suitable for application under SOFC conditions. The issue of chromium poisoning, therefore, persists.

1.1 Chromium Volatilisation

The chromium poisoning literature is broadly divided into two topics; (a) Cr-species evaporation from interconnects and (b) the formation of Cr-phases within the cathode. This review will concentrate heavily upon the latter of these two areas but it remains useful to recap the former for background understanding. Under SOFC operating conditions there is a tendency for the chromia species to react with oxygen and moisture and migrate towards the cathode in gaseous form. The vaporisation of this chromia layer has been studied thermodynamically [**15–17**] and experimentally **[13,18**].

It is generally agreed [**13**,**15**,**16**,**19**] that CrO_3 and $CrO_2(OH)_2$ are the most common and abundant species that are formed. This occurs via the following reactions [**16**]:

$$Cr_2O_3(s) + 1.5O_2(g) \rightarrow 2CrO_3(g) \quad (1)$$

$$Cr_2O_3(s) + 1.5O_2(g) + 2\,H_2O(g) \rightarrow 2CrO_2(OH)_2(g) \quad (2)$$

It has been shown that the relative quantities of such species vary as a strong function of oxygen partial pressure and humidity [**15**,**17**,**20**]. Lower valency Cr-gases may become dominant at lower oxygen partial pressures [**20**]. In addition, a thermodynamic study conducted by Yin et al. [**17**] has shown that chromium evaporation rates increase at higher temperatures. In particular, the formation of the CrO_3 species increases significantly as the temperature is increased from 600 to 1000˚C.

Much research has sought to reduce the rate at which chromium is evaporated from steel interconnect materials. Indeed, there are a range of interconnect alloys that have been considered within the SOFC literature and there are several reviews [**21–23**] which summarise the developments in this area. The use of alloys that are capable of forming Cr-Mn spinel layers have been shown to reduce degradative effects **[24–26**]. These spinel phases form on top of the Cr_2O_3 layer and reduce the rate at which chromium is vaporised from the interconnect. Researchers have successfully engineered spinel phases (e.g, Cu-Mn spinel, Co-Mn spinels etc) as coating materials in attempts to deliberately reduce volatilisation rates [**27–29**]; perovskite coatings [**13**,**28**,**30**] have also

been shown to offer great promise in achieving this. The use of suitable interconnect materials can help to alleviate the issue of chromium poisoning but the studies of such materials have also shown that although reduced, the chromium release rate still remains too high to safeguard sufficient SOFC lifetime for stationary applications, in the order of magnitude of 40,000 to 100,000 hours. It is worth noting that the selection of suitable interconnect alloys represents a key step with respect to mitigating the effects of chromium poisoning. Nevertheless, the additional application of protective coatings will be necessary.

1.2 Chromium Deposition

After the gaseous chromium species is formed, it is able to diffuse into the porous cathode structure where it is subsequently deposited. Whilst the process of chromium deposition may appear, at first glance, a simple concept, there is a significant body of work highlighting that this is not the case. Indeed, the exact mechanisms by which this process occurs has, historically, been a subject of some debate. Further to this, the manner in which the cathodes are poisoned is greatly dependent upon the cathode materials in question, as demonstrated in work by Simner et al. [**25**].

Where the interconnect material directly touches the cathode material – i.e. along the contacting ribs - chromium can also directly migrate by solid state diffusion. In this case the necessity of volatilisation is sidestepped, but the final effect is the same: the formation of chromia or other chromium composites within the cathode structure.

1.3 Scope

This review aims to summarise the work already conducted on the chromium resistance of various cathode materials. Firstly, we consider the current understanding of chromium poisoning in relation to the most popular cathode materials: the group of predominately electronic conductors, LSM ($La_{1-x}Sr_xMnO_{3-\delta}$), and that of the mixed ionic-electronic conductors (MIEC) LSC ($La_{1-x}Sr_xCoO_{3-\delta}$), LSF ($La_{1-x}Sr_xFeO_{3-\delta}$), and LSCF ($La_xSr_{1-x}Co_yFe_{1-y}O_{3-\delta}$). These materials, like many other cathode materials, adopt the ABO_3-type perovskite structure. We will compile from literature sources how chromium resilience can be improved by an appropriate choice of materials, considering various SOFC cathode compositions and the effect that chromium has on each of them. Then, a consideration of the research around alternative cathode structures (e.g. double perovskites and Ruddlesden-Popper phases) will be provided, with the goal of understanding if these alternative materials would suggest any specific benefits in resisting chromium poisoning.

For reference, a consideration on the properties of common cathode materials has been provided in table 1. It is important to note that there are discrepancies in the literature with respect to the recorded values of a number of these properties. As an example, conductivity measurements have

been shown to vary from study-to-study and may be dependent on environmental, synthesis and testing conditions. In some cases, the values found in the literature may vary by orders of magnitude, for a given material. Nevertheless, a review of the literature is able to offer context for the discussion in this review.

Table 1 – Properties of some SOFC cathode materials.

*$ denotes value that has been estimated based on graphical data *Measurement conducted in air/P_{O2}=0.21bar ~Readings extrapolated from similar compositions*

NOTE: ECR=Electrical Conductivity Relaxation, IEDP=Isotope Exchange Depth Profile, IIE=Isothermal Isotope Exchange

Composition	**Total Conductivity, σ (Scm^{-1})** *[Temperature of measurements as below unless otherwise specified]*			**Ionic Conductivity, σ_i (Scm^{-1})**	**Oxygen Diffusion Coefficient, D*/D_{chem} (cm^2 s^{-1})** *[# - measured via IEDP/SIMS, £ - measured via ECR]*	**Surface Exchange Coefficient, k*/k_{chem} (cm s^{-1})** *[# - measured via IEDP/SIMS, £ - measured via Electrical Conductivity Relaxation, ^ - measured via IIE]*	**Thermal Expansion Coefficient (x 10^{-6} ˚C^{-1})** *[Temperature range denoted in parenthesise. "r.t" denotes room temperature]]*
	T=500˚C	**T=700˚C**	**T=900˚C**				
$LaMnO_3$	44 (P_{O2}=1 bar) [**31**] $	71 (P_{O2}=1 bar) [**31**] $	84 (P_{O2}=1 bar) [**31**] $ 115 (T=984˚C) [**32**] $*	-	8.7 x 10^{-16} (T=706˚C) [**33**] # 7.7 x 10^{-15} (T=796˚C) [**33**] # 1.2 x 10^{-13} (T=896˚C) [**33**] #	7.58 x 10^{-9} (700˚C) [**34**] ^ 8.91 x 10^{-9} (850˚C) [**34**] ^	9.5 – 10.75 (r.t - 1000˚C) [**35**] 12.4 (1000-50˚C) [**36**]
$LaCoO_3$	800 [**37**] *$	900 [**37**] *$ 1024 (P_{O2}=not specified) [**38**]	1000 [**37**] *$	3 x 10^{-4} (T=850˚C) [**39**] *$ 1.6 x 10^{-3} (T=900˚C) [**39**] *$	9.2 x 10^{-13} (T=700˚C) [**40**] # 2.41 x 10^{-11}(800˚C) [**40**] # 5.31 x 10^{-10} (900˚C) [**40**] #	4.57 x 10^{-9} (700˚C) [**40**] # 3.47 x 10^{-7} (800˚C) [**40**] #	23.5 (100-700˚C) [**38**] 21 (300-950˚C) [**41**] 24 - 28 (25-1000˚C) [**37**]
$LaFeO_3$	0.15 [**37**] *$	0.2 [**37**] *$	0.25 [**37**] *$	-	9.84 x 10^{-13} (T=900˚C) [**42**] # 5.28 x 10^{-11}(T=1000˚C) [**42**] #	3.89 x 10^{-8} (900˚C) [**42**] # 1.67 x 10^{-7} (1000˚C) [**42**] # 8.89 x 10^{-9} (700˚C) [**34**] ^ 4.11 x 10^{-9} (850˚C) [**34**] ^	10.1 (25-1000˚C) [**37**]
$LaNiO_3$	125 [**43**] *$ 900 [**37**] *$	105 [**43**] *$ 750 [**37**] *$	100 [**43**] *$	-	-	-	9-14 (25-1000˚C) [**37**]
$LaCrO_3$	-	0.34 (P_{O2}=not specified) [44]	1 (1000˚C; ; P_{O2}=not specified) [**44**]	-	-	-	9.6 (100-850˚C) [**45**]

$La_{0.8}Sr_{0.2}MnO_{3-\delta}$ (**LSM-82**)	150 [**46**] *$ 135 (T=470˚C) [**47**] *$ -	-	210 (T=1000˚C ; P_{O2}=10^{-6}-1bar) [**48**] $ 220 (T=1000˚C ; P_{O2}=1atm) [**49**] $ 290 (T=1000˚C) [**47**] *$	4.2 x 10^{-10} (T=750˚C ; P_{O2}=1bar) [**50**] 4 x 10^{-8} (T=900 ˚C ; P_{O2}=not specified) [**51**] 5.93 x 10^{-7} (T=900 ˚C ; P=100 torr.) [**52**]	2 x 10^{-16} (T=700˚C), 5 x 10^{-15} (T=800˚C), 2 x 10^{-13} (T=900˚C) [34] # 5 x 10^{-7} (T=800˚C) [**53**] £ 1.8 x 10^{-12} (T=1000˚C) [**54**] £ $ 10^{-16} (T=700 ˚C), 10^{-12} (T=1000 ˚C) [**55**] # 1.27 x 10^{-12} (T=900˚C) [**52**] #	8.4 x 10^{-9} (775˚C) [**34**] ^ 4.19 x 10^{-9} (850˚C) [**34**] ^ 10^{-9} (700˚C), 10^{-7} (1000˚C) [**55**] #	11.8 (30-1000˚C) [**46**] 13.1 (200-800˚C) [**56**] 10.8-11.25 (r.t - 1000˚C) [**35**] 11.5 (r.t - 1000˚C) [**57**]
$La_{0.6}Sr_{0.4}MnO_{3-\delta}$ (**LSM-64**)	80 (P_{O2}=10^{-5}atm) [**58**] $	125 (P_{O2}=10^{-5}atm) [**58**] $	140 (P_{O2}=10^{-5}atm) [**58**] $	-	-	-	11.75-12.25 (r.t - 1000˚C) [**35**] 12 (r.t - 1000˚C) [**57**]
$La_{0.5}Sr_{0.5}MnO_{3-\delta}$ (**LSM-55**)	-	360 (P_{O2}=not specified) [**59**]	300 (P_{O2}=not specified) [**59**] 485 (T=1000˚C) [**47**] *	5 x 10^{-7} (T=900˚C ; P_{O2}=not specified) [**60**] 1.35 x 10^{-9} (T=750˚C ; P_{O2}=1bar) [**50**]	10^{-8} – 10^{-10} (T=695-840 ˚C) [61] £ 2 x 10^{-15} (T=700˚C) [59] # 8 x 10^{-14} (T=800˚C) [59] # 3 x 10^{-12} (T=900˚C) [59] #	1 x 10^{-8} (700˚C) [59] # 1 x 10^{-7} (800˚C) [59] # 9 x 10^{-8} (900˚C) [59] #	12-12.6 (r.t - 1000˚C) [**35**] 12.2 (r.t - 1000˚C) [**57**]
$La_{0.6}Sr_{0.4}Co_{0.2}Fe_{0.8}O_{3-\delta}$ (**LSCF-6428**)	330 [**62**] *$ 400 [**63**] *$	320 [**62**] *$ 440 [**63**] *$	210 [**62**] *$ 270 [**64**] * 220 [**65**] *	0.23 (T=900 ˚C) [66] 8 X 10^{-3} (T=800˚C) [**67**] * 0.023 (T=750˚C ; P_{O2} =1 bar) [**50**]	1 x 10^{-9} (T=650˚C) [**34**] # 5 x 10^{-9} (700˚C) [**34**] # 7.8 x 10^{-6} (800˚C) [**53**] £ 2.5 x 10^{-9} (700˚C) [68] # 1 x10^{-6} – 2.5 x 10^{-6} (650˚C) [69] £ $ 1 x10^{-6} – 5 x 10^{-6} (700˚C) [**69**] £ $ 5 x10^{-6} – 1 x 10^{-5} (800˚C) [**69**] £ $	2.46 x 10^{-8} (500˚C) [**34**] ^ 2.68 x 10^{-8} (600˚C) [**34**] ^ 2.74 x 10^{-8} (700˚C) [**34**] ^ 2.76 x 10^{-8} (800˚C) [**34**] ^ 1.1 x 10^{-6} (700˚C) [68] # 1 x 10^{-5} – 5 x 10^{-3} (650-800˚C) [**69**] £ $	15.3(100-600˚C) [**62**] 17.5 (r.t -1000˚C) [**64**] 16.8 (100-900˚C) [**63**] 23.6 (700-900˚C) [**63**]
$La_{0.6}Sr_{0.4}Co_{0.8}Fe_{0.2}O_{3-\delta}$ (**LSCF-6482**)	225 (P_{O2}=not specified) [**70**] $	205 (P_{O2}=not specified) [**70**] $	-	0.058 (T=800˚C) [**67**] * 0.005 (T=750˚C ; P_{O2}=1bar) [**50**]	-	-	21.4 (30-1000˚C) [**67**]
$La_{0.5}Sr_{0.5}Co_{0.8}Fe_{0.2}O_{3-\delta}$ (**LSCF-5582**)	-	-	-	-	3.62 x 10^{-6} (500˚C) [71] £ 7.94 x 10^{-6} (600˚C) [71] £	-	20.62 (25-650˚C) [**71**]

					1.47 x 10^{-5} (700˚C) [71] £		
$La_{0.8}Sr_{0.2}CoO_{3-\delta}$ (**LSC-82**)	1450 [**72**] *$ 1689 (T=600˚C) [**64**]*	1300 [**72**] *$ 1521 (T=800˚C) [**64**] *	1125 [**72**] *$ 1291 (T=1000˚C) [**64**] *	4.9 x 10^{-4} (T=750˚C ; P_{O2}=1bar) **[50]**	1 x 10^{-10} – 1 x10^{-8} (700˚C) [**34**] # 8 x 10^{-10} – 2 x 10^{-7} (800˚C) [**34**] # 1 x 10^{-8} – 1 x 10^{-6} (900˚C) [**34**] # 1 x 10^{-8} (700˚C) [**59**] # 2 x 10^{-8} (800˚C) [**59**] # 4 x 10^{-8} (900˚C) [**59**] # 8 x 10^{-8} (1000 ˚C) [**54**] # $	3.65 x 10^{-8} (600˚C) [**34**] ^ 3.87 x 10^{-8} (700˚C) [**34**] ^ 3.67 x 10^{-8} (800˚C) [**34**] ^ 3 x 10^{-6} (700˚C) [**59**] # 5 x 10^{-6} (800˚C) [**59**] # 2 x 10^{-5} (900˚C) [**59**] #	19.1 (30-1000˚C) [**46**] 19.7 (100-900˚C) [72]
$La_{0.6}Sr_{0.4}CoO_{3-\delta}$ (**LSC-64**)			1084 (T=1000˚C) [**64**] *	0.22 (T=800˚C) [**67**] * 4.09 x 10^{-3} (T=700˚C ; P_{O2} =0.1bar) [**73**]	1.09 x 10^{-6} (700˚C) [**73**] £ 2.5 x 10^{-6} (825˚C) [**53**] £	1.97 x 10^{-4} (700˚C) [**73**] £ 2.5 x 10^{-4} (825˚C) [**53**] £	20.5 (30-1000˚C) [**67**]
$La_{0.5}Sr_{0.5}CoO_{3-\delta}$ (**LSC-55**)	1899 (T=600˚C) [**64**]*	1356 (T=800˚C) [**64**] *	930 (P_{O2}=1atm) [60] $ 893 (T=1000˚C) [**64**] *	0.1 (T=900˚C ; P_{O2}=not specified) [**60**]	6.01 x 10^{-6} (500˚C) [**71**] £ 1.21 x 10^{-5} (600˚C) [**71**] £ 4.71 x 10^{-5} (700˚C) [**71**] £		21.37 (25-650˚C) [**71**]
$La_{0.5}Sr_{0.5}Co_{0.8}Ni_{0.2}O_{3-\delta}$ (**LSCN-5582**)	-	-	-		3.09 x 10^{-6} (500˚C) [**71**] £ 7.28 x 10^{-6} (600˚C) [**71**] £ 1.69 x 10^{-5} (700˚C) [**71**] £		21.38 (25-650˚C) **[71]**
$La_{0.5}Sr_{0.5}Co_{0.8}Cu_{0.2}O_{3-\delta}$ (**LSCCu-5582**)	-	-	-		7.91 x 10^{-6} (500˚C) [**71**] £ 1.25 x 10^{-5} (600˚C) [**71**] £ 3.44 x 10^{-5} (700˚C) [**71**] £		19.75 (25-650˚C) [**71**]
$La_{0.8}Sr_{0.2}FeO_{3-\delta}$ (**LSF-82**)	80 [**74**] *$ 90 [**72**] *$	90 [**74**] *$ 155 (T=750˚C) [**75**] *	80 [**74**] *$	4.68 x 10^{-2} (T=800˚C ; P_{O2}=1atm.) [**76**] 7.75 x 10^{-2} (T=900˚C ; P_{O2}=1atm)	-	10^{-5} - 10^{-4} (800˚C) [**77**] £ $	12 (30-1000˚C) [**75**] 12.2 (30-1000˚C) [**46**]

				[**76**]			12.6 (300-900˚C) [**72**]
$La_{0.6}Sr_{0.4}FeO_{3-\delta}$ (**LSF-64**)	240 [**74**] *$~	200 [**74**] *$~	115 [**74**] *$~	0.141 (T=800˚C ; P_{O2}=1atm) [**76**] @ 0.232 (T=900˚C ; P_{O2}=1atm) [**76**] @ 0.003 (T=750˚C ; P_{O2}=1bar) [**50**]	1.0-1.1 x 10^{-5} (800˚C) [**53**] £ 3 x 10^{-6}, 7 x 10^{-6}, 1 x 10^{-5} (725, 800, 875˚C) [**34**] £	1 x 10^{-3} (800˚C) [**53**] £ 2.79 x 10^{-8} (700˚C) [**34**] ^ 3.17 x 10^{-8} (800˚C) [**34**] ^	-
$LaNi_{0.6}Fe_{0.4}O_{3-\delta}$ (**LNF-64**)	625 [**78**] *$	595 [**78**] *$ 313 (P_{O2}=not specified) [**79**] 525 (T=750˚C) [**75**] *	297 (P_{O2}=not specified) [**79**]	-	4.3 x 10^{-9} (800˚C) [**80**] #	8.6 x 10^{-6} (800˚C) [**80**] #	13.2 (30-1000˚C) [**75**] 11.1 (30-800˚C) [**78**] 12.1 (r.t-900˚C) [**79**]
$La_{0.5}Ba_{0.5}Co_{0.9}Fe_{0.1}O_{3-\delta}$ (**LBCF-5591**)	560 [**81**] *$	375 [**81**] *$		-	-	-	23.75 (20-1000˚C) [**81**]
$La_{0.6}Sr_{0.4}Co_{0.8}Mn_{0.2}O_{3-\delta}$ (**LSCM-6482**)	1400 [**82**] $*	1000 [**82**] $*	800 [**82**] $*	-	-	-	18.1 (500-900˚C) [**82**]
$La_{0.5}Sr_{0.5}Co_{0.2}Mn_{0.8}O_{3-\delta}$ (**LSCM-5528**)	-	86 (P_{O2}=not specified) [**59**]	98 (P_{O2}=not specified) [**59**]	-	2 x 10^{-14} (700˚C) [**59**] # 2 x 10^{-13} (800˚C) [**59**] # 1 x 10^{-11} (900˚C) [**59**] #	2 x 10^{-8} (700˚C) [**59**] # 1 x 10^{-7} (800˚C) [**59**] # 2 x 10^{-7} (900˚C) [**59**] #	-
$Pr_{0.6}Sr_{0.4}Co_{0.8}Fe_{0.2}O_{3-\delta}$ (**PSCF-6482**)	955 (P_{O2}=not specified) [**83**] $	795 (P_{O2}=not specified) [**83**] $	-	-	-	-	19.69 (30-850˚C) [**83**]
$Pr_{0.8}Sr_{0.2}MnO_3$ (**PSM-82**)	-	-	-	-	-	-	9.5 (30-800˚C) [**56**] 10.1 (30-1000˚C) [**56**]
$Pr_{0.6}Sr_{0.4}MnO_3$ (**PSM-64**)	214 [**84**] *	242 (P_{O2}=10^{-5}bar) [**85**] $	237 (P_{O2}=10^{-5}bar) [**85**] $	-	-	-	12 (300-1000˚C) [**58**]
$Pr_{0.5}Sr_{0.5}MnO_3$ (**PSM-55**)	130 (P_{O2}=not specified) [**86**] $	115 (P_{O2}=not specified) [**86**] $	107 (P_{O2}=not specified) [**86**] $	-	-	-	12.2 (100-600˚C) [**84**] 13.6 (600-800˚C) [**84**]

	102 [**87**] $* 226 [**84**] *	130 [**87**] $* 230 [**84**] $*	150 [**87**] $*				11.43 (r.t.-300˚C) [**88**]
$Pr_{0.7}Sr_{0.3}CoO_{3-\delta}$ (**PSC-73**)	1685 (P_{O2}=not specified) [**89**] $ 1995 [**90**] *$	1510 (P_{O2}=not specified) [**89**] $ 1585 [**90**] *$	-	-	-	-	18.8 (30 - 800˚C) [**56**] 22 (100 -700˚C) [**90**]
$Sm_{0.5}Sr_{0.5}CoO_{3-\delta}$ (**SSC-55**)	1580 [**91**] $* 700 [**92**] $* 1260 ($P_{O2}$=not specified) [**93**] $	1110 [**91**] $* 500 [**92**] $*	650 [**91**] $* 350 (T=850˚C) [**92**] $* 630 ($P_{O2}$=not specified) [**93**] $	0.13 (T=750˚C ; P_{O2}=1 bar) [**50**]	1.56 x 10^{-6} (500˚C) [**94**] £ 3.63 x 10^{-5} (700˚C) [**94**] £ 3.9 x 10^{-8}-1.8 x 10^{-6} (597-887˚C) [**3**] #	3.7 x 10^{-6} (597˚C) [**3**] # 5.6 x 10^{-5} (887˚C) [**3**] #	20.5 (r.t - 900 ˚C) [**93**] 22.8 (30 - 900˚C) [**92**] 24 (200- 1000˚C) [**91**]
$Sm_{0.5}Sr_{0.5}MnO_{3-\delta}$ (**SSM-55**)	160 [**91**] $*	-	183 [**91**] $*	-	-	-	11.4 (r.t - 1000˚C) [**57**] 11.8 (200 - 1000˚C) [**91**]
$Sm_{0.5}Sr_{0.5}Co_{0.2}Fe_{0.8}O_3$ (**SSCF-5528**)	125 [**65**] $* 400 ($P_{O2}$=not specified) [**93**] $	185 [**65**]* 250 (P_{O2}=not specified) [**93**] $	122 (P_{O2}=0.21 bar) [**65**] 180 (P_{O2}=not specified) [**93**] $	-	-	-	15.75 (r.t - 900˚C) [**93**]
$Sm_{0.5}Sr_{0.5}Co_{0.8}Fe_{0.2}O_3$ (**SSCF-5582**)	1000 (P_{O2}=not specified) [**93**] $	595 (P_{O2}=not specified) [**93**] $	355 (P_{O2}=not specified) [**93**] $	-	-	-	20.6 (r.t - 900˚C) [**93**]
$Sm_{0.6}Sr_{0.4}Co_{0.8}Mn_{0.2}O_3$ (**SSCM-6482**)	470 [**82**] *$	555 [**82**] *$	590 [**82**] *$	-	-	-	21.6 (500 - 900˚) [**82**]
$Ba_{0.5}Sr_{0.5}Co_{0.8}Fe_{0.2}O_3$ (**BSCF-5582**)	28 [**95**] *$ 52 (P_{O2}=0.2bar) [**69**] $ 80 (P_{O2}=1bar) [**69**] $	32 [**95**] *$ 49 (P_{O2}=0.2bar) [**69**] $ 68 (P_{O2}=1bar) [**69**] $	65 (P_{O2}=1bar) [**69**] $	0.07, 0.25, 0.96 (T=600,700,800˚C ; P_{O2}=0.21-0.1atm) [**96**] @ 0.71 (T=750˚C ; P_{O2}=1bar) [**50**]	5 x 10^{-7} - 7.75 x 10^{-5} (600˚C) [**69**] £ $ 2.5 x 10^{-7}- 5 x 10^{-5} (700˚C) [**69**] £ $ 7.75 x 10^{-6}- 5 x 10^{-5} (800˚C) [**69**] £ $	2.7 x 10^{-4} – 4.1 x 10^{-3} (600-800˚C) [**96**] £ 5 x 10^{-5} – 5 x10^{-4} (600˚C) [**69**] £ $ 5 x 10^{-5} – 1 x10^{-2} (700˚C) [**69**] £ $	19.95 (50 - 1000˚C) [**95**] 12.7 (200 - 400˚C) [**69**] 27.3 (425 - 980˚C) [**69**]

$Ba_{0.5}Sr_{0.5}Co_{0.2}Fe_{0.8}O_3$ (**BSCF-5528**)	32 [**65**] *$ 19 [**97**] *$ 21 (in oxygen) [**97**] $	40 [**65**] *$ 11 [**97**] *$	16 [**65**] * 2 [**97**] *$ 9.5 (in oxygen) [**97**] $	-	-	-	23 (25 - 850˚C) [**98**]
$Ba_{0.6}Sr_{0.4}Co_{0.9}Nb_{0.1}O_{3-\delta}$ (**BSCN-6491**)	42.5 (P_{O2}=1 atm) [**99**] $ 32.5 [**99**] *$	46 (P_{O2}=1 atm) [**99**] $ 38 [**99**] *$ 39.7 [**100**] *	48 (P_{O2}=1 atm) [**99**] $ 43 (P_{O2}=0.21 atm) [**99**] $	0.45 (700˚C) [**100**] $* 0.9 (800˚C) [**100**] $* 1.38 (900˚C) [**100**] $*	1.3 x 10^{-4} (600˚C) [**99**] £	3.3 x 10^{-5} (600˚C) [**99**] £	14.4 (200 - 500˚C) [**99**] 21.9 (500 - 900˚C) [**99**]
$Ba_{0.5}Sr_{0.5}Fe_{0.9}Nb_{0.1}O_{3-\delta}$ (**BSFN-5591**)	12.25 [**101**] *$	7.5 (P_{O2}=0.21 atm) [**101**] $	6.5 [**101**] *$	-	-	-	19.2 (20 - 1000˚C) [**101**]
$BaCo_{0.7}Fe_{0.2}Nb_{0.1}O_{3-\delta}$ (**BCFN-721**)	11 (P_{O2}=1 atm) [102] $ 7.75 [102] *$	15 (P_{O2}=1 atm) [102] $ 11 [102] *$	18.5 (P_{O2}=1 atm) [102] $ 15 [102] *$	-	-	-	18.2 (30 - 900˚C) [**102**] 14.4 (30 - 500˚C) [**102**]
$Nd_{0.8}Sr_{0.2}MnO_{3-\delta}$ (**NSM-8210**)				-	-	-	-
$Nd_{0.6}Sr_{0.4}Co_{0.8}Mn_{0.2}O_3$ (**NSCM-6482**)	600 [**82**] *$	615 [**82**] *$	460 [**82**] *$	-	-	-	19.6 (500 - 900˚) [**82**]
$Gd_{0.6}Sr_{0.4}Co_{0.8}Mn_{0.2}O_3$ (**GSCM-6482**)	810 [**82**] *$	870 [**82**] *$	650 [**82**] *$	-	-	-	21.3 (500 - 900˚) [**82**]
$La_2NiO_{4+\delta}$ (**LNO-214**)	102 [**103**] *$ 83 [**104**] *$ 10 [**43**] *$ 6.1 [**105**] *$	85 [**103**] *$ 68 [**104**] *$ 9 [**43**] *$ 5.25 [**105**] *$	68 [**103**] *$ 8 [**43**] *$	5.6 x 10^{-3} (T=600˚C) [106] $* 1.7 x 10^{-2} (T=700˚C) [106] $* 4.0 x 10^{-2} (T=800˚C) [106] $*	10^{-9} - 10^{-7} (500-850˚C) [**106**] $# 2.71 x 10^{-8} – 1.39 x 10^{-7} (640-842˚C) [**107**] # 10^{-8} – 10^{-7} (600-850˚C) [**108**] #	10^{-7} – 10^{-6} (500-850˚C) [**106**] # $ 1.81 x 10^{-7} – 3.18 x 10^{-6} (640-842˚C) [**107**] # 10^{-8} – 10^{-6} (640-850˚C) [**108**] #	13.8 (75 - 900˚C) [**104**] 13.0 (27˚C - 900˚C) [**109**] 13.0 (100 - 900˚C) [**63**]
$Nd_2NiO_{4+\delta}$ (**NNO-214**)	42 [**109**] *$	37 [**109**] *$	32 [**109**] *$	4.44 X 10^{-4} (T=700˚C ; P_{O2} =0.1bar) [**73**]	5.73 x 10^{-7} (700˚C) [**73**] £	1.31 x 10^{-4} (700˚C) [**73**] £	12.7 (27˚C - 900˚C) [**109**]

2 LSM-based cathodes

The perovskite material $La_{1-x}Sr_xMnO_3$ (LSM) has traditionally been a popular choice as an SOFC cathode material and its performance and associated degradation phenomena have received significant research attention. LSM cathodes have, however, been shown to be susceptible to a substantial performance deterioration in the presence of a chromium source [**18**,**110–112**]. Work by De Haart et al. [**113**], in which a series of LSM-based stacks were galvanostatically tested over a 3,000 hour interval within the Real-SOFC project [**114**], determined that this deterioration in performance comprised of three characteristic regions (see Figure 1). First, a considerable drop in performance, followed by a continuous degradation process with the final stage being one of progressive degradation towards the stack end-of-life. Assuming that this degradation behaviour was due to a single dominating process, e.g. cathode degradation due to chromium deposition, Roehrens et al. [**115**] proposed that this was likely to result from the manner in which the deposited species block an increasing portion of the active sites. The authors suggested that the initial (~100 hours) drop in performance proceeds via a "chemical pathway" with small amounts of secondary phases deposited within the electrode. Elsewhere [**116**], it was suggested to be driven by the adsorption of chromium gas species upon the cathode surface. The initial stage of degradation is then followed by a more gradual and linear reduction in voltage, determined by a further formation of solid chromium species within the cathode. An acceleration in the degradation rate can then be expected, as further formation of such species cause "*disproportionately large performance loss*" [**115**]. In a different context, Kulikovski **[117**] described a mathematical model of such progressive degradation based on performance loss by an increasing electrode poisoning effect. Although chromium poisoning is a major contributor to the loss of performance seen in Fig. 1, it is not the sole cause of degradation as has been shown in further research (e.g. [**118**]).

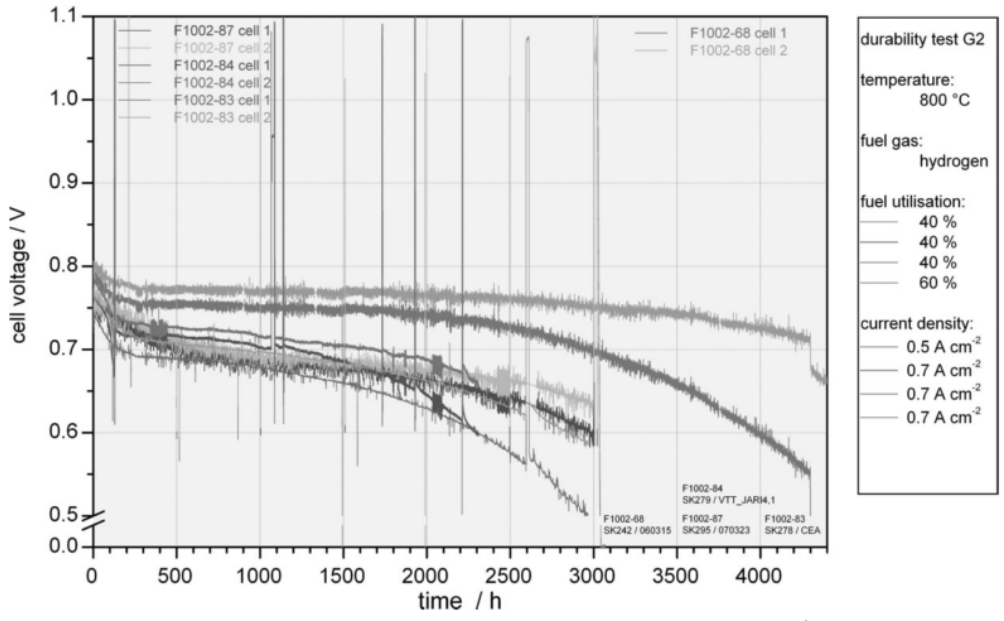

Figure 1 – Voltage loss of galvanostatically-operated fuel cell stacks [**113**]*. The stacks contain an LSM-based cathode material and a steel alloy interconnect. Re-printed with kind permission.*

The degradation in performance which has been related to chromium in the literature has been observed to result from the formation of solid chromium species, notably $(Cr,Mn)_3O_4$ and Cr_2O_3. Such species are typically observed at the electrode-electrolyte interface across a number of LSM compositions [**18**,**111**,**119**,**120**]. Historically, there has been some disagreement in the literature as to the exact mechanism by which these phases are deposited within the cell [**26**]. Two popular theories commonly discussed in the literature involve (a) the electrochemical deposition of chromium gas species at the triple phase boundaries [**20**] or, alternatively, (b) the chemical reaction between the chromium-containing gas and the reduced Mn^{2+} species [**120**]. In addition to these theories, the role of oxygen pressure gradients (as the oxygen is electrochemically reduced across the cathode) have been suggested to play some role in the deposition process [**18**,**121**].

2.1 Cr-Deposition Theories for LSM

2.1.1 Electrochemical Deposition Theory

In thermodynamic studies by both Das et al. [**20**] and Hilpert et al. [**15**], it was proposed that Chromium vapours (e.g. CrO_3 or $CrO_2(OH)_2$) could be electrochemically reduced at the cathode via one of the following reactions:

$$2CrO_3\,(g) + 6e^- \rightarrow Cr_2O_3(s) + 3O^{2-} \quad (3)$$

$$2CrO_2(OH)_2\,(g) + 6e^- \rightarrow Cr_2O_3(s) + 2H_2O(g) + 3O^{2-} \quad (4)$$

Subsequent work [**110**,**112**,**122**], investigating chromium poisoning of LSM cathodes, has shared the view that this so-called electrochemical deposition mechanism is a likely cause of chromium-related degradation. It has been anticipated that such reactions would be most likely seen at the triple phase boundaries, where oxygen reduction readily occurs [**15**,**123**]. Deposition in these areas, as suggested by Paulson and Birss [**123**], could not only reduce the rate of oxygen reduction but could also provide deposits which block the all-important reaction sites. Chromia deposition, however, has typically been observed along the whole boundary between the cathode and electrolyte, and not exclusively at the TPBs [**111,122**,**123**], as seen in Figure 2. Further to this, Paulson and Birss observed the growth of a chromia layer [**123**] *away* from an LSM cathode (and hence away from the TPBs) and along a YSZ electrolyte material. The authors proposed that the newly formed chromia (initially deposited upon the TPB), must provide an extended reaction site upon which further reduction of the chromium gas phase can occur.

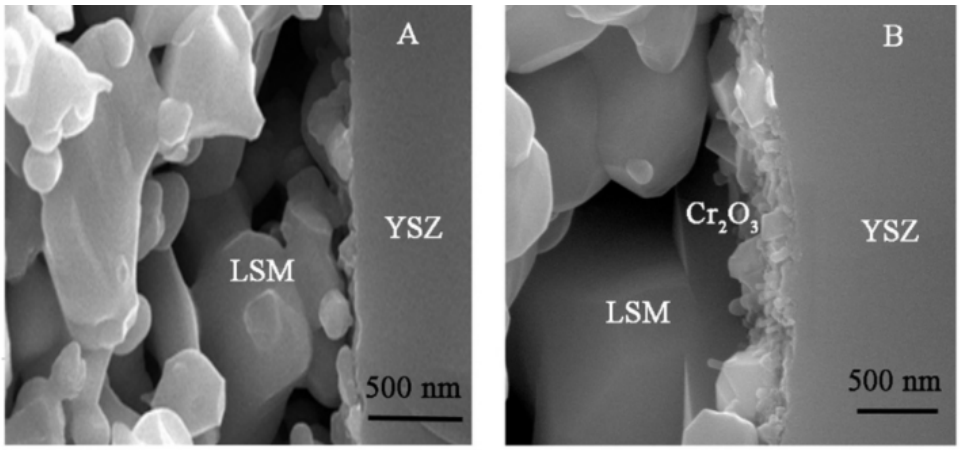

Figure 2 – (a, left) YSZ/LSM interface prior to exposure to chromium, (b, right) chromia scale formed along the electrolyte/cathode boundary as seen in work by Hu et al. [**111**]. *The authors utilised SEM and EDS to perform morphological and elemental analysis. Reprinted with kind permission.*

2.1.2 Chemical deposition theory

In a series of papers by Jiang et al. [**120**,**124–127**], a significant opposition to the theory described in section 2.1.1 has been presented. In the first of these studies [**120**], the authors observed the formation of chromia at anodic, cathodic and open circuit conditions and concluded that this makes deposition by electrochemical means unlikely. It is suggested that, instead, the formation of chromia occurs via the precipitation of Cr-Mn-O nuclei:

$$Mn^{2+}\ (LSM\ surface) \rightarrow Mn^{2+}\ (YSZ\ surface) \quad (5)$$

$$Mn^{2+}\ (YSZ\ surface) + CrO_3(g) \rightarrow Cr-Mn-O\ (nuclei, YSZ) \quad (6)$$

$$Cr - Mn - O\ (nuclei, YSZ\ surface) + CrO_3(g) \rightarrow Cr_2O_3(YSZ) \quad (7)$$

$$Cr_2O_3(YSZ) + CrO_3(g) + Mn^{2+}\ (YSZ\ surface) \rightarrow (Cr,Mn)_3O_4(YSZ) \quad (8)$$

The reduced manganese species (Mn^{2+}), mentioned above, are suggested to originate from two sources; (1) the reduction of Mn^{3+} or Mn^{4+} during cathodic polarisation (as observed during in-situ XPS experiments by Lee et al. [**128**]) and (2) transfer from the cathode to the electrolyte during manufacture. As such, Jiang et al. [**120**] offer an alternative explanation as to the apparent accelerating effect that polarisation appears to have upon chromium deposition (i.e. an increased number of nucleation sites becoming available due to the increase in the amount of Mn^{2+}). The transfer of Mn to the electrolyte would also explain the observation of chromium phases upon the electrolyte as observed in Figure 2.

In order to further explore their proposed theory, Jiang et al.[**125**] studied the effect of chromium deposition on the oxygen reaction kinetics of LSM cathodes. Their findings indicated that the formation of Cr-species has the effect of hindering oxygen diffusion processes. Li et al. [**119**], meanwhile, have pointed to the formation of Cr_2O_3 and $(Cr,Mn)_3O_4$ at areas away from the TPBs as further evidence that the theory outlined in section 2.1.1 may be flawed. Additionally, it has been suggested that the effects of chromium upon platinum electrodes (discussed in section 4.1) offers further proof of the theories outlined here.

2.1.3 Oxygen Activity Theory

Taniguchi et al. [**18**] proposed that the formation of chromia at the LSM cathode/electrolyte interface arises from the drop in oxygen activity which is experienced as the oxygen is electrochemically reduced. The authors hypothesised that the lower oxygen pressure at the interface drives one of the following:

$$2CrO_3(g) \rightarrow Cr_2O_3(s) + 1.5O_2(g) \quad (9)$$

$$2CrO_2(OH)_2(g) \rightarrow Cr_2O_3(s) + 1.5O_2(g) + 2H_2O(g) \quad (10)$$

As such, the relationship between oxygen activity and chromium deposition is considered to be the key driver of the poisoning effect. As the oxygen activity decreases, greater quantities of chromia are found at the electrolyte-cathode interface. This theory is also supported in a thermodynamic analysis conducted by Yokokawa et al.[**121**]. In that work, the authors suggest that the accelerated rate at which chromium deposits under polarisation is due to the resulting oxygen potential gradient that exists in the cathode layer as the ORR is allowed to proceed.

2.1.4 Discussion

Whilst many authors have sought to prove or disprove a single theory, it is perfectly possible that several reaction mechanisms may, in fact, be taking place. These mechanisms may be competing with each other, possibly depending on the set of materials present or the operating conditions.

The deposition of chromium in LSM cathodes has been reported at open circuit conditions [**115**,**120**,**129–131**]. However, it is generally agreed that the formation of chromium species under such conditions is not as significant as that which may be seen under polarisation. In work by Jiang et al. [**120**] the authors reported that, when their LSM cathode was placed under an open circuit condition, the formation of Cr-containing phases only occurred at temperatures in excess of 1000˚C. It may be pertinent to point out, however, that this work considered a comparatively short 50h testing period. Longer term testing may have revealed some deposition of chromium. Further, there appears to be a general consensus within the aforementioned studies, that chromium poisoning may indeed occur in the absence of polarisation. Whilst it is certainly an accelerating factor, the current flow condition (i.e. polarisation) does not appear to be a *requirement* for chromium poisoning to occur.

It has been observed by Konysheva et al. [**129**] that, under open circuit conditions, the deposition of chromium becomes much more random across the width of the cathode. This is also consistent with works by Jin and Lu [**130,131**] who observed the migration of chromium from a stainless steel alloy into LSM cathode layers deposited on a YSZ electrolyte. In comparison, the deposition of chromium under polarisation is seen to occur at the interface between the cathode and electrolyte. These apparently differing characteristics could hint at the possibility of multiple processes driving the formation of the chromium species. Indeed, that is a suggestion which is proposed in the previously mentioned work by Roehrens et al. [**115**]. After a series of 3000h tests at different current conditions, the authors concluded that both a chemical or electrochemical degradation mechanism may be possible. In that work, the chemical deposition mechanism is hypothesised to dominate at low current densities (or at OCV conditions) with the electrochemical deposition becoming more significant at higher current densities. The formation of Cr-Mn spinels (via a thermodynamic driving force), will subsequently result in the depletion of manganese in the LSM matrix and a subsequent breakdown of the perovskite structure. We will further discuss the drivers of chromium poisoning in the coming sections of this review and with a summary provided at the end of the paper.

2.2 Further work on LSM Cr-degradation

Regardless of the drivers of chromium poisoning, it is clear that the effects on LSM cathodes offer a challenge for long lifetimes of SOFC systems using this material. Further work has been undertaken

in this area in order to establish the mitigating factors that may help to reduce or overcome the poisoning effect.

2.2.1 Effect of Operating Conditions

As previously discussed, current flow has been demonstrated [**119**,**120**,**129**,**132**] to have a profound effect on the rates of LSM cathode degradation, when in the presence of a chromium source. The reduction of current is not a particularly attractive solution to preventing chromium poisoning given that the maximisation of electrical output is desirable. Other operational parameters, however, offer a more attractive route to reducing chromium deposition (or its effects).

A study of the literature indicates that degradation resulting from chromium poisoning is intensified at higher humidity [**24**,**132–134**]. Most authors [**132–134**] have attributed this to the increased partial pressure of chromium-containing gas which results at this condition (as seen in work by Hilpert et al. [**15**]). As the humidity increases, the rate of volatised chromium will also increase and the resulting quantities of chromium that are deposited within the cathode will subsequently grow. However, there is evidence to suggest that, even in the absence of a chromium source, the performance and degradation of LSM cathodes may worsen under the influence of water in both the short and long-term [**135**]. As such, it would be advantageous to reduce humidity whether chromium-containing alloys are used or not.

There appears to be some confusion within the literature with respect to the effects of operating temperature. In some cases at least, an increase in temperature has been seen to intensify the formation of solid chromium species within the LSM cathodes [**18**,**124**]. This may be unsurprising given the increased volatilisation rates that are seen at higher temperatures [**15**]. Taniguchi et al. [**18**] noted that, despite higher levels of chromium found within the cathode at elevated temperatures, the voltage loss as a function of time was larger at *lower* temperatures. Research led by the Argonne National Laboratory in the United States [**122**,**136**], reports a somewhat different phenomenon. In these studies, not only is the degradation rate greater at lower temperatures but the amount of chromium deposited is also seen to be greater. Importantly, one further conclusion that can be drawn from this work is that the chromium has a greater impact on the voltage loss per wt% of chromium. This, perhaps, could be accounted for by the lower activity of the cathode at lower temperature. Thus, the effect of a given amount of chromium could be expected to have a greater impact upon the performance of the cathode with lower activity (i.e, the cathode at lower temperature).

It has been observed [**18**] that, at higher temperatures, the deposition of chromium becomes more varied across the width of the cathode, as may be noted for an LSM/YSZ composite cathode shown

in Figure 3. Whilst this study was carried out on a composite cathode, whereby the use of the YSZ ionic phase in mixture with LSM effectively extends the TPB into the body of the cathode, there is further evidence to indicate that this would also be observed for single phase LSM cathodes. Two separate studies [**120**,**137**] indicate that, under open circuit conditions, chromium deposition can be expected at temperatures in excess of 1000˚C. As a side note, Jiang et al. [**120**] suggest that the formation of solid chromium species at higher temperatures provides additional support for their chemical deposition theory. The authors indicated that the increased mobility of the nucleation agent (Mn^{2+}) at higher temperatures provides a source of the deposition which cannot be explained by the electrochemical reduction theory.

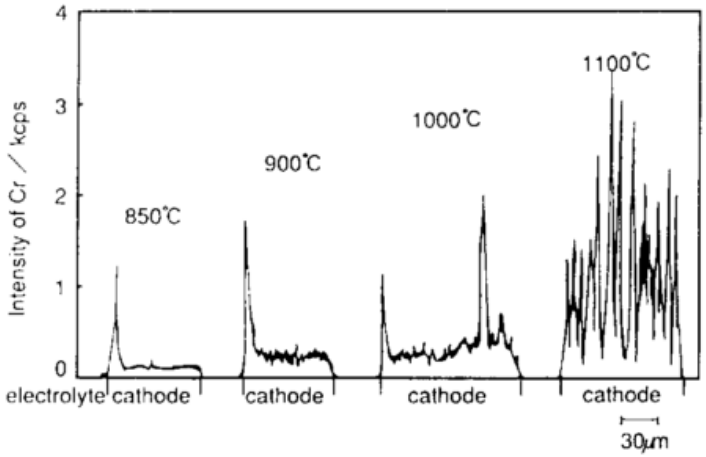

Figure 3 – Effect of temperature upon the distribution of chromium in LSM/YSZ cathodes. The left most edge of the scan corresponds to the electrolyte/cathode interface. It is seen that chromium is deposited at areas other than the electrolyte/cathode interface when operational temperatures begin to exceed 900˚C [**18**]*. This analysis was performed with the use of EPMA and SEM analysis.* ***Re-printed with kind permission.***

This section of the review has heavily concentrated on commonly discussed operating parameters such as current, humidity and temperature but this is not to suggest that these are the only factors to be considered. As an example of this, Schuler et al. [**138**] have considered the effects that higher than expected SO_2 contents may have on the extent of chromium poisoning. In addition to this, Jiang et al. [**126**] have explored the effects that airflow can have upon the poisoning effects. Such factors could prove just as relevant as the previously discussed parameters.

2.2.2 Optimisation of LSM cathodes

It has been suggested by Aphale et al. [139] that there are four possible approaches to reducing the extent of Cr poisoning; (a) altering the chemistry of the interconnect alloys, (b) the use of surface coatings, (c) the use of Cr-getters and (d) the use of Cr-resistant cathode materials. Indeed, the performance of the LSM cathodes in the presence of chromium containing interconnects would

suggest that at least one of these solutions is necessary to ensure the required SOFC cell lifetime can be achieved.

It has been shown that the chemical composition of the LSM phase can have an effect on chromium poisoning. LSM cathodes with A-site deficiencies are commonly utilised within the literature and many of the aforementioned studies have employed such materials. Work by Jiang et al. [**140**] has shown that A-site sub-stoichiometry can improve the stability, adherence and shelf-life of the LSM phase. Considering the relationship between A-site stoichiometry and chromium poisoning, meanwhile, Fu et al. [**141**] argued that a 5% A-site deficient LSM material ($La_{0.75}Sr_{0.2}MnO_{3-\delta}$) could also offer an improvement on a comparable A-site stoichiometric sample of $La_{0.8}Sr_{0.2}MnO_{3-\delta}$, in terms of resistance to chromium poisoning. Somewhat contrary to this, Jin and Lu [**142**] determined that A-site deficiency actually led to greater amounts of chromium deposition. The authors reported that this was due to the relative excess of Mn in the material, which promoted the formation of chromium species. Interestingly Lu et al. [**143**] found that, whilst A-site deficient LSM cathodes were indeed more susceptible to the deposition of chromium, this behaviour did not actually lead to poorer overall performance. The authors argue that this is a result of the manner in which Sr segregates out of LSM during the formation of chromium species, reducing the conductivity of the perovskite and hence the performance of the cathode. In addition to this, Mitterdorfer and Gauckler [**144**] have previously reported that Mn excess (and, hence, A-site deficiency) can suppress the formation of a $La_2Zr_2O_7$ phase, which is a common cause of degradation that leads to an increase in the Ohmic resistance. As a result, whilst more chromium deposition may result, those materials with A-site deficiency appear to offer better overall performance.

The use of composite LSM/YSZ cathodes was briefly mentioned earlier. Cathodes of such materials demonstrate an improvement in general performance due to an apparent extension of the TPB sites [**145**,**146**] and have also been shown to enhance resistance to the effects of chromium poisoning [**129**,**147**]. Zhen and Jiang [**148**] compared the performance of pure LSM cathodes with composite cathodes of LSM/YSZ (varying YSZ wt%) and GDC-impregnated-LSM. Within the study, it is noted that such composites have the potential to greatly improve resilience to chromium poisoning, with the GDC-impregnated cathodes showing particularly exciting resistance to degradation. The authors also suggest that the use of the ionic phases promotes the ORR in addition to offering a favourable extension of the TPBs.

Studies upon the geometry of cathodes have been conducted by Konysheva et al. [**129**] who investigated the variation of thickness in the so-called “Functional Layer” (FL). In this case, the

cathode is comprised of two sections; the FL of the LSM/YSZ composite and a second layer of LSM (as a current collection layer). It has been observed that increasing the thickness of the FL can reduce degradation due to chromium poisoning. The use of such functional layers will also result in a change in the manner in which chromium is deposited across the cathode structure (Figure 4). Similar observations have been noted by Schuler et al. [**149**] but, whilst Konysheva et al.[**129**] suggest that the LSM/YSZ layer could be acting as a trap for the chromium, Schuler et al. argue that it is more likely due to the additional cathode thickness operating as a diffusion barrier.

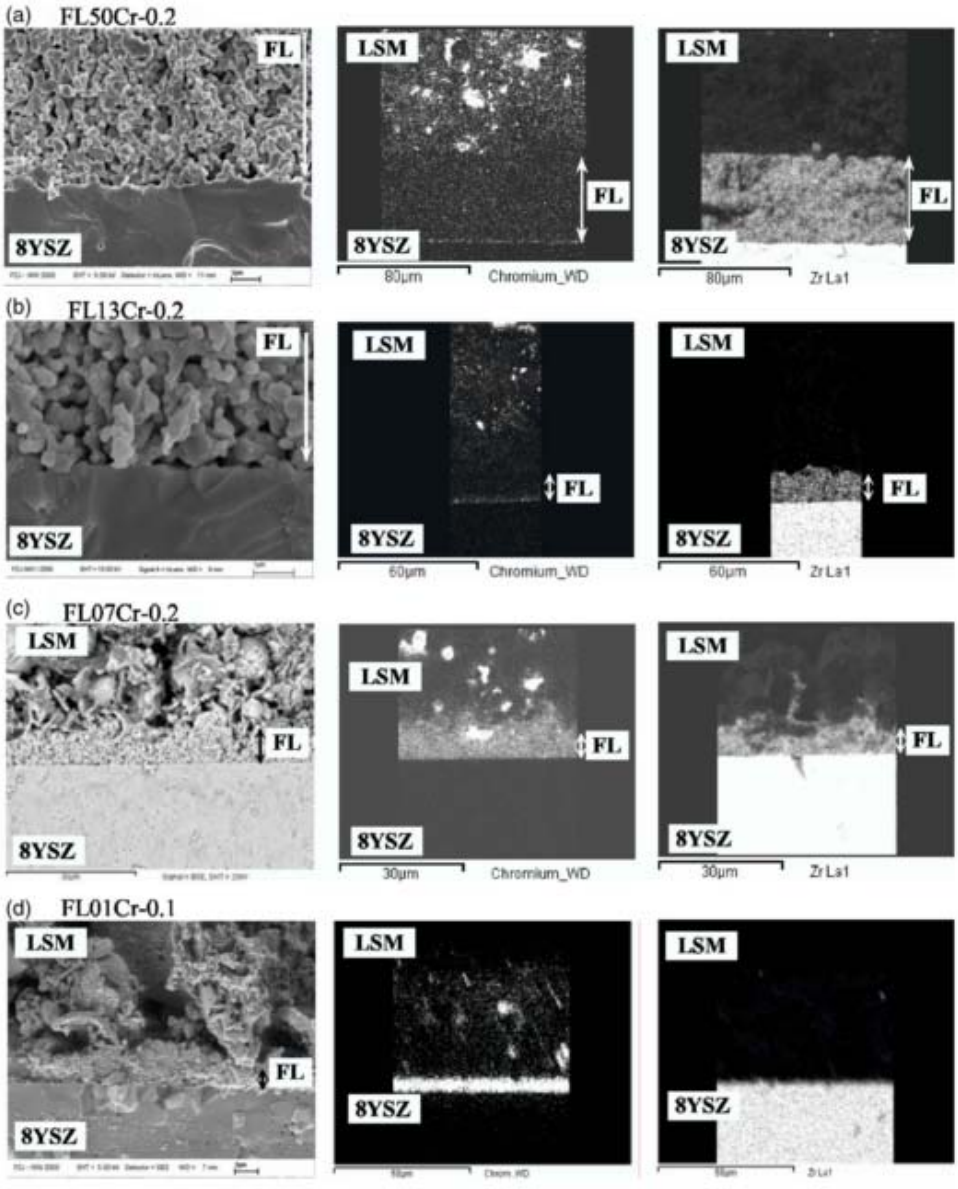

Figure 4 - A series of SEM and elemental mapping images exploring the effects of a chromium source on LSM/YSZ cathodes with (a) a 50-micron functional layer (FL) thickness, (b) a 13-micron thickness, (c) a 7-micron thickness and (d) a 1-micron thickness. The chromium mapping images indicate that, as the width of the functional layer increases, the deposition of chromium moves away from the electrolyte/electrode interface and into the LSM layer [**129**]. *Re-printed with kind permission.*

The effects that different electrolyte materials can have upon the poisoning process has also been considered **[112**]. LSM cathodes were screen-printed onto four different electrolyte materials (YSZ, ScSZ, SDC and LSGM) and exposed to chromium vapours under galvanostatic conditions. The authors noted a much-reduced degradation rate when the LSM cathodes were deposited onto SDC and LSGM, compared to that seen when electrolytes of YSZ or ScSZ were used. However, based on the analysis provided in that same paper it is not entirely clear as to whether or not the degradation rate is indeed a result of chromium poisoning or whether it is driven by some other means (e.g. reactions between electrolyte and electrode materials).

3 LSCF/LSC/LSF cathodes

3.1 LSCF

LSCF cathodes ($La_{1-x}Sr_xCo_{1-y}Fe_yO_{3-\delta}$) have shown great promise within SOFC operating conditions [**150**] and a significant research effort has gone into understanding their performance. Key research players, Forschungszentrum Jülich, have demonstrated an LSCF-cathode containing fuel cell stack with an operation time of 100,000h [**12**,**151**]. At 70,000h a degradation rate of 0.6% per 1000h for this stack was noted [**151**] and a further improvement observed (0.3% per 1000h with over 30,000h of operation) when an improved interconnect coating was utilised. Such results offer encouragement especially when considering the degradation target, as set by SECA, the Solid State Energy Conversion Alliance, at 0.2 % per 1000 hours [**10**]. Despite this promising performance, cathodes of LSCF are known, like their LSM counterparts, to suffer from the poisoning effects brought about by chromium-containing interconnects [**152**]. In this section, the resistance to chromium poisoning of LSCF cathodes shall be explored further. Within the LSCF family of materials, the $La_{0.6}Sr_{0.4}Co_{0.2}Fe_{0.8}O_{3-\delta}$ composition represents the most studied material. The great majority of the studies which will be discussed here consider this composition when studying exposure to chromium.

3.1.1 Comparison with LSM

LSCF cathodes perform somewhat differently to their LSM counterparts. The mixed ionic and electronic conduction (MIEC) properties of the material increases the effective triple phase boundary, ensuring that the electrochemical activity of the cathode is not confined simply to the TPB located around the cathode-electrolyte interface.

Comparative experimental studies indicate that cells that utilise LSCF as a cathode material have an improved resilience to chromium poisoning, compared to those cells with LSM-based cathodes [**25**,**112**,**113**,**127**,**153**]. This statement, however, may be something of an over-simplification since LSM cathodes may be optimised to rival LSCF in certain scenarios. Work by Zhen and Jiang [148] indicates that, whilst LSCF outperformed both LSM and composite LSM-YSZ cathodes, LSM cathodes which were impregnated with GDC could offer competitive performance and resilience to the effects of chromium. Despite such considerations, there appears to be a general agreement within the literature that LSCF shows improved resistance to the degrading effects of chromium poisoning. In addition to this, there have been efforts to further improve the performance of these cathodes.

De Haart et al. [**113**] noted that the degradation of cells with LSCF cathodes is manifested (Figure 5) in a different manner to that which was observed for those cells with LSM cathodes (Figure 1).

During a 10,000h experiment, the authors noted the absence of the initial and sudden drop in voltage that was present for the LSM test cases. In addition to this, the third stage of the degradation profile seen in Figure 1 (characterised by an acceleration in the rate of voltage reduction) can be avoided when utilising the LSCF cathodes, albeit at the lower operating temperature of 700˚C. These findings highlight the importance of test duration when considering cell degradation. Many of the studies discussed in this review provide a direct comparison between cathode materials by studying the effects of chromium on the increase in overpotential. The performance of LSM cathodes is utilised as a typical "bench mark". A number of studies also consider such performance over a time period of less than 100 hours. Cathode materials are commonly referred to as offering "promising" behaviour when out-performing LSM cathodes during this period. However, what is often not considered is the potentially misleading increased degradation rate of LSM cathodes during the initial stages of operation. In isolation, a consideration of voltage drop during this initial time period may lead to misleading results and longer testing periods should be considered for a full analysis of a cathode's resilience to chromium poisoning,

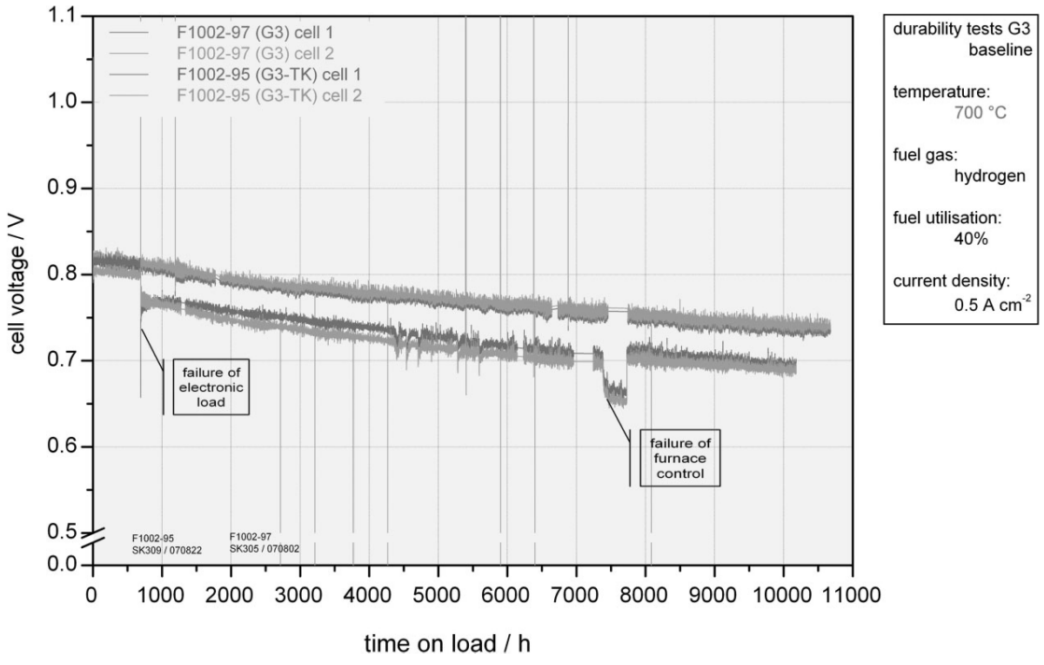

Figure 5 - LSCF-based stack testing over 10,000h at 700˚C under galvanostatic conditions [**113**]. ***Re-printed with kind permission.***

3.1.2 Cr-Deposition Theories for LSCF

It has been reported by a number of authors that Sr has a tendency to segregate to the surface, often in the form of SrO [**17**,**154–158**]. In isolation, the segregation and enrichment of Sr has been shown to have a detrimental effect upon cell performance [**154**,**155**] but, additionally, the segregated SrO also acts as a chromium-getter which can deteriorate performance further.

Moreover, SrO has been shown to be reactive with the often-utilised electrolyte material YSZ, forming an insulating $SrZrO_3$ phase [**17**,**159**]. A protective interlayer has commonly been employed in order to prevent this from occurring [**150**,**160**]. Work by Zhao and other authors [**157**,**158**,**161**] has demonstrated that Co also has the tendency to segregate out of the bulk material in the form of CoO_x but the authors also concluded, via the use of FIB-EDS and Raman spectroscopy, that such segregation does not affect Cr-deposition. Interestingly, however, the authors did observe the potential for the reaction between the segregated Co and the Cr_2O_3 (forming Co-Cr spinels) when in the absence of the segregated Sr. The Cr, therefore, appears to prefer a reaction with the Sr species.

Yin et al. [**17**] have suggested that there are *four* possible reactions which may result from the reaction between the segregated Sr and the gaseous CrO_3 species:

$$SrO(s) + CrO_3(g) \rightarrow SrCrO_4(s) \quad (11)$$

$$SrO(s) + CrO_3(g) \rightarrow SrCrO_3(s) + \frac{1}{2}O_2(g) \quad (12)$$

$$SrO(s) + \frac{2}{3}CrO_3(g) \rightarrow \frac{1}{3}Sr_3Cr_2O_8(s) + \frac{1}{6}O_2(g) \quad (13)$$

$$SrO(s) + \frac{1}{2}CrO_3(g) \rightarrow \frac{1}{5}Sr_2CrO_4(s) + \frac{1}{4}O_2(g) \quad (14)$$

In that study, it was indicated that the Sr-Cr-O phase that forms is dependent upon oxygen partial pressure, chromium-gas partial pressure, the activity of SrO, and the temperature. The formation of $SrCrO_4$ is most commonly reported in the experimental literature and is generally noted to nucleate upon the surface of the LSCF cathodes [**24**,**127**,**152**,**162**]. Chen et al. [**163**] utilised 3-D imaging techniques to demonstrate (a) the preference of the chromium deposited on the surface of the LSCF cathodes and (b) the resulting decrease in porosity at the surface of the cathode (Figure 6). The authors suggested that the resulting effects on the diffusion of oxygen through the cathode drives the voltage drop.

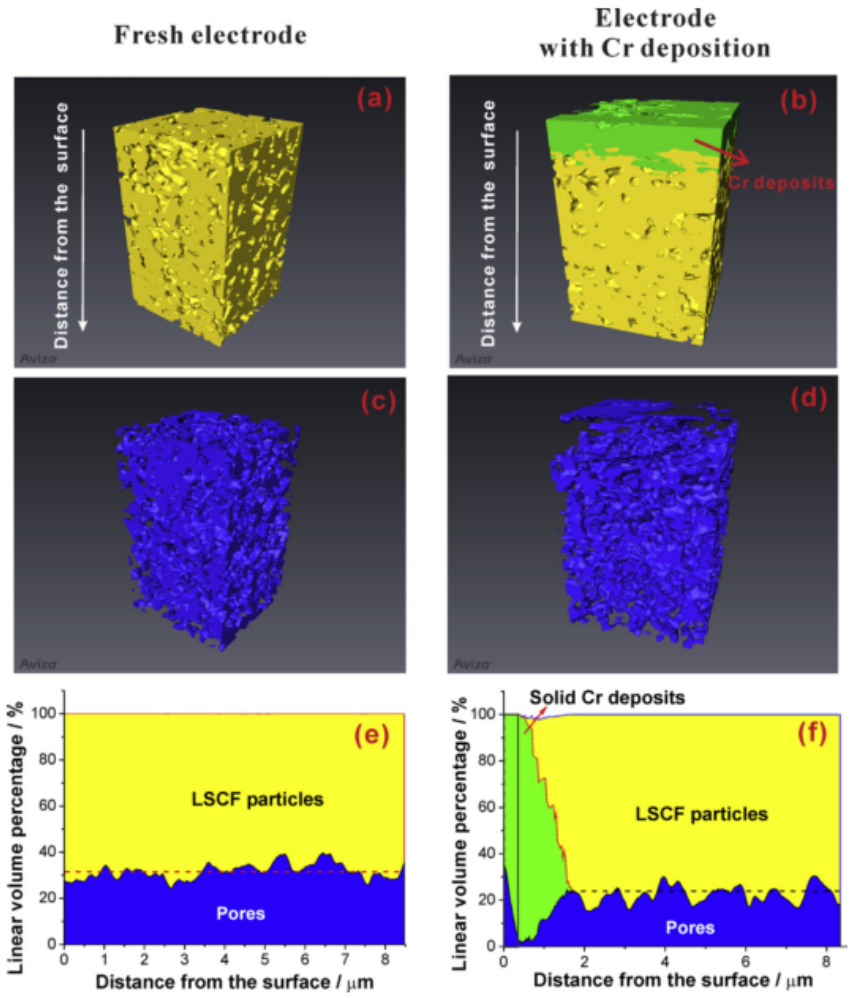

Figure 6 – The deposition of chromium at the surface of the LSCF electrode is shown by Chen et al. **[163]** *via Transmission X-ray Microscopy (TXM).* ***Re-printed with kind permission.***

In addition to the formation of solid Cr species at the cathode surface, there are several studies that have also reported the formation of chromium towards the cathode-electrolyte interface region [**153**,**164**] as well as through the bulk of the cathode [**165**,**166**]. In general terms, however, there is a definite contrast when comparing the studies on LSCF to those on LSM (discussed in section 2), where chromium species primarily nucleate at the electrode-electrolyte interface. It is also notable that Sr-Cr-O-containing deposits are observed to form in the case of LSCF whereas the Cr-Mn spinel phases are reported form LSM, despite the presence of Sr in both cathodes. The literature indicates that this suggests a preferential deposition on the Mn (i.e. over the Sr).

There are several suggestions as to how the formation of solid Sr-Cr-O species may result in the observed reduction in voltage over time. It is commonly suggested that such species have the ability to block the active sites and, hence, reduce the electrochemical activity as well as the electrical conductivity [**165–167**]. Work reported by Zhao et al. [**158**] concluded that the segregation of Sr and

subsequent deposition of Cr reduces the oxygen surface exchange coefficient and the authors argued that it is this phenomenon that causes the poisoning effect. Elsewhere, it has been hypothesised that a loss of porosity at the surface of the cathodes could drive a corresponding decrease in oxygen diffusion [**152**,**163**,**165**,**166**]. Such an effect would have obvious implications for the rate at which the ORR proceeds. The impact of the Sr segregation on the bulk perovskite material has also been cited as a source of degradation. Oh et al. [**167**] observed a depletion of Sr in the bulk LSCF material, resulting from the segregation of Sr and the precipitation of $SrCrO_4$. This effect, the authors concluded, results in a decrease in the number of available oxygen vacancies (or the electron hole concentration) and a reduction in the oxygen reaction kinetics.

Jiang et al. [**152**] suggest that the formation of the $SrCrO_4$ results from the reaction between the segregated Sr and the chromium gaseous species, a theory that is also supported elsewhere [**162**]. Wang et al. [**162**] used Raman spectroscopy to show that the formation of $SrCrO_4$ can readily occur at temperatures between 700 and 900˚C. In this study, it was shown that, whilst the formation of solid-chromium species did not require current flow, it was aggravated at higher temperatures. Wei et al. [**168**] also observed the deposition of $SrCrO_4$ in the absence of current during their OCV study on LSCF cathodes in the presence of a chromium source.

It is interesting to further consider the aforementioned spatial distribution of chromium-containing phases in LSCF cathode materials. Several authors have observed the deposition of chromium in areas other than the surface of the cathode. On the one hand, Jiang et al. [**127**] concluded that Cr-phases observed at the cathode-electrolyte interface in their study were due to the presence of impurities (which acted as nucleation agents). On the other, it has been suggested that this is evidence of an electrochemical deposition route [29] and it could even be suggested that the notable formation of Cr-phases at the surface of LSCF could be accommodated by the MIEC properties of the cathode material. Whilst Konysheva et al.[**166**] suggest that increased polarisation results in increased deposition at the electrolyte interface (and reduced deposition on the electrode surface), chromium deposits in this region have also been reported under OCV conditions [**127**,**165**]. This latter observation would appear to question the validity of conclusions on electrochemical deposition routes. Again, these observations may suggest multiple deposition routes are possible (i.e. electrochemical *and* chemical routes possible). Alternatively, the role of partial pressures on the chemical reaction may offer an explanation. Beez et al. [**19**] further considered the role of oxygen pressure on the reaction between the LSCF cathode material and the Cr-containing vapours. It was indicated that a reduction in oxygen pressure (towards the cathode-electrolyte interface) influences the equilibrium of the reaction and deposits can be formed in these areas. The authors also indicate that chromium phases are possibly formed throughout the cathode but are likely to be below the

detection limits of SEM/EDX (which is typically employed for analysis of chromium in cathodes). Nevertheless, it is difficult to categorically rule out the possibility of an electrochemical degradation process playing some role in the poisoning process.

3.1.3 Further work

3.1.3.1 Effect of Operating Conditions

Within the literature, there are a limited number of attempts to further understand the effects of current upon the poisoning process of LSCF cathodes. In terms of Area Specific Polarisation resistance (ASR_p), Bentzen et al. [169] have published results that would indicate that increased polarisation rates can actually reduce the observed degradative effects (although the inverse relationship is seen when considering the electrode overpotential). Whilst the authors of that study suggest this surprising result could be brought about by corresponding increases in temperature, similar observations have been reported elsewhere. Konysheva [**166**] reported that open circuit conditions offered the greatest degradation rate when the cathodes were exposed to chromium. There are also some observations on the *amount* of chromium that is observed under different current conditions. Work by Jiang et al. [127**]** indicates that chromium deposition may become more pronounced in the absence of polarisation rather than in its presence. In their study, however, only one polarisation condition ($200mAcm^{-2}$) was compared against the open circuit condition. Both Park et al. [**170**] and Konysheva [**166**] noted a non-linear relationship between chromium deposition and polarisation current density with deposition seemingly peaking around the $200mAcm^{-2}$ condition in both instances. A significant deposition of chromium was seen to be possible even under open circuit conditions as observed by Lau et al. [**171**].

The effect of temperature on the chromium poisoning of LSCF is generally agreed upon within the literature. Comparing performance at atmospheric temperatures of 700, 800 and 900˚C, Wang et al. [**162**] found increased deposition of solid chromium species with increasing temperature. This is an observation corroborated in articles by other authors [**65**,**152**,**154**]. The work by Wang et al. [**162**] reports both an increase in the number and size of particles. The authors have attributed this to, not only, the increased volatilisation rates but, additionally, the quantity of segregated Sr at the higher temperatures. The increase in segregation with temperature is also noted in work by Oh et al. [**156**]. Humidity has been seen to have a similar impact on chromium poisoning of LSCF cathodes. Zhao and authors [**158**,**161**] have commented on the acceleration of Sr segragation at higher humidities and, as a result, the increased formation of $SrCrO_4$ under such conditions. Increases in degradation rate at higher humidities are also documented elsewhere [**172**,**173**].

3.1.3.2 Optimisation of LSCF cathodes

In recent times there have been a number of efforts at optimising the chromium resistance of LSCF cathodes. Some research points to the suppression of Sr segregation as the key for achieving this [**174**,**175**]. Ding et al. [**174**] propose that segregation is driven by strain relaxation and surface charge minimisation and suggest the need to reduce both of these factors. It is indicated that this can be achieved via the use of different dopants or the use of an interface lattice mismatch (i.e. different electrolytes) in order to reduce the segregation effect. Work by Yu et al. [**175**] supports this conclusion, also observing the effects of altering the fraction of Sr doping.

In an attempt to improve the performance of LSCF cathode materials, a number of parameters relating to their chemistry and synthesis have been considered. As examples of this, factors such as sintering temperature [**165**] and A-site stochiometry [**176**] have been demonstrated to have an effect on the extent of chromium poisoning. Xiong et al. [**165**] showed that increased sintering temperatures resulted in reduced degradation rates for LSCF-GDC composite cathodes. This, the authors concluded, is driven by differences in microstructure ; greater sintering temperatures are seen to result in larger cathode particle sizes and, as a result, less surface area (per unit volume) for reaction. Li et al. [**176**] observed differing chromium poisoning effects for $(La_{0.6}Sr_{0.4})_x(Co_{0.2}Fe_{0.8})O_{3-\delta}$ when the A-site stoichiometry was altered. In that study, it was proposed that, in the case of the A-site deficient material (i.e, x=0.95), Cr took up some of the A-sites (i.e. less preferential deposition upon segregated Sr) and this actually helped to reduce the rate of degradation.

One popular method of improving chromium resistance is via the impregnation of cathode materials with secondary phases to form composite cathodes. GDC-impregnated [**177**] LSCF cathodes have been shown to demonstrate improved performance in resisting chromium-related degradation. Shen and Lu [**178**] found that, whilst SDC-impregnated cathodes had reduced resistance to the formation of $SrCrO_4$, the overall stability could be improved by the addition of SDC. This serves to remind the reader that, whilst chromium poisoning represents a significant degradation effect, it is not the only cause of cell deterioration and it is important to engineer new materials that offer an improvement in all areas. In work by Chen et al. [**179**], LSCF cathodes were infiltrated with BaO and an increase in chromium resistance was reported. It was found that, instead of $SrCrO_4$, the formation of $BaCrO_4$ was favoured. This phase is said to have better electrical conductivity than the $SrCrO_4$ phase and thus reduces the rise in ohmic resistance as the chromium containing phase is formed. In addition, this also enables the integrity of the LSCF perovskite to be maintained. The authors indicate that this could only offer a complimentary improvement (e.g. to an interconnect coating) since, eventually, the BaO would be exhausted and the Cr will begin to react upon the segregated Sr.

In a recent paper, Zhao et al. [**252**] decorated LSCF cathodes with nickel and iron phases in an attempt to improve the chromium poisoning resistance of the material. The authors observed a notable improvement in the manner in which ohmic and polarisation resistance developed over operating time. This was ascribed to the way in which these phases helped to reduce the Sr and Co segregation, with $Sr(Co,Ni)O_3$ forming on the surface of the cathode and offering some level of protection against the incorporation of chromium.

3.2 LSC

The removal of iron from the LSCF composition offers another material which has been studied for use as an SOFC cathode. LSC ($La_{1-x}Sr_xCoO_{3-\delta}$) cathodes have excellent electrical and ionic conductivity but suffer from a high thermal expansion coefficient [**67**]. The addition of iron into LSC, to form the familiar LSCF, helps to reduce the thermal expansion coefficient [**72**]. LSC is reactive towards the typical YSZ electrolyte and a protective barrier layer is required [**160**] to prevent the formation of an insulating $La_2Zr_2O_7$ phase. Despite these issues, there remains a body of work observing the performance of LSC in a chromium-containing atmosphere. The $La_{0.6}Sr_{0.4}CoO_{3-\delta}$ composition has had the most research attention due to offering the most favourable performance [**67**].

LSC cathodes suffer from similar issues to those previously reported for LSCF-based cathodes. The segregation of Sr [**180**,**181**] as well as the already-mentioned reaction between cathode and electrolyte, have been described above. As was also seen in the case of LSCF, the formation of chromium containing phases are seen upon the surface of LSC electrodes after exposure to a chromium-containing atmosphere [**182**]. This behaviour has also been noted by other authors [**172**,**183**], with Schrödl et al. [**183**] observing the formation of $SrCrO_4$, $La_xCr_yO_Z$, $CoCr_{2-x}Co_xO_4$ and Co_3O_4.

Work by Bucher et al. [**172**] focused on comparing the relative performance of an LSCF and an LSC cathode in a chromium-containing atmosphere via the measurement of the oxygen exchange coefficient (k_{chem}). The analysis indicated that LSC may offer better resilience to chromium poisoning in comparison to that of LSCF, though the poisoning effect is still observed, particularly in humid atmospheres. In another study, Yang et al. [**184**] approached the effects of chromium deposition in a slightly different manner to that described previously. The authors purposefully coated LSC samples with very thin (~nm) layers of chromium to understand the effects that such deposition would have upon the surface exchange coefficient. Even with a chromium coating as thin as 10nm there was a profound effect upon k_{chem}. The performance fell further with an increasing chromium-layer thickness.

Schrödl et al.[**185**] considered the effect of humidity upon the poisoning of LSC. It was seen that both the surface exchange coefficient and the diffusion coefficient of LSC within dry atmospheres were stable. This reiterates the importance of controlling operational parameters in reducing the degradation effect brought about by chromium. In a recent study by Kageyama et al.[**186**], the authors utilised a "model electrode" in order to confirm the accelerating effects of polarisation on chromium poisoning. In this case, a dense electrode was prepared and defined areas were removed via ion beam milling in order to control the quantities of triple phase boundaries. Significant chromium deposition was observed on the surface of the electrode which was close to the triple phase boundary with comparatively less seen in areas further away.

Ou and Cheng [**253**] studied the fundamental effects of the addition of MnO_2 into a $La_{0.7}Sr_{0.3}CoO_3$ material. The authors observed that the MnO_2 reduced the rate at which $SrCrO_4$ was formed after heating at 800˚C for 1000 h in the presence of a chromium-containing alloy. There was a marked preference for the formation of the Cr-Mn spinel phase. When considering the effects on conductivity, it was apparent that this led to a much reduced degradation which the authors concluded was a result of the improved stability of Sr in the material. The use of such an approach (i.e. where "sacrificial" materials are used in order to form less destructive phases) has recently been more commonly reported in the literature.

3.3 LSF

LSF ($La_{1-x}Sr_xFeO_{3-\delta}$), like LSC, is related to the LSCF composition (this time via the removal of Co from the material) and is a predecessor to LSCF. This material has been shown to offer reasonable electrochemical reactivity and favourable thermal expansion properties [**75**] for use as an SOFC cathode material. There is evidence, however, to indicate that such cathodes ($La_{0.8}Sr_{0.2}FeO_3$ being popular) fail to offer an appropriate resistance to chromium poisoning. Simner et al.[**25**] noted greater chromium deposition within an LSF cathode than that for cathodes of either LSM or LSCF. The authors found that the significant performance deterioration of their LSF cathodes was coupled with the formation of a $SrFe_{12}O_{19}$ impurity phase.

Interestingly, the deposition of chromium has been reported to occur throughout the thickness of the cathode rather than demonstrating preferential deposition at either the interface or cathode surface as was seen for LSM and LSCF, respectively [**25**,**26**,**187**,**188**]. Combined with the extent of the poisoning effect, a high level of reactivity between LSF and the hexavalent chromium species is apparent.

Whilst literature indicates that LSF has high reactivity with chromium vapours under operation, when compared with LSM [**26**,**188**], this does not necessarily mean that LSF is less tolerant to

chromium poisoning. Horita et al. [**188**] found that, although larger quantities of chromium deposits are expected in LSF cathodes, the electrochemical performance does not deteriorate as much as seen for LSM within which lower levels of chromium are detected. The polarisation resistance of the LSM cathodes was seen to increase by up to 15 times its initial value in a 300h time period, compared to up to 2.3 times for LSF. It is highly likely that this is a result of the increased number of reaction sites brought about by the mixed conduction properties of LSF. This is a conclusion that is supported in analysis by Yokokawa et al.[**121**]. The authors noted that, whilst LSF was less stable than LSM in the presence of chromium containing vapours, the wider area for electrochemical activity likely results in a lower sensitivity to chromium deposition. Generally speaking, LSCF appears to be preferred to LSF and it has been shown that the former offers better resilience to chromium poisoning [**25**].

4 Other materials

Whilst it has become commonplace to utilise coated steel interconnects as a method of reducing the rate of chromium migration (and hence poisoning) [**189**], there is evidence to indicate that this may not offer a complete solution to the issues discussed so far. Firstly, chromium containing vapours have been observed to emanate from BoP components within the fuel cell system [**190**] and, as such, coatings of the interconnects alone may not necessarily eradicate the presence of mobile chromium. The application of coatings on interconnects also offers further complication and additional expense in manufacturing SOFC stacks. Further, such coatings are subject to their own degradation mechanisms and, thus, such a solution may become less effective with time. With these factors considered, the pursuit and development of new chromium-tolerant cathode materials could offer significant advantages. By further analysing research efforts, it is possible to consider the various strategies that have been employed by the research community in order to offset the poisoning effects.

It is clear that LSM and LSCF-based composites have received the greatest level of research attention but the effects of chromium upon many other cathode materials have also been investigated. It is often difficult to provide direct comparisons between these materials as the extent to which they have been analysed in relation to one another is often limited and the experimental techniques used frequently vary in terms of operational parameters as well as in terms of experimental set-up. Typically, the performance of alternative cathode materials are contrasted with that of LSM or LSCF. In a number of the cases described, promising performance has been reported and yet there remains limited literature to support these claims and, often, the materials are not studied for extended periods (commonly <100 hours).

4.1 Platinum

Platinum electrodes are more typically associated with the lower temperature PEMFC but the material also offers an interesting case study for chromium poisoning under SOFC-type conditions. A review of the work conducted is revealing.

Jiang et al. [**127**] compared LSM, LSCF and platinum electrodes in a chromium containing atmosphere. By observing the overpotential under galvanostatic conditions, there was seen to be an apparently large poisoning effect on the Pt-electrode. Remarkably, however, the authors did not observe significant deposition of chromium, suggesting that the loss of performance was unrelated to chromium poisoning. Whilst it is not clear why the degradation was more significant under a chromium-containing atmosphere, the findings in the study appear to offer further proof that

deposition is not brought about by electrochemical reduction of the gaseous species and is, moreover, related to material selection.

In two papers by Wang and Fergus [**191,192**] platinum electrodes were utilised to study poisoning effects when combined with doped and undoped YSZ electrolytes. Though there was seen to be very little evidence of chromium poisoning on the platinum electrodes themselves, it was seen that doping of the YSZ with Mn, Fe and Co promoted the poisoning effect, with little chromium noted upon the undoped YSZ. This is an interesting finding and, again, points towards a chemical (rather than electrochemical) deposition mechanism. To complicate matters, however, the experimental work was conducted under both polarisation and non-polarisation conditions. Significant deposition of chromium was observed under polarisation conditions alone, indicating that the current flow has some accelerating effect in this process.

4.2 Other La-based Perovskites

Besides the La-based perovskites discussed previously, there has also been a significant drive to research other perovskite materials, most of which concentrated towards materials with La at the A-site. Many of these materials have been explored, not only for use as cathodes, but also as interconnect coating materials.

4.2.1 LNF

Jiang et al. [**193**] hypothesised that, based upon their theory of LSM deposition mechanisms (see 2.1.2), the next generation of chromium-resistant materials can be brought about via the production of cathode materials which exclude nucleation agents like Mn and Sr. Experimental work by Komatsu et al. [**194**] would appear to go some way in justifying this statement. The authors have demonstrated the much-improved chromium-resistance of LNF ($LaNi_xFe_{1-x}O_{3-\delta}$) in comparison with LSM. This range of perovskites has received a notable amount of study, with the most common composition studied being $LaNi_{0.6}Fe_{0.4}O_{3-\delta}$.

Cathodes based upon the perovskite LNF have been reported to offer competitive performance at SOFC operating temperatures [**78**,**195**]. The performance of this subset of perovskites has been shown to be particularly promising when combined with ionic conductors such as GDC to form composite cathodes [**196**]. A number of studies suggested that such cathodes offer an advantage in avoiding chromium poisoning when compared with LSM and LSCF [**153**,**193**,**194**,**197**,**198**]. Work by Zhen et al. [**198**] compares the commonly utilised LSM and LSCF cathodes with the less widely studied LNF and LBCF during 20 hours of chromium exposure (Figure 7). It is seen that LNF shows highly promising resilience to the chromium poisoning effect. Elsewhere, Komatsu et al. [**199**] reported a much improved degradation rate compared to LSM over a 1000 hour test. In the case of

LNF, a 200mV drop was observed after 1000 hours at a current load of 2.3Acm^{-2} whereas the same voltage drop was seen for LSM within 350 hours at a current density of just 0.345Acm^{-2}.

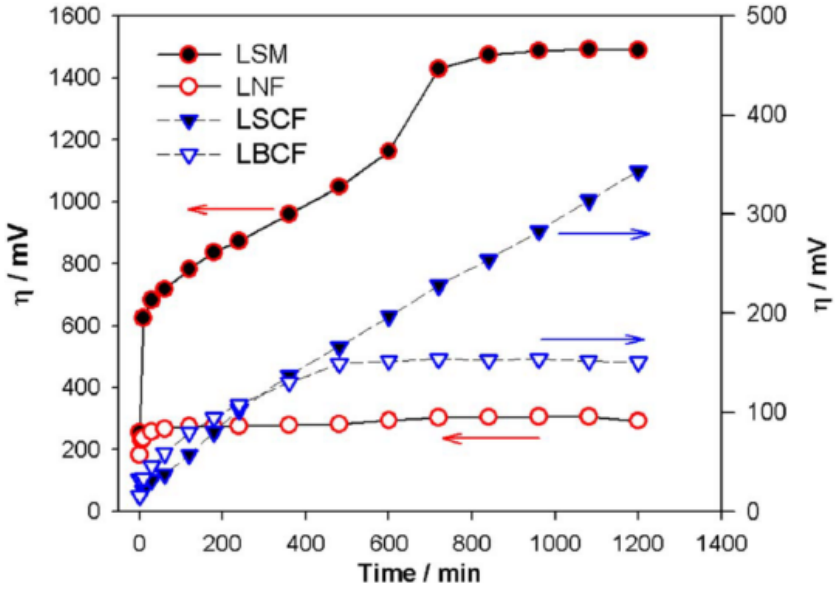

Figure 7 – Overpotential vs time for four different cathode materials in the presence of a chromium interconnect (galvanostatic condition of 200 mAcm^{-2} and operational temperature of 900˚C) [**198**]. *Re-printed with kind permission.*

Despite the aforementioned studies, suggesting an encouraging resilience to chromium poisoning, a thermodynamic study conducted by Yokokawa et al. [**121**] indicated that there remains potential for reaction between LNF cathodes and chromium vapours and reactions between these materials have been experimentally observed. Komatsu et al. [**153**] heated a mixture of Cr_2O_3 and LNF powders at 800˚C for 1000 hours and utilised XRD analysis to detect the formation of $NiCr_2O_4$. Though the formation of this spinel phase was confirmed, the authors also commented that the consumption of the chromium is significantly slower than that seen for both LSCF and LSM; indicating an improved chemical stability, a conclusion also supported elsewhere [**171**]. During a similar reactivity study at the lower SOFC temperature of 600˚C, Stodolny et al. [**200**] initially reported that no extra phases or reactions could be observed after a 1000 hour test. Subsequent work by the same authors, however, has shown that chromium-related degradation is still observed at this lower temperature, when LNF cathodes are employed **[201]**. The lower temperatures do, however, bring about a reduction in the degradation rate.

At 800˚C and under a current load of 400mAcm^{-2}, Stodolny et al. [**202**] found that, despite an initial stable performance for around 200 hours, their LNF cathodes exhibited a dramatic increase in ohmic and polarisation resistance after a further 800h. Work by these authors [**200–202**] has sought to determine the exact mode of degradation that drives the loss of performance. It was concluded that chromium is incorporated into the LNF perovskite structure via chemical reaction, with a resulting

segregation and precipitation of nickel out of the bulk material. Thermodynamic work by Yokokawa et al. subsequently agreed that this reaction is thermodynamically feasible [**121**]. In one particular study [**202**], the deposition of chromium under galvanostatic operation is noted to be apparent throughout the cathode. There is, however, an apparent preference for deposition upon the cathode surface, at the cathode-barrier layer interface and, surprisingly, within the GDC barrier layer itself. This latter effect is thought to offer a deterioration in the ionic conduction properties of the barrier layer. Interestingly, the authors of that study concluded that the reduction in nucleation agents (such as Mn and Sr) enables the chromium vapours to reach the interlayer and have this poisoning effect. In other words, the removal of these nucleating agents has shifted a large quantity of the deposited chromium to an alternate component within the cell.

As has been seen for other materials, chromium poisoning resistance is dependent on a number of compositional and microstructural features. As an example of this, Stodolny et al. [**203**] observed that electrodes with high porosities, small grain sizes and larger particle surface areas were more susceptible to chromium poisoning with respect to both increases in resistance and deposition of chromium. Impregnation of LNF with GDC has demonstrated improved electrochemical performance, whilst also offering the opportunity to still further improve resistance to chromium poisoning [**204–206**]. This is believed to result from the increase of the TPB area and, hence, the increase in the number of reaction sites. By varying the content of ionic conductor CGO, Chen et al. [**207**] found that the general performance was optimised at 30wt%CGO, whilst Huang et al. [**196**] reported optimisation of their LNF-GDC cathodes at 21wt%GDC .

Overall the literature indicates that, whilst LNF still suffers from the issue of chromium poisoning, the material may offer an improvement in this area relative to other systems, particularly when used to form a composite with an ionic conducting phase such as GDC.

4.2.2 LBCF

Like LNF, the MIEC cathode material LBCF ($La_{1-x}Ba_xCo_{1-y}Fe_yO_{3-\delta}$) has also been reported to offer an improvement in resilience to chromium poisoning when compared to LSCF and LSM [**198**,**208**,**209**]. In the papers referenced here, $La_{0.6}Ba_{0.4}Co_{0.2}Fe_{0.8}O_3$ has proven a common composition but others have also been studied including $La_{0.5}Ba_{0.5}Co_{0.9}Fe_{0.1}O_3$ which is referenced in Table 1. The performance of LSCF, LSM, LNF and LBCF cathodes over a 20 hour period is compared in Figure 7 [**198**]. It can be noticed that, after an initial increase in overpotential, the performance of LBCF becomes much more stable, albeit over the relatively small testing period which was studied. Although the formation of $BaCrO_4$ was observed to occur upon the surface of the LBCF cathodes, Chen et al. [**208**] reported much lower quantities of this phase than when considering the formation

of $SrCrO_4$ upon LSCF. The lower degradation rate (relative to LSCF) indicates that Ba has a lower affinity to the formation of chromium species when compared with Sr, which was discussed previously to offer a site for the nucleation of such phases. Alternatively, this may be due to the fact that the resulting $BaCrO_4$ is less destructive to the performance of the electrode.

Despite the studies which indicate promising performance with respect to resisting chromium poisoning, it is also important to consider the other properties of interest. The thermal expansion coefficient of the LBCF family (between 20-30 x 10^{-6} $^{\circ}C^{-1}$ [**81**,**210**]), suggests that it may be difficult to utilise cathodes of such a material. Setevich et al. [**210**] found a significant increase in polarisation resistance over a 200 hour period which the authors concluded to have arisen from a thermal expansion mismatch with the electrolyte. In addition, Ba-containing cathodes have been observed to suffer from poor stability in CO_2, leading to the formation of Ba-carbonates [**218**,**219**]. We are unaware of any reports that have searched for this phenomenon specifically in LBCF but the Ba-content would indicate that this is a likely degradation mechanism. The drawbacks described above are most likely the reason why there has been only limited interest in the LBCF family of perovskites.

4.2.3 Other

Some researchers have looked to synthesise new cathodes that effectively offer an "intermediate" between two of the materials that have already been discussed. As an example of this, $La_{1-y}Sr_yCo_xMn_{1-x}O_{3-\delta}$ is a perovskite material which, by varying the Co-Mn content, can explore the range of systems between LSM (i.e. x=0) and LSC (i.e. x=1). Often it is seen that the chromium resistance that is offered lies between that of the two materials at either end of this range. Materials that have been investigated in a similar manner are LSBCF (e.g. $La_{0.6}Sr_{0.4-x}Ba_xCo_{0.2}Fe_{0.8}O_{3-\delta}$ [**208**]), LSBCFN (e.g. $La_{0.24}Sr_{0.16}Ba_{0.6}Co_{0.5}Fe_{0.44}Nb_{0.06}O_{3-\delta}$ [**211**]) and LSCM (e.g. $(La_{0.8}Sr_{0.2})_{0.95}Mn_{1-x}Co_xO_{3\pm\delta}$ [**182**]). Even LSCF can be considered as an amalgamation of two other cathode materials, combining the excellent conductivity of LSC with the improved stability of LSF. By conducting such research, authors have been able to make direct comparisons between materials in terms of the extent of the poisoning effect and the mechanism of deposition for each material.

One field of cathode research which is particularly interesting is the use of Cr-doped perovskite materials within SOFC cells. This may seem a somewhat counter-intuitive concept given the poisoning effects of chromium which have been discussed thus far. Nevertheless a number of studies [**212–214**] have reported the potential of such materials. We are unaware of any studies observing the effect of chromium-poisoning on these cathodes and this may be an area of interest for those designing new cathodes with improved resilience.

4.3 Other ABO_3-type perovskites (i.e, A= Ba, Pr, Nd, Sm)

As may be appreciated at this stage, all of the materials discussed so far have made use of La at the A-site of the ABO_3 structure. In essence, those studies observed the effects of altering the A-site dopant and/or B-site species on the electrode performance (specifically, with respect to chromium poisoning). Elsewhere, attempts to synthesise new perovskites via the replacement of La with alternative lanthanides (e.g. neodymium) or with alkaline earth metals (e.g. barium) have also been demonstrated. These have the ability to offer new cathode materials with differing properties and there is a significant body of work that reviews the effect that this has upon the general performance of cathodes. It would appear that conclusions on the preferred A-site material differ dependent upon composition and operating temperature (e.g. [**82**,**159**,**215**]). A thorough analysis of the general benefits of each material is out of the scope of this article (although some references to such work are provided for the purpose of context). Importantly, however, some authors have looked to see if such an approach can have a beneficial effect in reducing chromium poisoning. These studies thus offer an insight into the role of the host species at the A-site in the poisoning process and this work may be relevant in helping the community to develop new chromium-tolerant cathodes. Here, some of these studies shall be discussed.

4.3.1 Ba at the A-site

BSCF ($Ba_xSr_{1-x}Co_yFe_{1-y}O_{3-\delta}$) is a commonly studied cathode material amongst researchers with Shao and Haile [**216**] amongst the first to comment upon its promise. These authors studied a $Ba_{0.5}Sr_{0.5}Co_{0.8}Fe_{0.2}O_{3-\delta}$ composition but alternatives within this BSCF family have also been considered. The favourability of such materials has been called into question by some researchers. Significantly, BSCF has been found to be unstable around common SOFC operating temperatures (i.e. below 800˚C) [**217**]. Niedrig et al. [**217**] found the transition of the BSCF structure from cubic to hexagonal, at temperatures below 840˚C leading to a corresponding drop in conductivity. In addition, the material has been shown to have the tendency to react with CO_2 to form carbonates, especially at lower operating temperatures, being especially prominent around 500˚C [**218**,**219**]. In work conducted by Shen and Lu [**65**], the electrical conductivity of the $Ba_{0.5}Sr_{0.5}Co_{0.2}Fe_{0.8}O_3$ composition is reported to be notably smaller than comparable LSCF and SSCF compositions ($La_{0.6}Sr_{0.4}Co_{0.2}Fe_{0.8}O_{3-\delta}$ and $Sm_{0.5}Sr_{0.5}Co_{0.2}Fe_{0.8}O_{3-\delta}$). The relatively poor electrical conductivity may also be noted in work by Wei et al. [**95**]. In studies by Patra et al. [**220**] and Wei et al. [**95**] it is indicated that a reduction in the Ba-Sr ratio is capable of significantly improving the electrical conductivity of the material, particularly when the volume ratio of Sr is increased above 0.6. However, this introduces other issues. Firstly, it was seen that increased Sr-content increased the thermal expansion coefficient and worsened the thermomechanical mismatch between electrolyte and

cathode. As will be discussed later, altering the composition in this manner also has a knock-on effect with respect to the performance of the cathode in a chromium-containing atmosphere.

Parallels may be drawn between the effects of chromium on BSCF cathodes and those on the previously discussed LBCF and LSCF. Chromium has been observed to deposit on the surface of BSCF cathodes, believed to be in the form of $BaCrO_4$ as well as in the form of $SrCrO_4$ [**221**]. The formation of chromium compounds on the surface of the BSCF cathodes has been observed to worsen at higher currents/overpotentials [**222**] and at higher temperatures [**221**]. This is reflected in the resulting deterioration in performance. In separate work observing chromium deposition, BSCF cathodes have been compared with Mn-containing perovskite LSM, PrSM and NdSM [**222**] as well as with similar colbalt-ferrite-containing perovskites LSCF and SSCF [**65**]. The BSCF cathodes are generally shown to outperform the Mn-containing cathodes with respect to chromium poisoning resilience [**222**] but it is, perhaps, the work conducted by Shen and Lu [**65**] which should be viewed most keenly due to the obvious similarities between LSCF, SSCF and BSCF. Interestingly, the study indicates that BSCF may offer an advantage over LSCF and SSCF when the cells in question are operated at the lower temperature of 600˚C (in terms of electrochemical performance) yet this does not account for the previous considerations on the phase stability of BSCF. As the temperature is increased, the polarisation resistance for all three materials increases markedly; LSCF and SSCF begin to outperform BSCF under these conditions. Despite this apparent drop in performance, the authors indicate that BSCF may offer a better chromium resistance in the long-term due to (a) the avoidance of Sr segregation and (b) the improved conduction properties of $BaCrO_4$ relative to $SrCrO_4$. This was a theory also discussed in earlier work by Chen et al. who studied the performance of BaO-infiltrated LSCF cathodes [**179**]. Nevertheless, the alkaline earth element Ba, like Sr, favours the formation of a chromium phase which offers a source of degradation.

Kim et al. [**223**] reported that the performance of BSCF cathodes in resisting poisoning effects is strongly dependent upon the Sr-content. Reduced Sr-content was seen to improve the stability of the material over a 20 hour period of time. This is an interesting observation and much of the work reporting on the stability of BSCF has concentrated heavily on a Ba-Sr ratio of 1:1 [**65**,**221**,**222**,**224**], with the $Ba_{0.5}Sr_{0.5}Co_xFe_{1-x}O_{3-\delta}$ dominating. The reported resilience in those papers could thus be enhanced by increasing the Ba-content. However, as discussed at the beginning of this section, BSCF offers particularly poor electrical conductivity at low Sr ratios [**220**]. Further to this, Lumeij et al. [**225**] suggest that an increase in the Ba-Sr ratio, drives a reduction in the structural stability of BSCF with the Ba-rich materials preferring the undesirable hexagonal structure. As a result of these considerations, any reduction in Sr content to achieve improved chromium resistance is done so at the expense of other factors.

In a recent paper by Qiu et al. [**226**], the possibility of improving chromium poisoning resistance by coating a $Ba_{0.5}Sr_{0.5}Co_{0.8}Fe_{0.2}O_{3-\delta}$ cathode with a $LaCoO_3$ layer was explored. The authors observed both improved resilience and an improvement in the overall performance of the cathode. Indeed, the impregnation of cathode materials with secondary phases is a technique which has been seen elsewhere [**227**,**228**] and appears to offer some potential in improving chromium poisoning resistance.

Other perovskite cathodes that utilise Ba at the A-site include BSCN ($Ba_{1-x}Sr_xCo_{1-y}Nb_yO_{3-\delta}$), BSFN ($Ba_{1-x}Sr_xFe_{1-y}Nb_yO_{3-\delta}$) and BCFN ($BaCo_{0.9-x}Fe_xNb_{0.1}O_{3-\delta}$). These materials have not received the same level of attention as that seen for BSCF but there remains some work of interest. The use of niobium-doping at the B-site gives BCFN (often the composition $BaCo_{0.7}Fe_{0.2}Nb_{0.1}O_{3-\delta}$ has been studied) which offers excellent chemical stability, but the material also suffers from poor electrical conductivity (σ<20 Scm^{-1}) [**102**,**229**,**230**]. In a study conducted by Zhao et al. [**229**], $BaCo_{0.7}Fe_{0.2}Nb_{0.1}O_{3-\delta}$ was observed to have a promising stability when exposed to chromium during operation, though this study only observed the performance during a 20-hour time frame. There have been some further efforts to take advantage of the apparent high-level of stability of this material and these efforts shall be discussed further in section 4.3.2. Contrary to this, however, a more recent study by Wang et al.[**231**] has cast some doubt upon the resistance of BCFN to chromium poisoning. The authors have indicated that there is some poisoning effect on BCFN cathodes above 700˚C and it is thus not immune to this degradation effect.

Like BCFN, it has been observed that compositions of BSFN ($Ba_{0.5}Sr_{0.5}Fe_{0.9}Nb_{0.1}O_{3-\delta}$; σ<20 Scm^{-1}) [**101**] and BSCN ($Ba_{0.6}Sr_{0.4}Co_{0.9}Nb_{0.1}O_{3-\delta}$; σ<50 Scm^{-1}) [**99**] offer relatively disappointing electrical conductivity. Although we are unaware of any chromium poisoning studies upon either BSFN or BSCN, it seems likely that, due to their Sr-content, they will poison in a similar manner to that considered for other Sr-containing perovskites such as LSCF or LSC (i.e, formation of $SrCrO_4$) and/or via the formation of $BaCrO_4$ as seen for BSCF.

4.3.2 Alternative Lanthanide elements (Sm, Nd, Pr) at the A-site

Xiong et al. [**232**] compared the poisoning effect of an SSM cathode ($Sm_{0.5}Sr_{0.5}MnO_{3-\delta}$) with that of an LSM cathode (of unspecified composition). The authors noted that the use of this SSM material resulted in a slower deterioration of the polarisation resistance when compared with LSM. This is interesting given that the common nucleation agents (i.e, Sr and Mn) are present in both materials although, in the absence of information on the LSM composition, this may be simply due to a differing A-site dopant concentration. In this same work, the authors noted the formation of $SrCrO_4$ on the SSM cathode surface, instead of the $(Cr,Mn)_3O_4$ phase that is commonly seen at the LSM-

electrolyte interface. This would suggest two differing poisoning effects despite the similarities between the materials. The authors of that study, in fact, attributed the change in behaviour to the ionic size difference between La^{3+} and Sm^{3+}. The smaller Sm ion is said to allow the Sr to segregate out more easily as a result of elastic energy minimisation whilst also reducing the rate at which Mn segregates (Figure 8). In a separate study, an SSCF composition ($Sm_{0.5}Sr_{0.5}Co_{0.2}Fe_{0.8}O_{3-\delta}$) was observed to degrade in the same manner as SSM (i.e, via the formation of $SrCrO_4$), though it was also noted that the poisoning effect was more profound in this case than it was with LSCF [**65**]. This observation would be consistent with the relationship between the smaller ion size and the ease with which Sr may segregate out of the perovskite structure. However, it is also notable that the authors compared their SSCF cathode against an LSCF material with lower Sr-content ($La_{0.6}Sr_{0.4}Co_{0.2}Fe_{0.8}O_3$). In such a case, a greater quantity of $SrCrO_4$ could be anticipated and a greater rate of degradation would be expected.

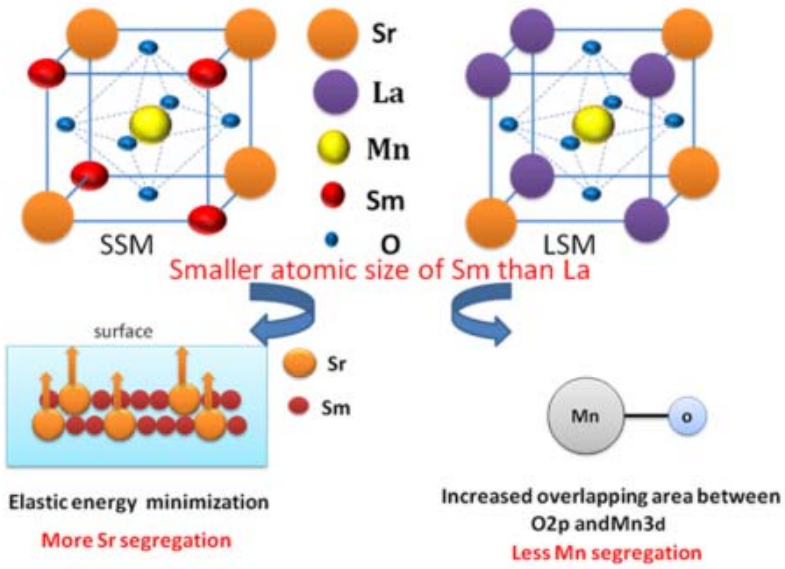

Figure 8 – A schematic of the effect of different A-site atomic sizes on Sr-segregation [**232**]. ***Re-printed with kind permission.***

A family of novel SSBCFN ($Sm_{0.5(1-x)}Sr_{0.5(1-x)}Ba_xCo_{1-0.3x}Fe_{0.2x}Nb_{0.1x}O_{3-\delta}$) cathode materials has been investigated by Zhao et al. [**229**] with respect to their chromium-poisoning resilience. The materials were synthesised in an attempt to exploit the high performance of SSC ($Sm_{0.5}Sr_{0.5}CoO_{3-\delta}$) and the stability of BCFN ($BaCo_{0.7}Fe_{0.2}Nb_{0.1}O_{3-\delta}$). In that study, the authors reported a reasonable level of success, with the material offering desirable stability and performance. It was suggested that the small amount of Nb-doping is capable of improving the stability of the Ba and Sr at the A-site and thus reduces the rate at which the species is capable of segregating to the surface of the material. However, this material requires further consideration to assess its longer term stability given that this study concentrated upon the degrading effects within a short time frame only (<100 hours).

In work by Matsuzaki and Yasuda [**112**] a comparison between compositions of LSM, LSCF ($La_{0.6}Sr_{0.4}Co_{0.2}Fe_{0.8}O_{3-\delta}$) and PSM ($Pr_{0.6}Sr_{0.4}MnO_{3-\delta}$) was reported. When the electrodes were exposed to chromium containing vapour, the loss of voltage with time indicated a very similar behaviour between LSM and PSM over a 40 hour period. The authors, however, did not analyse the quantity of chromium deposited within the PSM cathode. Park et al. [**222**], on the other hand, did conduct such an analysis using Wavelength Dispersive Spectroscopy (SEM-WDS). The deposition of chromium within the PSM ($Pr_{0.8}Sr_{0.2}MnO_{3-\delta}$) and NSM ($Nd_{0.8}Sr_{0.2}MnO_{3-\delta}$) cathodes was seen to be similar to that of the LSM composition $(La_{0.8}Sr_{0.2})_{0.98}MnO_{3-\delta}$. Generally speaking, the presence of chromium appeared to affect the LSM cathode more profoundly with greater quantities deposited within the electrode and a resulting larger rate in the drop in voltage with time. This indicates that the replacement of lanthanum with either neodymium or praseodymium does indeed have some effect on the extent and impact of chromium-related degradation. Although it is questionable whether or not PSM or NSM may offer a significant-enough improvement to the incumbent electrode materials, the tactic of replacing La with Pr or Nd at the A-site may reap benefits in other perovskite materials.

4.4 Alternative Structures

4.4.1 Ruddlesden-Popper Phases

In recent times the Ruddlesden-Popper family of materials has generated interest with SOFC researchers, due to the promising electrochemical and thermomechanical stability that it can offer [**233**,**234**]. These materials have a general formula $A_{n+1}M_nO_{3n+1}$ whereby ABO_3 perovskite layers are separated by AO rock salt layers. Such structures possess a wide range of oxygen stoichiometries (both deficient and excess) and the oxide ion may be transported via both interstitial and vacancy mechanisms [**235**]. Today, the A_2BO_4 series (i.e. 'n=1') of materials has been the most commonly studied of the Ruddlesden-Popper phases.

A number of Ruddlesden-Popper materials have been proposed for use in SOFC applications but the analysis herein shall concentrate on two of the more popular of these materials. An emphasis is placed upon those materials that have been researched in terms of their chromium resistance. It is interesting to consider whether or not these structures can offer some improvement to the resistance to chromium poisoning or if this is determined by the constituents of the phase only (e.g. the presence or absence of Sr or Mn).

4.4.1.1 LNO-214

In relation to the K_2NiF_4-family, the effects of chromium upon the mixed conductor $La_2NiO_{4+\delta}$ (herein denoted LNO-214) have perhaps received the highest amount of attention amongst researchers. Hou et al.[**236**] concluded that LNO-214 could offer a promising chromium-resistant cathode for SOFC finding little evidence of chromium poisoning over a short-term test (~20h). Generally, the performance of LNO-214 in a dry, chromium-containing atmosphere has been shown to be relatively stable but, like many of the other materials discussed thus far, the degradation becomes significantly more prevalent in humid conditions [**185**,**237**,**238**]. Over the course of a 4000 hour test, Schrödl et al. [**238**] studied the effects of both chromium and silicon vapours upon the surface exchange coefficient of LNO-214, observing a notable deterioration in this property due to chromium. The authors identified (a) the segregation of Lanthanum from the bulk to the surface of the material, (b) the formation of $La(Cr,Ni)O_3$ as well as $La_{9.33}(SiO_4)O_2$ upon the cathode surface and (c) below the surface, the LNO-214 was seen to restructure to higher order Ruddlesden-Popper phases. It was seen that the performance was reasonably stable in dry conditions but that the presence of significant humidity offered a much more aggressive condition, resulting in significant degradation. Across two of their studies [**185**,**238**], Schrödl et al. observed a deterioration in oxygen exchange kinetics (represented by k_{chem}). Interestingly, this appeared to be greater at a temperature of 700˚C (a decrease in k_{chem} by a factor of 230 in relation to initial performance) than it did at 800˚C (a

decrease in k_{chem} by a factor of 25). This is an interesting observation given the higher volatilisation rates of Cr_2O_3 at elevated temperatures but, as should be expected, the electrode-properties of the material are also shown to be improved at higher temperatures.

In a recent work produced by Gong et al.[**239**], the formation of $La(Ni_{0.7}Cr_{0.3})O_3$ was observed to occur within LNO-214 cathodes (consistent with the aforementioned work [**238**]). The authors noted that there was no real tendency for chromium to deposit around the electrolyte/cathode interface (unlike that seen in the case of the LSM/YSZ cathode). Importantly, the authors confirmed that this material can offer a significant improvement in resisting the degradative effects of chromium when compared with that seen for LSM/YSZ.

Lee et al. [**240**] sought to observe the impact that chromium deposition would have on the performance of LNO-214 cathodes by depositing small amounts of chromium into the material. At low levels of chromium incorporation (<0.5% of the total cations in the material) the polarisation resistance was seen to remain relatively stable but, at greater concentrations, the resistance was observed to increase significantly. Despite this, the authors note that the deterioration in performance was less than that seen for LSCF cathodes, which is hypothesised to be a result of the reasonable catalytic performance of the resulting $LaCrO_3$ and $LaNiO_3$ phases.

Ling et al. [**241**] studied an iron-doped LNO-214 cathode with a composition of $La_2Ni_{0.9}Fe_{0.1}O_{4+\delta}$. The authors also considered an electrode of this composition, when infiltrated with GDC. The addition of the oxide-conducting phase notably improved the polarisation resistance of the cathode but it also reduced the degradation rate over the 300-hour test period. This is consistent with those studies that have been mentioned previously, relating to dual phase cathodes.

It has been suggested that, in fact, higher order phases $La_3Ni_2O_7$ (LNO-327) and $La_4Ni_3O_{10}$ (LNO-4310) may offer improved performance as cathode electrode materials in comparison to the LNO-214. We are unaware of any work which has considered the response of these materials to a chromium-rich environment. Indeed, it may be of interest to examine if these higher-order phases can offer any improvement in this regard and this may also reveal more about the role of the crystal structure in the poisoning process.

4.4.1.2 NNO-214

The isostructured Nd-nickelate NNO-214 ($Nd_2NiO_{4+\delta}$) has shown reasonable conduction properties [**73**] and, like LNO-214, its lack of the classic nucleation agents, Sr and Mn, would suggest that the material should offer a high-level of resilience to a chromium-containing environment. This is the conclusion that was reached by Lee et al. [**242**] who reported only a minimal poisoning effect when

NNO-214 was exposed to chromium vapours. This work studied the effects of chromium when the cells were under both in open circuit and polarisation state. Interestingly, this appeared to have little effect with respect to the deposition of chromium with only small amounts reported throughout the cathode structure. Further work on NNO-214 by Yang et al. [**184**] suggested a reasonable level of tolerance to chromium deposition, with the authors demonstrating only a minimal impact upon k_{chem} when a 10nm layer of chromium was deposited on the cathode. In comparison, and as discussed in section 3.2, the performance of LSC was noted to be affected even at this low level of chromium deposition (though the initial performance was better). Contrary to these studies, Schuler et al. [**243**] concluded that cathodes of NNO-214 remain susceptible to poisoning via chromium-sources (forming $NdCrO_4$), as well as from sources of other contaminants such as silicon and sulphur. Observing a precipitation of nickel out of the material (as familiar to the previously discussed LNF material), the authors describe a "*contamination induced decomposition of the nickelate structure*".

Choe et al. [**244**] built upon the earlier work on the Nd_2NiO_4 material, by analysing the effect of copper-doping ($Nd_2Ni_{1-x}Cu_xO_{4+\delta}$). Finding that the lowest ASR and polarisation resistance could be achieved with a Cu content of x=0.05, the authors then analysed the effects of chromium poisoning in comparison with that of LSCF. At 800˚C (and under the presence of gaseous chromium species), it was observed that the ASR of LSCF increased by a factor of 4.5 whilst that of the $Nd_2Ni_{0.95}Cu_{0.05}O_{4+\delta}$ only increased by a factor of 1.7.

4.4.2 Double perovskites

Double perovskites are another subset of materials which have received some interest for use as SOFC cathodes. Such structures describe a perovskite variant, where the A or B site is occupied by two types of cation (e.g, $A_2BB'O_6$ or $AA'B_2O_6$) [**245**]. To date, there are few studies considering these materials with respect to their resistance to chromium poisoning.

There exist a handful of Cr-poisoning studies that relate to the $LnBaCo_2O_{5+\delta}$ (Ln=Lanthanide) subset of double perovskites. Wei and co-authors first studied the reactivity of chromium with SBCO ($SmBaCo_2O_{5+\delta}$) [**246**] before later studying its reactivity with PBCO ($PrBaCo_2O_{5+\delta}$) [**247**]. In both instances, the formation of $BaCrO_4$ was observed to have a notable effect upon the electrochemical performance of the cathode. In the absence of chromium, the authors observed the segregation of Co and Ba species from the bulk PBCO material, assumed to be in the form of Co_3O_4 and BaO [**247**]. The chromium vapours were seen to react, preferentially, with the BaO, forming $BaCrO_4$. Across the two studies, the authors concluded that neither PBCO nor SBCO offered resilience to poisoning. Indeed, this was consistent with earlier work by Gu et al. [**248**] who found that NBCO ($NdBaCo_2O_{5+\delta}$) exhibited a strong loss in performance when exposed to chromium for just a few hours.

In another study conducted by Li et al. [**228**] the authors again noted a strong poisoning effect, this time on PBSCF ($PrBa_{0.5}Sr_{0.5}Co_{1.5}Fe_{0.5}O_{5+\delta}$). The authors found, however, that when the cathode was infiltrated with LNO ($La_2NiO_{4+\delta}$), the performance could be greatly improved. This highlights the promise that cathodes with non-nucleating agents can offer in resisting the phenomena of chromium deposition. From the limited work in the area of chromium poisoning on double perovskites, there does not appear to be any apparent advantage in such a structure with respect to suppressing the formation of secondary phases although further work is necessary to confirm this. It may be interesting to consider the effects of chromium on double perovskites that do not contain the traditional nucleation agents (i.e. Mn, Sr, Ba).

5 Discussion

5.1 Conventional Materials and the Mechanism of Chromium Poisoning

The traditional cathode material LSM has been shown to suffer from a significant deterioration in performance as a direct result of the deposition of chromium species at the cathode/electrolyte interface. A number of solutions have been proposed to extend the life of LSM cathodes. The use of oxide conducting phases (such as YSZ or GDC) to extend the amount of TPB sites throughout the cathode has been shown to offer a reduced degradation rate.

LSCF cathodes, which have replaced LSM as the "state-of-the-art", have also been shown to be susceptible to chromium poisoning, yet their MIEC properties (and hence increased number of active sites) appear to reduce the impact that the resulting chromium phases have on the cathode performance. Nevertheless, the formation of the $SrCrO_4$ phase offers a serious degradation mechanism which, ideally, should be eliminated to further extend the life of SOFCs. As a side note on LSCF, a move away from Co-containing materials (for cost and ethical reasons) also offers a reason for the research and development of alternative materials.

Earlier in this review we considered the evidence for different theories on the mechanism of chromium poisoning. The great majority of this work has been conducted on LSM and LSCF cathodes, reflecting the historical and current importance of such materials. Early work in this area commented on the likelihood of an electrochemical reduction of chromium species during the polarisation of the cathodes [**15**, **20**]. Work by Jiang and collaborators [**6**] preferred a theory relating to the formation of chromium species on 'nucleation agents'.

The argument laid out in the review by Jiang et al. [**6**] appears to be fairly comprehensive and there has yet to be a compelling counter-argument to disprove the theory presented. Therefore, on the weight of the current evidence, we concur with the conclusions in that paper. That is to say, the phenomenon is *predominantly* driven by a reaction between the chromium species and the cation species within the cathode material (e.g. Mn^{2+}, Sr^{2+}). The acceleration of the poisoning process under polarisation and at higher temperatures is said to be related to the valence stability of the cation species and/or the segregation of certain species (e.g. SrO). This has important implications on the development of new cathode materials. We will consider this further, shortly. Whilst it is difficult to *categorically* rule out the possibility of an electrochemical deposition route playing some role in the poisoning process (however minor), the evidence does not appear to be as compelling.

5.2 Considerations on Operating Conditions

In order to minimise chromium poisoning, a key operating parameter that could potentially be controlled is humidity. All cathode materials discussed in this review have been observed to poison in humid environments (with the exception of perhaps platinum). This is linked with the increased quantity of Cr-VI gas produced from the steel interconnects under such conditions. Operation in dry air appears to considerably reduce the effect of chromium poisoning due to a much reduced volatility of chromium species.

The effects of temperature and, moreover, the definition of an optimal SOFC operating temperature are less clear. Higher temperatures have the obvious advantage of improved SOFC performance (e.g. faster reaction kinetics) and yet higher operating temperatures also result in greater amounts of chromium release and subsequent deposition in the cathode structure. However, as discussed previously, it would appear that this does not necessarily lead to a greater degradation in performance terms. The literature suggests that, whether a material degrades more quickly at a lower or higher operating temperature is influenced by the material in question (and probably the chromium species which is formed).

Further to conflicting reports on the effects of operating temperature, it is worth commenting on the fact that experimental work in the chromium-poisoning area is often focused on a single temperature. It is, therefore, very difficult to identify from literature a single temperature that would be the optimal to operate at in terms of reducing chromium poisoning (whilst simultaneously maximising performance). Ultimately, the SOFC operating temperature is likely to be determined by the properties of the individual stack and cell material in question and the application itself, rather than solely based on considerations with respect to reducing chromium-poisoning related degradation.

In considering the minimisation of chromium poisoning (and hence the maximisation of lifetime), research should consider the valence stability of the studied cathode materials. Jiang et al. [**6**] suggested that Cr-poisoning was reduced for materials with high valence stability. As an example of how this may be of interest, we can consider the Ruddlesden-Popper nickelate cathode materials ($La_{n+1}Ni_nO_{3n+1}$). Amow et al. [**249**] have discussed this series of materials in a review paper from 2006. It was suggested that the La_2NiO_4 species is less stable below 900˚C (i.e. at SOFC operating temperatures) than the “n=2 and 3” species. This, the authors concluded, is a result of the fact that the Ni^{2+} is less favourable at temperatures below 900˚C, compared with the Ni^{3+} species. Applying this knowledge to the observations on the relationship between valence stability and chromium deposits, we can tentatively propose which one of the nickelate series is likely to have improved

chromium resilience. The doped $LaNiO_3$ subset of perovskites, which contain the Ni^{3+} species, may thus offer improved stability and improved resistance to chromium poisoning over the Ruddlesden-Popper phases (which contain the Ni^{2+} species as well as the Ni^{3+} species in the case of $La_3Ni_2O_7$ and $La_4Ni_3O_{10}$). As such, the former would be more applicable for operation at temperatures under 900˚C. It would be of interest to confirm the validity of such a relationship.

5.3 Improving Chromium Resilience

The further development of chromium resistant cathode materials is important in extending the life of SOFC stacks. In essence, cathodes can be developed to either (a) reduce the rate at which chromium species are formed or (b) reduce the impact such species have on SOFC cell performance. Engineering cathode materials that 'fail well' in the presence of chromium (i.e. those that form phases which are less destructive to the performance of the cathode) may be one option for future cell development. Alternatively, this may be enabled by engineering materials that have very high performance, providing greater 'head room' for the loss of performance that may result from many 10,000 hours of operation.

5.3.1 Resilience via appropriate elemental selection

To date, a variety of SOFC cathode materials have been developed and considered for application. In this review we have discussed only a limited selection of these (i.e. those which have been studied in terms of chromium poisoning resistance). From this it is possible to observe the effects of different materials on the influences of chromium poisoning. An overview of some of the studies discussed is presented in Table 2. Due to the nature of these reports, it is very difficult to directly compare degradation rates from study-to-study and offer some definitive ranking of the materials, e.g. due to different testing conditions, varying cathode compositions etc. Instead, and where possible, we have sought to identify those materials which appear to offer reduced degradation rates in comparison with typical SOFC materials, LSCF and LSM. This is with a view to identifying those materials which may offer improved long-term resilience relative to today's state-of-the-art. The reader should note that the table does not reflect information on the initial performance of the cathodes (i.e. prior to degradation). The purpose of the table is to summarise our discussion so far and to identify trends within the studied cathode materials which could be used for further cathode development. Optimisation of these 'chromium-tolerant' cathode materials is likely to be imperative.

One proposed approach to producing cathodes with improved resistance to chromium poisoning is to synthesise materials that omit the common 'nucleation agents' Sr and Mn. This tactic appears to have resulted in some success in terms of reducing chromium-related degradation rates. As an example, the literature indicates that LNF cathodes demonstrate reduced degradation rates relative

to LSM and LSCF [**153**,**193**,**194**,**197**,**198**]. However, it is critical to acknowledge that the removal of Sr from the perovskite structure is likely to lead to poorer general performance (as can be appreciated by a consideration of Table 1). The replacement of Sr with Ba has been attempted in some cases and appears to offer some advantages (e.g. LBCF) [**198**,**208**,**209**]. In terms of its reaction with chromium, the formation of $BaCrO_4$ has been observed in Ba-containing cathodes. This appears to be preferred over the formation of $SrCrO_4$ in relation to the rate at which the performance of the cathode degrades. Jiang et al. already suggested the activity of nucleation agents with chromium oxides is of the following order; Mn > Sr > Ba ~ Co [6]. However, the use of Ba is likely to drive other issues such as poor stability with carbon dioxide and so this approach is likely to offer only limited interest. It appears that the use of alkaline earth elements in cathode systems should ideally be avoided for improved long-term cathode stability.

Evidence from the literature indicates that the classic ABO_3-type perovskites have all been shown to poison in some way, although the effect is characteristic of the material and, as discussed, some materials offer better resilience than others. Altering the A and B-site species as well as the dopant species and concentrations, all appear to impact on the response to chromium poisoning and need to be tailored accordingly. As previously mentioned, one approach to achieving this, which is highlighted by Jiang et al. [**6**], is to stabilise the crystal structure, improve the valence stability of the cations and reduce the segregation of nucleation agents such as SrO. This, the authors indicated, could be achieved via an appropriate doping strategy. As briefly discussed earlier, a number of Nb-doped perovskite materials have been investigated and, in part at least, this is with a view to achieve this improved stability. Indeed, Chen and Jiang [**211**] reported that their $La_{0.24}Sr_{0.16}Ba_{0.6}Co_{0.5}Fe_{0.44}Nb_{0.06}O_{3-\delta}$ had "*excellent stability and tolerance towards chromium deposition and poisoning*". Zhao et al.[**229**], meanwhile, engineered a family of cathodes of type $Sm_{0.5(1-x)}Sr_{0.5(1-x)}Ba_xCo_{1-0.3x}Fe_{0.2x}Nb_{0.1x}O_{3-\delta}$, reporting "*high activity, stability and high tolerance towards contamination by Cr".* However, Nb-doping should not be considered to offer a 'blanket solution' to improving chromium resistance. Wang et al.[**231**] more recently considered a $Ba_{0.9}Co_{0.7}Fe_{0.2}Nb_{0.1}O_{3-\delta}$ composition and reported poor chromium resistance. Nevertheless, it seems that such an approach may be worthy of further investigation.

Based on the evidence in this review it appears that engineering materials that will form less 'destructive' phases when reacted with chromium will help to reduce the impact of chromium poisoning. An overview of the electrical conductivities of common Cr-containing phases is seen in Table 3, offering an idea of how the formation of such phases may impact the conductivity properties of different cathodes. In the case of the La-nickelate materials, $(La,Cr,Ni,Fe)O_3$ perovskite phases are commonly said to form as a result of reaction with chromium species. (although Ni-Cr

spinel is also reported). This would be expected to drive a much slower degradation rate than that which would be seen for $SrCrO_4$ (observed in LSCF and LSC cathodes). However, the general performance of the nickelates needs to be optimised to compete with the conventional cathode materials. If these materials can be further enhanced without compromising the Cr-resilience of the material, these may offer an ideal replacement for the incumbent materials. Indeed, this is an approach taken by a number of authors [**250**, **251**] who have looked at the effect of doping La_2NiO_4. It is interesting that these referenced works have considered the use of Sr-doping. For the aforementioned reasons, this would likely reduce the chromium poisoning resistance unless the nickelate structure had the effect of reducing the SrO segregation. We are unaware of any chromium-poisoning related studies on Sr-doped nickelate systems. With respect to engineering new materials, the challenge is to select A and B-site materials which will offer chromium resistance without compromising the premium performance that has been previously achieved with materials such as LSCF.

5.3.2 Alternative crystal structures

Alternative perovskite-related structures, such as the A_2BO_4 type and the double perovskites, have been suggested as having potential as SOFC cathode materials. Research on these is mainly concentrated on the general performance of the materials as electrodes, though a limited amount of studies have focused on the effects that chromium has upon individual materials which adopt this structure. In terms of their general performance, it is not currently clear if these materials are preferable to the more conventional materials and more work is required in this area to understand if they can replace the existing, preferred cathodes. Based on the literature, it is also not currently clear if there is any significant relationship between the underlying crystal structure of the cathode material (e.g. perovskite, double perovskite, Ruddlesden-Popper) and the chromium poisoning resistance of the material. Do certain crystal structure features promote better chromium tolerance? For example, do the rock salt-type layers that exist between the perovskite layers in the Ruddlesden-Popper phases have any effect on chromium incorporation? This could be analysed by considering the effect of chromium on a series of materials with differing crystal structures but with the same elemental make-up (e.g. $LaNiO_3$, La_2NiO_4, $La_3Ni_2O_7$, $La_4Ni_3O_{10}$). Current understanding would suggest that chromium poisoning is determined entirely by the constituents of the cathode material (e.g. absence or presence of Sr). An understanding on the relationship between chromium poisoning and cathode crystal structures would help to advance understanding around cathode development and upon the mechanism of chromium poisoning itself.

5.3.3 Dual phase cathodes

As previously acknowledged, the research community has found it difficult to offer a material with excellent chromium resilience that will also match the performance of LSCF. One possible approach to overcoming this issue is to use dual-phase cathode structures which aim to exploit the benefits of a Cr-tolerant material whilst also drawing on the excellent performance of a less-tolerant material, like LSCF. One particularly novel concept is the idea of coating a high-performance cathode material with another chromium-tolerant one. Indeed, similar approaches have been attempted in recent times with some success reported [**179**, **226**, **228**, **252**, **253**]. Such dual phases may offer a more realistic approach of obtaining high-performance, long-life cathodes as opposed to searching for a 'holy grail' material which can achieve all of this in isolation.

5.4 Concluding Remarks

It may seem an obvious statement but it is not enough to seek materials that offer excellent resistance to chromium poisoning. Research needs to ensure that alternative cathode materials can offer not only reduced degradation rates but they must also exhibit competitive electrochemical and thermomechanical properties relative to the state-of-the-art cathode materials. Today, there appears to be a reluctance to move research (and industry) effort away from the conventional LSM, LSC and LSCF materials which have been well studied and have been proven to offer reasonable performance over many 1000's of hours. New cathode materials need to out-perform these materials whilst offering improved resistance to chromium poisoning. In the future, this could be achieved via the optimisation of materials such as the lanthanum nickelates but care must be taken to avoid introducing features that will likely reduce their chromium tolerance (e.g. whether Sr-doping leads to SrO segregation and formation of $SrCrO_4$ in these materials). Alternatively, efforts must be made to further the lifetime of the conventional materials. This may be achieved via the use of interconnect coatings, Cr-getters, careful control of the operating conditions and/or the use of novel cathode structures. The use of dual phase cathodes may represent a solution that minimises concerns relating to changing to a totally new material, whilst also allowing improved Cr tolerance.

*Table 2 – Overview of Cr-phase formation in SOFC cathode materials and consideration of degradation rates relative to common cathode materials ; *Denotes tests run for less than 100h [A]Denotes test taken at 750˚C ; Y/N – Denotes 'Yes'/'No' (i.e. Yes=evidence of lower degradation rate) ; For comparisons with LSM, A-site stoichiometry is denoted (e.g. $^{0.9}$=$(La_{0.8}Sr_{0.2})_{0.9}MnO_3$)*

Material Group	Composition	Degradative Chromium Phase Observed Reported in Literature						Evidence for Lower Deg. Rate than $(La_{0.8}Sr_{0.2})_xMnO_3$ in presence of Chromium			Evidence for Lower Deg. Rate than $La_{0.6}Sr_{0.4}Co_{0.2}Fe_{0.8}O_3$ in presence of chromium		
		Cr_2O_3	$(Cr,Mn)_3O_4$	$SrCrO_4$	$BaCrO_4$	$La(Cr,M)O_3$ (e.g. M=Fe)	Other Cr Phases / Secondary Phases / Comments	700˚C	800˚C	900˚C	700˚C	800˚C	900˚C
LSM	$(La_{0.8}Sr_{0.2})_xMnO_3$ (x=0.9-1)							-	-	-	-	N[254][1]	N [148]*[/0.9]
LSM/YSZ	$(La_{0.8}Sr_{0.2})_{0.9}MnO_3$/8YSZ (90%-10%)	✓	✓			✓	Increasing YSZ content shows reduced degradation rates [148]. Use of LSM/YSZ Functional Layers also seen to reduce the degradation rate [129].	-	-	Y [148]*[/0.9]	-	-	N [148]*[/0.9]
	$(La_{0.8}Sr_{0.2})_{0.9}MnO_3$/8YSZ (70%-30%)							-	-	Y [148]*[/0.9]	-	-	N [148]*[/0.9]
	$(La_{0.8}Sr_{0.2})_{0.9}MnO_3$/8YSZ (50%-50%)							-	-	Y [148]*[/0.9]	-	-	N [148]*[/0.9]
LSM/GDC	$(La_{0.8}Sr_{0.2})_{0.9}MnO_3$/GDC							-	-	Y [148]*[/0.9]	-	-	Y [148]*[/0.9]
LSC	$La_{0.8}Sr_{0.2}CoO_3$			✓			Formation/Precipitation of Co_3O_4, Co-Cr spinel also reported [183]	-	-	Y [182]*[/0.95]	-	-	-
	$La_{0.6}Sr_{0.4}CoO_3$			✓		✓		-	-	-	-	-	-
LSCF	$La_{0.6}Sr_{0.4}Co_{0.2}Fe_{0.8}O_3$			✓			Formation of (La,Sr,Cr)(CoFe)O_3 [176] & Co-Cr spinel [153] has also been reported	-	Y [254][1.0]	Y [198]*[/0.9]	-	-	-
LSF	$La_{0.8}Sr_{0.2}FeO_3$	✓		✓		✓	Precipitation of $SrFe_{12}O_{19}$ reported [25]. Unclear if different Cr-phases related to Sr-content	Y [188][0.95]	Y [25][A 0.99]	-	-	N [25][A]	-
	$La_{0.6}Sr_{0.4}FeO_3$			✓				-	-	-	-	-	-
Pt	Pt						No Cr-deposits observed.	-	-	N [127]*[/0.9]	-	-	N [127]*
LNF	$LaNi_{0.6}Fe_{0.4}O_3$					✓	(Ni,Fe)(Fe,Cr)$_2O_4$ [200]. (Ni,Cr)$_2O_4$, NiO [153]	Y [194][1.0]	-	Y [198]*[/0.9]	Y [153]	-	Y [198]*
LBCF	$La_{0.6}Ba_{0.4}Co_{0.2}Fe_{0.8}O_3$				✓			-	-	Y [198]*[/0.9]	-	-	Y [209]*
LSCM	$(La_{0.8}Sr_{0.2})_{0.95}Mn_{0.8}Co_{0.2}O_3$		✓	✓			More Mn leads to more Cr-Mn spinel at electrolyte surface, more Co leads to more $SrCrO_4$ at surface. Degradation is largest when Co=0.4 and smallest when Co=0.8 or 1. [182]*	-	-	N [182]*[/0.95]	-	-	-
	$(La_{0.8}Sr_{0.2})_{0.95}Mn_{0.6}Co_{0.4}O_3$							-	-	N [182]*[/0.95]	-	-	-
	$(La_{0.8}Sr_{0.2})_{0.95}Mn_{0.4}Co_{0.6}O_3$							-	-	N [182]*[/0.95]	-	-	-
	$(La_{0.8}Sr_{0.2})_{0.95}Mn_{0.2}Co_{0.8}O_3$							-	-	Y [182]*[/0.95]	-	-	-
LSBCF	$La_{0.6}Sr_{0.3}Ba_{0.1}Co_{0.2}Fe_{0.8}O_3$			✓	✓		Chromium deposition is reduced with increasing Ba-content. In general, increasing Ba-content reduces degradation [208]	-	-	-	-	-	N [208]*
	$La_{0.6}Sr_{0.2}Ba_{0.2}Co_{0.2}Fe_{0.8}O_3$							-	-	-	-	-	Y [208]*
	$La_{0.6}Sr_{0.1}Ba_{0.3}Co_{0.2}Fe_{0.8}O_3$							-	-	-	-	-	Y [208]*
LSBCFN	$La_{0.24}Sr_{0.16}Ba_{0.6}Co_{0.5}Fe_{0.44}Nb_{0.06}O_3$				✓		$BaCr_2O_4$ is a possible reaction product [211]*	-	-	-	-	-	**Y** [211]*
BSCF	$Ba_{0.5}Sr_{0.5}Co_{0.2}Fe_{0.8}O_3$				✓		No $SrCrO_4$ formation reported [65]	-	-	-	N [65]	N [65]	N [211]*
	$Ba_{0.3}Sr_{0.7}Co_{0.8}Fe_{0.2}O_3$			✓	✓		Increasing Sr-content leads to increasing $SrCrO_4$ formation and increased performance loss [223]. (Co,Fe)CrO_4 reported for BSCF-5582 [224]	-	-	-	-	-	-
	$Ba_{0.5}Sr_{0.5}Co_{0.8}Fe_{0.2}O_3$							Y [222][0.98]	-	-	-	-	-
	$Ba_{0.7}Sr_{0.3}Co_{0.8}Fe_{0.2}O_3$							-	-	-	-	-	-
BCFN	$Ba_xCo_{0.7}Fe_{0.2}Nb_{0.1}O_3$ (x=0.9, 1)				✓		Conflicting conclusions on Cr-stability [229,231]	-	-	-	-	-	Y [211]*
SmSCF	$Sm_{0.5}Sr_{0.5}Co_{0.2}Fe_{0.8}O_3$			✓			Very similar degradation behaviour to LSCF [65]	-	-	-	N [65]	N [65]	-
SmSM	$Sm_{0.5}Sr_{0.5}MnO_3$			✓				-	Y [232][A]	-	-	-	-
SmSBCFN	$Sm_{0.25}Sr_{0.25}Ba_{0.5}Co_{0.85}Fe_{0.1}Nb_{0.05}O_3$						Cr deposited in cathode (phase unknown) [229]	-	-	-	-	-	Y [229]*
PrSM	$Pr_{0.8}Sr_{0.2}MnO_3$						Cr-poisoning is apparent for PrSM and NdSM. Cr-Mn spinel and Cr_2O_3 probable [222]	N [222][0.98]	-	-	N [112]*	-	-
NdSM	$Nd_{0.8}Sr_{0.2}MnO_3$							N [222][0.98]	-	-	-	-	-
LNO	La_2NiO_4					✓	NiO precipitation [240]	-	Y [239][0.95]	-	-	-	-
NNO	Nd_2NiO_4						$NdCrO_4$, NiO [243]	-	-	-	-	-	-
NNCuO	$Nd_2Ni_{0.95}Cu_{0.5}O_4$							-	-	-	-	-	Y [244]*
PBCO	$PrBaCo_2O_5$				✓		Co_3O_4, $Pr_4Co_3O_{10}$ precipitated [247]	-	-	-	-	-	-
SBCO	$SmBaCo_2O_5$	✓			✓		$SmCoO_3$, Co_3O_4 precipitated [246]	-	-	-	-	-	-
NBCO	$NdBaCo_2O_5$				✓		$CrNdO_3$, $CoCr_2O_4$ reported [248]	-	-	-	-	-	-

Table 3 – Electrical Conductivity of Cr-containing phases

Chromium-Containing Phase	Conductivity (Scm^{-1})		
	600˚C	**700˚C**	**800˚C**
Cr_2O_3	0.009 [**255**]	0.015 [**255**]	0.02 [**255**]
$MnCr_2O_4$	0.0003 [**256**]	0.00136 [**256**]	0.004 [**256**]
$Mn_{1.5}Cr_{1.5}O_4$	0.004 [**256**]	0.014 [**256**]	0.036 [**256**]
Mn_2CrO_4	0.13 [**256**]	0.38[**256**]	0.94 [**256**]
$CoCr_2O_4$	-	-	7.4 [**257**]
$NiCr_2O_4$	-	-	0.73 [**257**]
$SrCrO_4$	1.00×10^{-6} [**258**]	2.00×10^{-5} [**258**]	0.000182 [**258**]
$BaCrO_4$	5.15×10^{-5} [**259**]	5.13×10^{-4} [259]	0.0045 [**259**]
$LaCrO_3$	0.50 [**260**]	0.63 [**260**]	0.68 [**260**]
$LaCr_{0.9}Ni_{0.1}O_3$	3.55 [**260**]	4.07 [**260**]	4.47 [**260**]
$LaCr_{0.8}Ni_{0.2}O_3$	6.92 [**260**]	8.13 [**260**]	8.91 [**260**]
$LaCr_{0.6}Ni_{0.4}O_3$	15.49 [**260**]	16.98 [**260**]	18.20 [**260**]
$LaCr_{0.4}Ni_{0.6}O_3$	54.95 [**260**]	57.54 [**260**]	60.26 [**260**]
$LaCr_{0.2}Ni_{0.8}O_3$	147.91 [**260**]	165.96 [**260**]	173.78 [**260**]
$LaCr_{0.1}Ni_{0.9}O_3$	218.78 [**260**]	234.42 [**260**]	245.47 [**260**]
$LaCr_{0.8}Fe_{0.2}O_3$	0.075 [**261**]	0.090 [**261**]	0.100 [**261**]

[1] K. Huang, Solid Oxide Fuel Cells, in: M. Gasik (Ed.), Mater. Fuel Cells, Woodhead Publishing Limited, Cambridge, 2008: pp. 280–343.

[2] D.J.L. Brett, A. Atkinson, N.P. Brandon, S.J. Skinner, Intermediate temperature solid oxide fuel cells, Chem. Soc. Rev. 37 (2008) 1568. doi:10.1039/b612060c.

[3] I.C. Fullarton, J.A. Kilner, B.C.H. Steele, P.H. Middleton, Characterisation of oxygen ion transport in selected perovskite structured oxided by 18O/16O isotopic exchange and dynamic secondary ion mass spectrometry, in T.A.Ramanarayanan, W.L.Worrell, H.L.Tuller (eds.): Proc. Second Int. Symp. Ion. Mix. Conduct. Ceram., The Electrochemical Society, Pennington, (1994), pp. 9–26.

[4] M. Janousek, W. Köck, M. Baumgärtner, H. Greiner, Development and Processing of Chromium Based Alloys for Structural Parts in Solid Oxide Fuel Cells, ECS Proc. Vol. 1997–40 (1997) 1225–1233. doi:10.1149/199740.1225pv.

[5] M. Bianco, M. Linder, Y. Larring, F. Greco, J. Van herle, Lifetime Issues for Solid Oxide Fuel Cell Interconnects, in: Solid Oxide Fuel Cell Lifetime Reliab., Elsevier Ltd, 2017: pp. 121–144. doi:10.1016/B978-0-08-101102-7.00007-6.

[6] S.P. Jiang, X. Chen, Chromium deposition and poisoning of cathodes of solid oxide fuel cells – A review, Int. J. Hydrogen Energy. 39 (2014) 505–531. doi:10.1016/J.IJHYDENE.2013.10.042.

[7] J.W. Fergus, Effect of cathode and electrolyte transport properties on chromium poisoning in solid oxide fuel cells, Int. J. Hydrogen Energy. 32 (2007) 3664–3671. doi:10.1016/J.IJHYDENE.2006.08.005.

[8] Z. Yang, M. Guo, N. Wang, C. Ma, J. Wang, M. Han, A short review of cathode poisoning and corrosion in solid oxide fuel cell, Int. J. Hydrogen Energy. 42 (2017) 24948–24959. doi:10.1016/j.ijhydene.2017.08.057.

[9] A. Arregui, L.M. Rodriguez-Martinez, S. Modena, M. Bertoldi, J. Van Herle, V.M. Sglavo, Stability of ferritic perovskite cathodes in anode-supported solid oxide fuel cells under different processing and operation parameters, Electrochim. Acta. 58 (2011) 312–321. doi:10.1016/j.electacta.2011.09.048.

[10] S.D. Vora, W.L. Lundberg, J.F. Pierre, Overview of U.S. Department of energy office of Fossil energy's solid oxide fuel cell program, ECS Trans. 78 (2017) 3–19. doi:10.1149/07801.0003ecst.

[11] H. Nirasawa, Current Status of National SOFC Projects in Japan, ECS Trans. 78 (2017) 33–40.

[12] Forschungszentrum Julich, High-Temperature Fuel Cell Achieves Lifetime of More Than 11 Years, Fz-Juelich.De. (2019). https://www.fz-juelich.de/SharedDocs/Pressemitteilungen/UK/EN/2019/2019-02-07-sofc-en.html?nn=2409938 (accessed November 22, 2019).

[13] C. Gindorf, L. Singheiser, K. Hilpert, Chromium vaporisation from Fe,Cr base alloys used as interconnect in fuel cells, Steel Res. 72 (2001) 528–533. doi:10.1002/srin.200100163.

[14] Z. Yang, K.S. Weil, D.M. Paxton, J.W. Stevenson, Selection and Evaluation of Heat-Resistant Alloys for SOFC Interconnect Applications, J. Electrochem. Soc. 150 (2003) A1188. doi:10.1149/1.1595659.

[15] K. Hilpert, D. Das, M. Miller, D.. Peck, R. Weiss, Chromium Vapor Species over Solid Oxide Fuel Cell Interconnect Materials and Their Potential for Degradation Processes, J. Electrochem. Soc. 143 (1996) 3642. doi:10.1149/1.1837264.

[16] C. Gindorf, L. Singheiser, K. Hilpert, Vaporisation of chromia in humid air, J. Phys. Chem. Solids. 66 (2005) 384–387. doi:10.1016/J.JPCS.2004.06.092.

[17] X. Yin, L. Bencze, V. Motalov, R. Spatschek, L. Singheiser, Thermodynamic perspective of Sr-related degradation issues in SOFCs, Int. J. Appl. Ceram. Technol. 15 (2018) 380–390. doi:10.1111/ijac.12809.

[18] S. Taniguchi, M. Kadowaki, H. Kawamura, T. Yasuo, Y. Akiyama, Y. Miyake, T. Saitoh, Degradation phenomena in the cathode of a solid oxide fuel cell with an alloy separator, J. Power Sources. 55 (1995) 73–79. doi:10.1016/0378-7753(94)02172-Y.

[19] A. Beez, X. Yin, N.H. Menzler, R. Spatschek, M. Bram, Insight into the Reaction Mechanism of $(La_{0.58}Sr_{0.40})(Co_{0.20}Fe_{0.80})O_{3-\delta}$ Cathode with Volatile Chromium Species at High Current Density in a Solid Oxide Fuel Cell Stack, J. Electrochem. Soc. 164 (2017) F3028–F3034. doi:10.1149/2.0051710jes.

[20] D. Das, M. Miller, H. Nickel, K. Hilpert, Chromium evaporation from SOFC interconnector alloys and degradation process by chromium transport, in: 1st Eur. Solid Oxide Fuel Cell Forum, 1994: pp. 703–714.

[21] W.J. Quadakkers, J. Piron-Abellan, V. Shemet, L. Singheiser, Metallic interconnectors for solid oxide fuel cells – a review, Mater. High Temp. 20 (2003) 115–127. doi:10.1179/mht.2003.015.

[22] J.C.W. Mah, A. Muchtar, M.R. Somalu, M.J. Ghazali, Metallic interconnects for solid oxide fuel cell: A review on protective coating and deposition techniques, Int. J. Hydrogen Energy. 42

(2017) 9219–9229. doi:10.1016/J.IJHYDENE.2016.03.195.

[23] M. Bianco, M. Linder, Y. Larring, F. Greco, J. Van herle, Chapter 7 – Lifetime Issues for Solid Oxide Fuel Cell Interconnects, in: Solid Oxide Fuel Cell Lifetime Reliab., 2017: pp. 121–144. doi:10.1016/B978-0-08-101102-7.00007-6.

[24] E. Konysheva, H. Penkalla, E. Wessel, J. Mertens, U. Seeling, L. Singheiser, K. Hilpert, Chromium Poisoning of Perovskite Cathodes by the ODS Alloy Cr5Fe1Y_2O_3 and the High Chromium Ferritic Steel Crofer22APU, J. Electrochem. Soc. 153 (2006) A765–A773. doi:10.1149/1.2172563.

[25] S.P. Simner, M.D. Anderson, G.-G. Xia, Z. Yang, L.R. Pederson, J.W. Stevenson, SOFC Performance with Fe-Cr-Mn Alloy Interconnect, J. Electrochem. Soc. 152 (2005) A740. doi:10.1149/1.1864332.

[26] M. Krumpelt, T.A. Cruse, M.C. Hash, Chromium interactions with cathode materials, Electrochem. Soc. Proc. (2005) 1578–1583. doi:10.1149/200507.1578PV.

[27] R. Wang, Z. Sun, U.B. Pal, S. Gopalan, S.N. Basu, Mitigation of chromium poisoning of cathodes in solid oxide fuel cells employing $CuMn_{1.8}O_4$ spinel coating on metallic interconnect, J. Power Sources. 376 (2018) 100–110. doi:10.1016/j.jpowsour.2017.11.069.

[28] H. Kurokawa, C.P. Jacobson, L.C. DeJonghe, S.J. Visco, Chromium vaporization of bare and of coated iron–chromium alloys at 1073 K, Solid State Ionics. 178 (2007) 287–296. doi:10.1016/J.SSI.2006.12.010.

[29] X. Li, J. Lee, B.N. Popov, Performance studies of solid oxide fuel cell cathodes in the presence of bare and cobalt coated E-brite alloy interconnects, J. Power Sources. 187 (2009) 356–362. doi:10.1016/j.jpowsour.2008.11.018.

[30] K. Fujita, K. Ogasawara, Y. Matsuzaki, T. Sakurai, Prevention of SOFC cathode degradation in contact with Cr-containing alloy, J. Power Sources. 131 (2004) 261–269. doi:10.1016/j.jpowsour.2003.12.051.

[31] J. Mizusaki, Y. Yonemura, H. Kamata, K. Ohyama, N. Mori, H. Takai, H. Tagawa, M. Dokiya, K. Naraya, T. Sasamoto, H. Inaba, T. Hashimoto, Electronic conductivity, Seebeck coefficient, defect and electronic structure of nonstoichiometric $La_{1-x}Sr_xMnO_3$, Solid State Ionics. 132 (2000) 167–180. doi:10.1016/S0167-2738(00)00662-7.

[32] Z. Zhong-Tai, O. Lin, T. Zi-Long, Synthesis and Characteristics of $La_{1-x}Sr_xMnO_3$ Ceramics for Cathode Materials of SOFC, ECS Proc. Vol. 1995–1 (1995) 502–511.

doi:10.1149/199501.0502PV.

[33] A. Berenov, J.L. MacManus-Driscoll, J.A. Kilner, Oxygen tracer diffusion in undoped lanthanum manganites, Solid State Ionics. 122 (1999) 41–49. doi:10.1016/S0167-2738(99)00077-6.

[34] E.N. Armstrong, K.L. Duncan, E.D. Wachsman, Effect of A and B-site cations on surface exchange coefficient for ABO_3 perovskite materials, Phys. Chem. Chem. Phys. 15 (2013) 2298–2308. doi:10.1039/c2cp42919e.

[35] A. Hammouche, E. Siebert, A. Hammou, Crystallographic, thermal and electrochemical properties of the system $La_{1-x}Sr_xMnO_3$ for high temperature solid electrolyte fuel cells, Mater. Res. Bull. 24 (1989) 367–380. doi:10.1016/0025-5408(89)90223-7.

[36] M. Mori, Y. Hiei, N.M. Sammes, G.A. Tompsett, Thermal-Expansion Behaviors and Mechanisms for Ca- or Sr-Doped Lanthanum Manganite Perovskites under Oxidizing Atmospheres, J. Electrochem. Soc. 147 (2000) 1295–1302. doi:10.1149/1.1393353.

[37] H. Nagamoto, I. Mochida, K. Kagotani, H. Inoue, A. Negishi, Change of thermal expansion coefficient and electrical conductivity of $LaCo_{1-x}M_xO_3$ (M = Fe, Ni), J. Mater. Res. 8 (1993) 3158–3162. doi:10.1557/JMR.1993.3158.

[38] V. Øygarden, T. Grande, Crystal structure, electrical conductivity and thermal expansion of Ni and Nb co-doped $LaCoO_3$, Dalt. Trans. 42 (2013) 2704–2715. doi:10.1039/C2DT32399K.

[39] F. Figueiredo, F.M.B. Marques, J.R. Frade, Electrochemical permeability of $La_{1-x}Sr_xCoO_{3-\delta}$ materials, Solid State Ionics. 111 (1998) 273–281. doi:10.1016/S0167-2738(98)00192-1.

[40] T. Ishigaki, S. Yamauchi, J. Mizusaki, K. Fueki, H. Tamura, Tracer diffusion coefficient of oxide ions in $LaCoO_3$ single crystal, J. Solid State Chem. 54 (1984) 100–107. doi:10.1016/0022-4596(84)90136-1.

[41] F. Figueiredo, J.R. Frade, F.M.B. Marques, Electrical and electrochemical behaviour of $LaCoO_{3-\delta}$ + $La_2(Zr,Y)_2O_7$-based electrode materials, Solid State Ionics. 118 (1999) 81–87. doi:10.1016/S0167-2738(98)00470-6.

[42] T. Ishigaki, S. Yamauchi, J. Mizusaki, K. Fueki, H. Naito, T. Adachi, Diffusion of oxide ions in $LaFeO_3$ single crystal, J. Solid State Chem. 55 (1984) 50–53. doi:10.1016/0022-4596(84)90246-9.

[43] D.O. Bannikov, V.A. Cherepanov, Thermodynamic properties of complex oxides in the La–Ni–

O system, J. Solid State Chem. 179 (2006) 2721–2727. doi:10.1016/j.jssc.2006.05.026.

[44] W.Z. Zhu, S.C. Deevi, Development of interconnect materials for solid oxide fuel cells, Mater. Sci. Eng. A. 348 (2003) 227–243. doi:10.1016/S0921-5093(02)00736-0.

[45] H. Hayashi, M. Watanabe, H. Inaba, Measurement of thermal expansion coefficient of $LaCrO_3$, Thermochim. Acta. 359 (2000) 77–85. doi:10.1016/S0040-6031(00)00507-4.

[46] F. Tietz, I. Arul Raj, M. Zahid, D. Stover, Electrical conductivity and thermal expansion of $La_{0.8}Sr_{0.2}(Mn,Fe,Co)O_{3-\delta}$ perovskites, Solid State Ionics. 177 (2006) 1753–1756. doi:10.1016/j.ssi.2005.12.017.

[47] Z. Li, M. Behruzi, L. Fuerst, D. Stöver, Crystalline Structure and Electrical Conductivity of Bulk-Sintered and Plasma-Sprayed $La_{1-x}Sr_xMnO_{3-\delta}$ with $0 \leq x \leq 0.9$, ECS Proc. Vol. 1993–4 (1993) 171–179. doi:10.1149/199304.0171PV.

[48] I. Yasuda, M. Hishinuma, Electrical Conductivity and Chemical Diffusion Coefficient of Strontium-Doped Lanthanum Manganites, J. Solid State Chem. 123 (1996) 382–390. doi:10.1006/jssc.1996.0193.

[49] H. Kamata, Y. Yonemura, J. Mizusaki, H. Tagawa, K. Naraya, T. Sasamoto, High temperature electrical properties of the perovskite-type oxide $La_{1-x}Sr_xMnO_{3-d}$, J. Phys. Chem. Solids. 56 (1995) 943–950. doi:10.1016/0022-3697(95)00019-4.

[50] J. Hwang, Y. Ando, S. Watanabe, Materials Search of Perovskite Cathode in SOFC by Statistical Analysis, ECS Trans. 68 (2015) 549–556. doi:10.1149/06801.0549ecst.

[51] Y. Ji, J.A. Kilner, M.F. Carolan, Electrical properties and oxygen diffusion in yttria-stabilised zirconia (YSZ)-$La_{0.8}Sr_{0.2}MnO_{3\pm\delta}$ (LSM) composites, Solid State Ionics. 176 (2005) 937–943. doi:10.1016/j.ssi.2004.11.019.

[52] I. Yasuda, K. Ogasawara, M. Hishinuma, T. Kawada, M. Dokiya, Oxygen tracer diffusion coefficient of (La, Sr)$MnO_{3\pm\delta}$, Solid State Ionics. 86–88 (1996) 1197–1201. doi:10.1016/0167-2738(96)00287-1.

[53] J. Richter, P. Holtappels, T. Graule, T. Nakamura, L.J. Gauckler, Materials design for perovskite SOFC cathodes, Monatshefte Für Chemie - Chem. Mon. 140 (2009) 985–999. doi:10.1007/s00706-009-0153-3.

[54] A. Weber, E. Ivers-Tiffée, Materials and concepts for solid oxide fuel cells (SOFCs) in stationary and mobile applications, J. Power Sources. 127 (2004) 273–283.

doi:10.1016/j.jpowsour.2003.09.024.

[55] B.C.H. Steele, Survey of materials selection for ceramic fuel cells II. Cathodes and anodes, Solid State Ionics. 86–88 (1996) 1223–1234. doi:10.1016/0167-2738(96)00291-3.

[56] F. Tietz, Thermal expansion of SOFC materials, Ionics (Kiel). 5 (1999) 129–139. doi:10.1007/BF02375916.

[57] Y. Sakaki, Y. Takeda, A. Kato, N. Imanishi, O. Yamamoto, M. Hattori, M. Iio, Y. Esaki, $Ln_{1-x}Sr_xMnO_3$ (Ln=Pr, Nd, Sm and Gd) as the cathode material for solid oxide fuel cells, Solid State Ionics. 118 (1999) 187–194. doi:10.1016/S0167-2738(98)00440-8.

[58] T. Ishiham, T. Kudo, H. Matsuda, Y. Takita, Doped Perovskite Oxide, $PrMnO_3$, as a New Cathode for Solid-Oxide Fuel Cells that Decreases the Operating Temperature, J. Am. Ceram. Soc. 77 (1994) 1682–1684. doi:10.1111/j.1151-2916.1994.tb09779.x.

[59] S. Carter, A. Selcuk, R.J. Chater, J. Kajda, J.A. Kilner, B.C.H. Steele, Oxygen transport in selected nonstoichiometric perovskite-structure oxides, Solid State Ionics. 53–56 (1992) 597–605. doi:10.1016/0167-2738(92)90435-R.

[60] R.A. De Souza, J.. Kilner, Oxygen transport in $La_{1-x}Sr_xMn_{1-y}Co_yO_{3\pm\delta}$ perovskites Part I. Oxygen tracer diffusion, Solid State Ionics. 106 (1998) 175–187. doi:10.1016/S0167-2738(97)00499-2.

[61] A. Belzner, T. Gur, R. Huggins, Oxygen chemical diffusion in strontium doped lanthanum manganites, Solid State Ionics. 57 (1992) 327–337. doi:10.1016/0167-2738(92)90166-M.

[62] L.-W. Tai, M.M. Nasrallah, H.U. Anderson, D.M. Sparlin, S.R. Sehlin, Structure and electrical properties of $La_{1-x}Sr_xCo_{1-y}Fe_yO_3$. Part 2. The system $La_{1-x}Sr_xCo_{0.2}Fe_{0.8}O_3$, Solid State Ionics. 76 (1995) 273–283. doi:10.1016/0167-2738(94)00245-N.

[63] M. Chen, B.H. Moon, S.H. Kim, B.H. Kim, Q. Xu, B.-G. Ahn, Characterization of $La_{0.6}Sr_{0.4}Co_{0.2}Fe_{0.8}O_{3-\delta}$ + $La_2NiO_{4+\delta}$ Composite Cathode Materials for Solid Oxide Fuel Cells, Fuel Cells. 12 (2012) 86–96. doi:10.1002/fuce.201100106.

[64] A. Petric, P. Huang, F. Tietz, Evaluation of La–Sr–Co–Fe–O perovskites for solid oxide fuel cells and gas separation membranes, Solid State Ionics. 135 (2000) 719–725. doi:10.1016/S0167-2738(00)00394-5.

[65] F. Shen, K. Lu, Perovskite-type $La_{0.6}Sr_{0.4}Co_{0.2}Fe_{0.8}O_3$, $Ba_{0.5}Sr_{0.5}Co_{0.2}Fe_{0.8}O_3$, and $Sm_{0.5}Sr_{0.5}Co_{0.2}Fe_{0.8}O_3$ cathode materials and their chromium poisoning for solid oxide fuel cells, Electrochim. Acta. 211 (2016) 445–452. doi:10.1016/j.electacta.2016.06.070.

[66] J.W. Stevenson, T.R. Armstrong, R.D. Carneim, L.R. Pederson, W.J. Weber, Electrochemical properties of mixed conducting perovskites La1-xMxCo1-yFeyO3-δ (M = Sr, Ba, Ca), J. Electrochem. Soc. 143 (1996) 2722–2729. doi:10.1149/1.1837098.

[67] H. Ullmann, N. Trofimenko, F. Tietz, D. Stöver, A. Ahmad-Khanlou, Correlation between thermal expansion and oxide ion transport in mixed conducting perovskite-type oxides for SOFC cathodes, Solid State Ionics. 138 (2000) 79–90. doi:10.1016/S0167-2738(00)00770-0.

[68] M. Sahibzada, S.J. Benson, R.A. Rudkin, J.A. Kilner, Pd-promoted $La_{0.6}Sr_{0.4}Co_{0.2}Fe_{0.8}O$ cathodes, Solid State Ionics. 113–115 (1998) 285–290. doi:10.1016/S0167-2738(98)00294-X.

[69] P. Ried, E. Bucher, W. Preis, W. Sitte, P. Holtappels, Characterisation of $La_{0.6}Sr_{0.4}Co_{0.2}Fe_{0.8}O_{3-\delta}$ and $Ba_{0.5}Sr_{0.5}Co_{0.8}Fe_{0.2}O_{3-\delta}$ as Cathode Materials for the Application in Intermediate Temperature Fuel Cells, in: ECS Trans., ECS, 2007: pp. 1217–1224. doi:10.1149/1.2729221.

[70] K. Dumaisnil, D. Fasquelle, M. Mascot, A. Rolle, P. Roussel, S. Minaud, B. Duponchel, R.-N. Vannier, J.-C. Carru, Synthesis and characterization of $La_{0.6}Sr_{0.4}Co_{0.8}Fe_{0.2}O_3$ films for solid oxide fuel cell cathodes, Thin Solid Films. 553 (2014) 89–92. doi:10.1016/j.tsf.2013.11.136.

[71] Y.-P. Fu, A. Subardi, M.-Y. Hsieh, W.-K. Chang, Electrochemical Properties of $La_{0.5}Sr_{0.5}Co_{0.8}M_{0.2}O_{3-\delta}$ (M=Mn, Fe, Ni, Cu) Perovskite Cathodes for IT-SOFCs, J. Am. Ceram. Soc. 99 (2016) 1345–1352. doi:10.1111/jace.14127.

[72] L.-W. Tai, M.M. Nasrallah, H.U. Anderson, D.M. Sparlin, S.R. Sehlin, Structure and electrical properties of $La_{1-x}Sr_xCo_{1-y}Fe_yO_3$. Part 1. The system $La_{0.8}Sr_{0.2}Co_{1-y}Fe_yO_3$, Solid State Ionics. 76 (1995) 259–271. doi:10.1016/0167-2738(94)00244-M.

[73] A. Egger, E. Bucher, W. Sitte, Oxygen Exchange Kinetics of the IT-SOFC Cathode Material $Nd_2NiO_{4+\delta}$ and Comparison with $La_{0.6}Sr_{0.4}CoO_{3-\delta}$, J. Electrochem. Soc. 158 (2011) B573–B579. doi:10.1149/1.3569697.

[74] E. V. Bongio, H. Black, F.C. Raszewski, D. Edwards, C.J. McConville, V.R.W. Amarakoon, Microstructural and High-Temperature Electrical Characterization of $La_{1-x}Sr_xFeO_{3-\delta}$, J. Electroceramics. 14 (2005) 193–198. doi:10.1007/s10832-005-0957-4.

[75] S.P. Simner, J.F. Bonnett, N.L. Canfield, K.D. Meinhardt, V.L. Sprenkle, J.W. Stevenson, Optimized Lanthanum Ferrite-Based Cathodes for Anode-Supported SOFCs, Electrochem. Solid-State Lett. 5 (2002) A173–A175. doi:10.1149/1.1483156.

[76] J. Bahteeva, I. Leonidov, M. Patrakeev, E. Mitberg, V. Kozhevnikov, K. Poeppelmeier, High-temperature ion transport in $La_{1-x}Sr_xFeO_{3-\delta}$, J. Solid State Electrochem. 8 (2004) 578–584.

doi:10.1007/s10008-003-0486-5.

[77] R. Ganeshananthan, A. V Virkar, Surface Exchange Coefficient Measurements on Porous $La_{0.8}Sr_{0.2}FeO_{3-\delta}$ by Conductivity Relaxation, in: 206th ECS Meet. October 3-8, Honolulu, HI, 2004. https://www.electrochem.org/dl/ma/206/pdfs/1684.pdf.

[78] R. Chiba, F. Yoshimura, Y. Sakurai, An investigation of $LaNi_{1-x}Fe_xO_3$ as a cathode material for solid oxide fuel cells, Solid State Ionics. 124 (1999) 281–288. doi:10.1016/S0167-2738(99)00222-2.

[79] R.N. Basu, F. Tietz, O. Teller, E. Wessel, H.P. Buchkremer, D. Stöver, $LaNi_{0.6}Fe_{0.4}O_3$ as a cathode contact material for solid oxide fuel cells, J. Solid State Electrochem. 7 (2003) 416–420. doi:10.1007/s10008-002-0330-3.

[80] M. Nishi, T. Horita, K. Yamaji, H. Yokokawa, T. Shimonosono, H. Kishimoto, M.E. Brito, D.H. Cho, F. Wang, Oxide Ion Conductivity of $LaNi_{0.6}Fe_{0.4}O_3$, ECS Trans. 45 (2012) 171–180. doi:10.1149/1.3701306.

[81] X. Li, X. Jiang, S. Pang, Q. Wang, Z. Su, Q. Zhang, Effect of iron substitution content on structure, thermal expansion behavior and electrochemical properties of $La_{0.5}Ba_{0.5}Co_{1-y}Fe_yO_{3-\delta}$, Int. J. Hydrogen Energy. 36 (2011) 13850–13857. doi:10.1016/j.ijhydene.2011.07.083.

[82] W. Chen, T. Wen, H. Nie, R. Zheng, Study of $Ln_{0.6}Sr_{0.4}Co_{0.8}Mn_{0.2}O_{3-\delta}$ (Ln=La, Gd, Sm or Nd) as the cathode materials for intermediate temperature SOFC, Mater. Res. Bull. 38 (2003) 1319–1328. doi:10.1016/S0025-5408(03)00143-0.

[83] X. Meng, S. Lü, Y. Ji, T. Wei, Y. Zhang, Characterization of $Pr_{1-x}Sr_xCo_{0.8}Fe_{0.2}O_{3-\delta}$ ($0.2 \le x \le 0.6$) cathode materials for intermediate-temperature solid oxide fuel cells, J. Power Sources. 183 (2008) 581–585. doi:10.1016/j.jpowsour.2008.05.052.

[84] G.C. Kostogloudis, N. Vasilakos, C. Ftikos, Preparation and characterization of $Pr_{1-x}Sr_xMnO_{3\pm\delta}$ (x = 0, 0.15, 0.3, 0.4, 0.5) as a potential SOFC cathode material operating at intermediate temperatures (500–700 °C), J. Eur. Ceram. Soc. 17 (1997) 1513–1521. doi:10.1016/S0955-2219(97)00038-1.

[85] T. Ishihara, T. Kudo, H. Matsuda, Y. Takita, Doped $PrMnO_3$ Perovskite Oxide as a New Cathode of Solid Oxide Fuel Cells for Low Temperature Operation, J. Electrochem. Soc. 142 (1995) 1519–1524. doi:10.1149/1.2048606.

[86] H.-R. Rim, S.-K. Jeung, E. Jung, J.-S. Lee, Characteristics of $Pr_{1-x}M_xMnO_3$ (M = Ca, Sr) as

cathode material in solid oxide fuel cells, Mater. Chem. Phys. 52 (1998) 54–59. doi:10.1016/S0254-0584(98)80006-0.

[87] T.-L. Wen, N. Sammes, O. Yamamoto, Ln(Pr, Nd, Sm, Gd, Yb and Y) Manganite Cathode Materials for SOFC Applications, ECS Proc. Vol. 1995–1 (1995) 463–471. doi:10.1149/199501.0463PV.

[88] J. Richter, P. Holtappels, T. Graule, L. Gauckler, Non-stoichiometry, thermal expansion and electrical properties of $Pr_{1-x}Sr_xMn_{1-y}In_yO_{3-\delta}$ perovskites, Solid State Ionics. 179 (2008) 2284–2289. doi:10.1016/j.ssi.2008.08.007.

[89] C. Zhu, X. Liu, D. Xu, D. Yan, D. Wang, W. Su, Preparation and performance of $Pr_{0.7}Sr_{0.3}Co_{1-y}Cu_yO_{3-\delta}$ as cathode material of IT-SOFCs, Solid State Ionics. 179 (2008) 1470–1473. doi:10.1016/j.ssi.2008.01.031.

[90] G. Kostogloudis, N. Vasilakos, C. Ftikos, Crystal structure, thermal and electrical properties of $Pr_{1-x}Sr_xCoO_{3-\delta}$ (x=0, 0.15, 0.3, 0.4, 0.5) perovskite oxides, Solid State Ionics. 106 (1998) 207–218. doi:10.1016/S0167-2738(97)00506-7.

[91] F. Dong, D. Chen, R. Ran, H. Park, C. Kwak, Z. Shao, A comparative study of $Sm_{0.5}Sr_{0.5}MO_{3-\delta}$ (M = Co and Mn) as oxygen reduction electrodes for solid oxide fuel cells, Int. J. Hydrogen Energy. 37 (2012) 4377–4387. doi:10.1016/j.ijhydene.2011.11.150.

[92] S. Yang, T. He, Q. He, $Sm_{0.5}Sr_{0.5}CoO_3$ cathode material from glycine-nitrate process: Formation, characterization, and application in $LaGaO_3$-based solid oxide fuel cells, J. Alloys Compd. 450 (2008) 400–404. doi:10.1016/j.jallcom.2006.10.147.

[93] H. Lv, Y. Wu, B. Huang, B. Zhao, K. Hu, Structure and electrochemical properties of $Sm_{0.5}Sr_{0.5}Co_{1-x}Fe_xO_{3-\delta}$ cathodes for solid oxide fuel cells, Solid State Ionics. 177 (2006) 901–906. doi:10.1016/j.ssi.2006.01.038.

[94] Y.-P. Fu, J. Ouyang, C.-H. Li, S.-H. Hu, Chemical bulk diffusion coefficient of $Sm_{0.5}Sr_{0.5}CoO_{3-\delta}$ cathode for solid oxide fuel cells, J. Power Sources. 240 (2013) 168–177. doi:10.1016/j.jpowsour.2013.03.138.

[95] B. Wei, Z. Lü, X. Huang, J. Miao, X. Sha, X. Xin, W. Su, Crystal structure, thermal expansion and electrical conductivity of perovskite oxides $Ba_xSr_{1-x}Co_{0.8}Fe_{0.2}O_{3-\delta}$ ($0.3 \le x \le 0.7$), J. Eur. Ceram. Soc. 26 (2006) 2827–2832. doi:10.1016/j.jeurceramsoc.2005.06.047.

[96] D. Chen, Z. Shao, Surface exchange and bulk diffusion properties of $Ba_{0.5}Sr_{0.5}Co_{0.8}Fe_{0.2}O_{3-\delta}$ mixed conductor, Int. J. Hydrogen Energy. 36 (2011) 6948–6956.

doi:10.1016/j.ijhydene.2011.02.087.

[97] Z. Chen, R. Ran, W. Zhou, Z. Shao, S. Liu, Assessment of $Ba_{0.5}Sr_{0.5}Co_{1-y}Fe_yO_{3-\delta}$ (y=0.0–1.0) for prospective application as cathode for IT-SOFCs or oxygen permeating membrane, Electrochim. Acta. 52 (2007) 7343–7351. doi:10.1016/j.electacta.2007.06.010.

[98] Z. Qingshan, J. Tongan, W. Yong, Thermal expansion behavior and chemical compatibility of $Ba_xSr_{1-x}Co_{1-y}Fe_yO_{3-\delta}$ with 8YSZ and 20GDC, Solid State Ionics. 177 (2006) 1199–1204. doi:10.1016/j.ssi.2006.04.029.

[99] C. Huang, D. Chen, Y. Lin, R. Ran, Z. Shao, Evaluation of $Ba_{0.6}Sr_{0.4}Co_{0.9}Nb_{0.1}O_{3-\delta}$ mixed conductor as a cathode for intermediate-temperature oxygen-ionic solid-oxide fuel cells, J. Power Sources. 195 (2010) 5176–5184. doi:10.1016/j.jpowsour.2010.02.080.

[100] J. Zhao, K. Zhang, D. Gao, Z. Shao, S. Liu, Optimization of $Ba_xSr_{1-x}Co_{0.9}Nb_{0.1}O_{3-\delta}$ perovskite as oxygen semi-permeable membranes by compositional tailoring, Sep. Purif. Technol. 71 (2010) 152–159. doi:10.1016/j.seppur.2009.11.014.

[101] S. Huang, G. Wang, X. Sun, C. Lei, T. Li, C. Wang, Cobalt-free perovskite $Ba_{0.5}Sr_{0.5}Fe_{0.9}Nb_{0.1}O_{3-\delta}$ as a cathode material for intermediate temperature solid oxide fuel cells, J. Alloys Compd. 543 (2012) 26–30. doi:10.1016/j.jallcom.2012.07.115.

[102] Y. Lin, W. Zhou, J. Sunarso, R. Ran, Z. Shao, Characterization and evaluation of $BaCo_{0.7}Fe_{0.2}Nb_{0.1}O_{3-\delta}$ as a cathode for proton-conducting solid oxide fuel cells, Int. J. Hydrogen Energy. 37 (2012) 484–497. doi:10.1016/j.ijhydene.2011.09.010.

[103] D. Huang, Q. Xu, F. Zhang, W. Chen, H. Liu, J. Zhou, Synthesis and electrical conductivity of $La_2NiO_{4+\delta}$ derived from a polyaminocarboxylate complex precursor, Mater. Lett. 60 (2006) 1892–1895. doi:10.1016/j.matlet.2005.12.044.

[104] G. Amow, I.. Davidson, S.. Skinner, A comparative study of the Ruddlesden-Popper series, $La_{n+1}Ni_nO_{3n+1}$ (n=1, 2 and 3), for solid-oxide fuel-cell cathode applications, Solid State Ionics. 177 (2006) 1205–1210. doi:10.1016/j.ssi.2006.05.005.

[105] S. Yoo, S. Choi, J. Shin, M. Liu, G. Kim, Electrical properties, thermodynamic behavior, and defect analysis of $La_{n+1}Ni_nO_{3n+1+\delta}$ infiltrated into YSZ scaffolds as cathodes for intermediate-temperature SOFCs, RSC Adv. 2 (2012) 4648–4655. doi:10.1039/c2ra20402a.

[106] H. Zhao, F. Mauvy, C. Lalane, J. Bassat, S. Fourcade, J. Grenier, New cathode materials for ITSOFC: Phase stability, oxygen exchange and cathode properties of $La_{2-x}NiO_{4+\delta}$, Solid State Ionics. 179 (2008) 2000–2005. doi:10.1016/j.ssi.2008.06.019.

[107] S. Skinner, J.A. Kilner, Oxygen diffusion and surface exchange in $La_{2-x}Sr_xNiO_{4+\delta}$, Solid State Ionics. 135 (2000) 709–712. doi:10.1016/S0167-2738(00)00388-X.

[108] S.J. Skinner, J.A. Kilner, A comparison of the transport properties of $La_{2-x}Sr_xNi_{1-y}Fe_yO_{4+\delta}$ where 0<x<0.2 and 0<y<0.2, Ionics (Kiel). 5 (1999) 171–174. doi:10.1007/BF02375836.

[109] E. Boehm, J. Bassat, P. Dordor, F. Mauvy, J. Grenier, P. Stevens, Oxygen diffusion and transport properties in non-stoichiometric $Ln_{2-x}NiO_{4+\delta}$ oxides, Solid State Ionics. 176 (2005) 2717–2725. doi:10.1016/j.ssi.2005.06.033.

[110] S.P.S. Badwal, R. Deller, K. Foger, Y. Ramprakash, J.P. Zhang, Interaction between chromia forming alloy interconnects and air electrode of solid oxide fuel cells, Solid State Ionics. 99 (1997) 297–310. doi:10.1016/S0167-2738(97)00247-6.

[111] B. Hu, S. Krishnan, C. Liang, S.J. Heo, A.N. Aphale, R. Ramprasad, P. Singh, Experimental and thermodynamic evaluation of $La_{1-x}Sr_xMnO_{3\pm\delta}$ and $La_{1-x}Sr_xCo_{1-y}Fe_yO_{3-\delta}$ cathodes in Cr-containing humidified air, Int. J. Hydrogen Energy. 42 (2017) 10208–10216. doi:10.1016/J.IJHYDENE.2017.01.040.

[112] Y. Matsuzaki, I. Yasuda, Dependence of SOFC Cathode Degradation by Chromium-Containing Alloy on Compositions of Electrodes and Electrolytes, J. Electrochem. Soc. 148 (2001) A126. doi:10.1149/1.1339869.

[113] L.G.J. De Haart, J. Mougin, O. Posdziech, J. Kiviaho, N.H. Menzler, Stack degradation in dependence of operation parameters; the real-SOFC sensitivity analysis, Fuel Cells. 9 (2009) 794–804. doi:10.1002/fuce.200800146.

[114] R. Steinberger-Wilckens, O. Bucheli, L.G.J. De Haart, A. Hagen, J. Kiviaho, J. Larsen, S. Pyke, B. Rietveld, J. Sfeir, F. Tietz, M. Zahid, Real-SOFC - A joint European effort to improve SOFC durability, ECS Trans. 25 (2009) 43–56. doi:10.1149/1.3205507.

[115] D. Roehrens, A. Neumann, A. Beez, I.C. Vinke, L.G.J. De Haart, N.H. Menzler, Formation of chromium containing impurities in (La,Sr)MnO_3 solid-oxide-fuel-cell cathodes under stack operating conditions and its effect on performance, Ceram. Int. 42 (2016) 9467–9474. doi:10.1016/j.ceramint.2016.03.010.

[116] L. Blum, L.G.J. De Haart, J. Malzbender, N.H. Menzler, J. Remmel, R. Steinberger-Wilckens, Recent results in Jülich solid oxide fuel cell technology development, J. Power Sources. 241 (2013) 477–485. doi:10.1016/j.jpowsour.2013.04.110.

[117] A.A. Kulikovsky, H. Scharmann, K. Wippermann, Dynamics of fuel cell performance

degradation, Electrochem. Commun. 6 (2004) 75–82. doi:10.1016/j.elecom.2003.10.018.

[118] R. Steinberger-Wilckens, J. Mergel, A. Glusen, K. Wippermann, I. Vinke, P. Batfalsky, M. Smith, Performance degradation and failure mechanisms of fuel cell materials, in: M. Gasik (Ed.), Mater. Fuel Cells, Woodhead Publishing Limited, 2008: pp. 425–465.

[119] J. Li, D. Yan, W. zhang, J. Pu, B. Chi, L. Jian, The investigation of Cr deposition and poisoning effect on Sr-doped lanthanum manganite cathode induced by cathodic polarization for intermediate temperature solid oxide fuel cell, Electrochim. Acta. 255 (2017) 31–40. doi:10.1016/J.ELECTACTA.2017.09.112.

[120] S.P. Jiang, J.P. Zhang, L. Apateanu, K. Foger, Deposition of Chromium Species at Sr-Doped $LaMnO_3$ Electrodes in Solid Oxide Fuel Cells I. Mechanism and Kinetics, J. Electrochem. Soc. 147 (2000) 4013–4022. http://jes.ecsdl.org/cgi/doi/10.1149/1.1393883.

[121] H. Yokokawa, T. Horita, N. Sakai, K. Yamaji, M.E. Brito, Y.-P. Xiong, H. Kishimoto, Thermodynamic considerations on Cr poisoning in SOFC cathodes, Solid State Ionics. 177 (2006) 3193–3198. doi:10.1016/J.SSI.2006.07.055.

[122] M. Krumpelt, T.A. Cruse, B.J. Ingram, J.L. Routbort, S. Wang, P.A. Salvador, G. Chen, The Effect of Chromium Oxyhydroxide on Solid Oxide Fuel Cells, J. Electrochem. Soc. 157 (2010) B228–B233. doi:10.1149/1.3266930.

[123] S.C. Paulson, V.I. Birss, Chromium Poisoning of LSM-YSZ SOFC Cathodes I. Detailed Study of the Distribution of Chromium Species at a Porous Single-Phase Cathode, J. Electrochem. Soc. 151 (2004) A1961–A1968. doi:10.1149/1.1806392.

[124] S.P. Jiang, S. Zhang, Y.D. Zhen, Early interaction between Fe–Cr alloy metallic interconnect and Sr-doped $LaMnO_3$ cathodes of solid oxide fuel cells, J. Mater. Res. 20 (2005) 747–758. doi:10.1557/JMR.2005.0101.

[125] S.P. Jiang, J.P. Zhang, K. Foger, Deposition of Chromium Species at Sr-Doped $LaMnO_3$ Electrodes in Solid Oxide Fuel Cells II. Effect on O_2 Reduction Reaction, J. Electrochem. Soc. 147 (2000) 3195–3205. doi:10.1149/1.1393883.

[126] S.P. Jiang, J.P. Zhang, K. Foger, Deposition of Chromium Species at Sr-Doped $LaMnO_3$ Electrodes in Solid Oxide Fuel Cells III. Effect of Air Flow, J. Electrochem. Soc. 148 (2000) C447–C455. http://jes.ecsdl.org/cgi/doi/10.1149/1.1393883.

[127] S.P. Jiang, J.P. Zhang, X.G. Zheng, A comparative investigation of chromium deposition at air electrodes of solid oxide fuel cells, J. Eur. Ceram. Soc. 22 (2002) 361–373. doi:10.1016/S0955-

2219(01)00280-1.

[128] H.Y. Lee, W.S. Cho, S.M. Oh, H. -D. Wiemhöfer, W. Göpel, Active Reaction Sites for Oxygen Reduction in $La_{0.9}Sr_{0.1}MnO_3$/YSZ Electrodes, J. Electrochem. Soc. 142 (1995) 2659–2664. doi:10.1149/1.2050070.

[129] E. Konysheva, J. Mertens, H. Penkalla, L. Singheiser, K. Hilpert, Chromium Poisoning of the Porous Composite Cathode Effect of Cathode Thickness and Current Density, J. Electrochem. Soc. 154 (2007) B1252–B1264. doi:10.1149/1.2784197.

[130] T. Jin, K. Lu, Chemical compatibility between Sr-doped lanthanum manganite air electrode and AISI 441 interconnect, Int. J. Hydrogen Energy. 36 (2011) 4440–4448. doi:10.1016/j.ijhydene.2011.01.013.

[131] T. Jin, K. Lu, Surface and interface behaviors of $(La_{0.8}Sr_{0.2})_xMnO_3$ air electrode for solid oxide cells, J. Power Sources. 196 (2011) 8331–8339. doi:10.1016/j.jpowsour.2011.06.052.

[132] R. Wang, M. Würth, U.B. Pal, S. Gopalan, S.N. Basu, Roles of humidity and cathodic current in chromium poisoning of Sr-doped $LaMnO_3$-based cathodes in solid oxide fuel cells, J. Power Sources. 360 (2017) 87–97. doi:10.1016/j.jpowsour.2017.06.005.

[133] X. Chen, Y. Zhen, J. Li, S.P. Jiang, Chromium deposition and poisoning in dry and humidified air at $(La_{0.8}Sr_{0.2})_{0.9}MnO_{3+\delta}$ cathodes of solid oxide fuel cells, Int. J. Hydrogen Energy. 35 (2010) 2477–2485. doi:10.1016/J.IJHYDENE.2009.12.185.

[134] R. Wang, U.B. Pal, S. Gopalan, S.N. Basu, Chromium Poisoning Effects on Performance of (La,Sr)MnO_3 -Based Cathode in Anode-Supported Solid Oxide Fuel Cells, J. Electrochem. Soc. 164 (2017) F740–F747. doi:10.1149/2.0441707jes.

[135] A. Hagen, K. Neufeld, Y.L. Liu, Effect of Humidity in Air on Performance and Long-Term Durability of SOFCs, J. Electrochem. Soc. 157 (2010) B1343–B1348. doi:10.1149/1.3459904.

[136] T.A. Cruse, B.J. Ingram, M. Krumpelt, S. Wang, P.A. Salvador, Effects of operating conditions on degradation by chromium, in: TMS 2008 Suppl. Proc. Vol. I Mater. Process. Prop., The Minerals, Metals and Materials Society, Pennsylvania, 2008: pp. 573–579.

[137] M.C. Tucker, H. Kurokawa, C.P. Jacobson, L.C. De Jonghe, S.J. Visco, A fundamental study of chromium deposition on solid oxide fuel cell cathode materials, J. Power Sources. 160 (2006) 130–138. doi:10.1016/j.jpowsour.2006.02.017.

[138] J.A. Schuler, H. Yokokawa, C.F. Calderone, Q. Jeangros, Z. Wuillemin, A. Hessler-Wyser, J. Van

herle, Combined Cr and S poisoning in solid oxide fuel cell cathodes, J. Power Sources. 201 (2012) 112–120. doi:10.1016/J.JPOWSOUR.2011.10.123.

[139] A. Aphale, C. Liang, B. Hu, P. Singh, Chapter 6 – Cathode Degradation From Airborne Contaminants in Solid Oxide Fuel Cells: A Review, in: Solid Oxide Fuel Cell Lifetime Reliab., 2017: pp. 101–119. doi:10.1016/B978-0-08-101102-7.00006-4.

[140] S.P. Jiang, J.P. Zhang, Y. Ramprakash, D. Milosevic, K. Wilshier, An investigation of shelf-life of strontium doped $LaMnO_3$ materials, J. Mater. Sci. 35 (2000) 2735–2741. doi:10.1023/A:1004766212164.

[141] C.J. Fu, K.N. Sun, X.B. Chen, N.Q. Zhang, D.R. Zhou, Electrochemical properties of A-site deficient SOFC cathodes under Cr poisoning conditions, Electrochim. Acta. 54 (2009) 7305–7312. doi:10.1016/J.ELECTACTA.2009.07.055.

[142] T. Jin, K. Lu, Chromium deposition and interfacial interactions of an electrolyte-air electrode-interconnect tri-layer for solid oxide fuel cells, J. Power Sources. 202 (2012) 143–148. doi:10.1016/j.jpowsour.2011.10.092.

[143] K. Lu, F. Shen, R. Roberts, G. Doucette, M. McGuire, W. Li, $(LaSr)_xMnO_3$ cathode stoichiometry effects on electrochemical performance in contact with AISI 441 steel interconnect, J. Power Sources. 268 (2014) 379–387. doi:10.1016/J.JPOWSOUR.2014.06.051.

[144] A. Mitterdorfer, L.J. Gauckler, $La_2Zr_2O_7$ formation and oxygen reduction kinetics of the $La_{0.85}Sr_{0.15}Mn_yO_3$, $O_2(g)$ | YSZ system, Solid State Ionics. 111 (1998) 185–218. https://ac.els-cdn.com/S0167273898001957/1-s2.0-S0167273898001957-main.pdf?_tid=5ecbaa0a-1363-4d37-b1b0-54c8c91526d3&acdnat=1521542538_76026e88633d84d81c280c1fae1204ab (accessed March 20, 2018).

[145] M.J.L. Østergård, C. Clausen, C. Bagger, M. Mogensen, Manganite-zirconia composite cathodes for SOFC: Influence of structure and composition, Electrochim. Acta. 40 (1995) 1971–1981. doi:10.1016/0013-4686(94)00332-U.

[146] T. Kenjo, M. Nishiya, $LaMnO_3$ air cathodes containing ZrO_2 electrolyte for high temperature solid oxide fuel cells, Solid State Ionics. 57 (1992) 295–302. doi:10.1016/0167-2738(92)90161-H.

[147] S.P. Jiang, Y.D. Zhen, S. Zhang, Interaction Between Fe–Cr Metallic Interconnect and $(La,Sr)MnO_3$/YSZ Composite Cathode of Solid Oxide Fuel Cells, J. Electrochem. Soc. 153 (2006) A1511–A1517. doi:10.1149/1.2207060.

[148] Y.D. Zhen, S.P. Jiang, Transition Behavior for O_2 Reduction Reaction on (La,Sr)MnO_3/YSZ Composite Cathodes of Solid Oxide Fuel Cells, J. Electrochem. Soc. 153 (2006) A2245–A2254. doi:10.1149/1.2357712.

[149] J.A. Schuler, P. Tanasini, A. Hessler-Wyser, C. Comninellis, J. Van Herle, Cathode thickness-dependent tolerance to Cr-poisoning in solid oxide fuel cells, Electrochem. Commun. 12 (2010) 1682–1685. doi:10.1016/j.elecom.2010.09.024.

[150] A. Mai, V.A.C. Haanappel, F. Tietz, D. Stöver, Ferrite-based perovskites as cathode materials for anode-supported solid oxide fuel cells: Part II. Influence of the CGO interlayer, Solid State Ionics. 177 (2006) 2103–2107. doi:10.1016/J.SSI.2005.12.010.

[151] L. Blum, L.G.J. de Haart, J. Malzbender, N. Margaritis, N.H. Menzler, Anode-Supported Solid Oxide Fuel Cell Achieves 70 000 Hours of Continuous Operation, Energy Technol. 4 (2016) 939–942. doi:10.1002/ente.201600114.

[152] S.P. Jiang, S. Zhang, Y.D. Zhen, Deposition of Cr Species at (La,Sr)(Co,Fe)O_3 Cathodes of Solid Oxide Fuel Cells, J. Electrochem. Soc. 153 (2006) A127–A134. doi:10.1149/1.2136077.

[153] T. Komatsu, R. Chiba, H. Arai, K. Sato, Chemical compatibility and electrochemical property of intermediate-temperature SOFC cathodes under Cr poisoning condition, J. Power Sources. 176 (2008) 132–137. doi:10.1016/j.jpowsour.2007.10.068.

[154] Z. Pan, Q. Liu, L. Zhang, X. Zhang, S.H. Chan, Effect of Sr Surface Segregation of $La_{0.6}Sr_{0.4}Co_{0.2}Fe_{0.8}O_{3-\delta}$ Electrode on Its Electrochemical Performance in SOC, J. Electrochem. Soc. 162 (2015) F1316–F1323. doi:10.1149/2.0371512jes.

[155] S.P. Simner, M.D. Anderson, M.H. Engelhard, J.W. Stevenson, Degradation Mechanisms of La–Sr–Co–Fe–O_3 SOFC Cathodes, Electrochem. Solid-State Lett. 9 (2006) A478. doi:10.1149/1.2266160.

[156] D. Oh, D. Gostovic, E.D. Wachsman, Mechanism of $La_{0.6}Sr_{0.4}Co_{0.2}Fe_{0.8}O_3$ cathode degradation, J. Mater. Res. 27 (2012) 1992–1999. doi:10.1557/jmr.2012.222.

[157] L. Zhao, J. Drennan, C. Kong, S. Amarasinghe, S.P. Jiang, Surface Segregation and Chromium Deposition and Poisoning on $La_{0.6}Sr_{0.4}Co_{0.2}Fe_{0.8}O_{3-\delta}$ Cathodes of Solid Oxide Fuel Cells, ECS Trans. 57 (2013) 599–604.

[158] L. Zhao, J. Zhang, T. Becker, S.P. Jiang, Raman Spectroscopy Study of Chromium Deposition on $La_{0.6}Sr_{0.4}Co_{0.2}Fe_{0.8}O_{3-\delta}$ Cathode of Solid Oxide Fuel Cells, J. Electrochem. Soc. 161 (2014) F687–F693. doi:10.1149/2.018406jes.

[159] H.. Tu, Y. Takeda, N. Imanishi, O. Yamamoto, $Ln_{0.4}Sr_{0.6}Co_{0.8}Fe_{0.2}O_{3-\delta}$ (Ln=La, Pr, Nd, Sm, Gd) for the electrode in solid oxide fuel cells, Solid State Ionics. 117 (1999) 277–281. doi:10.1016/S0167-2738(98)00428-7.

[160] H. Uchida, S. Arisaka, M. Watanabe, High Performance Electrode for Medium-Temperature Solid Oxide Fuel Cells La(Sr)CoO_3 Cathode with Ceria Interlayer on Zirconia Electrolyte, Electrochem. Solid-State Lett. 2 (1999) 428. doi:10.1149/1.1390860.

[161] L. Zhao, J. Drennan, C. Kong, S. Amarasinghe, S.P. Jiang, Insight into surface segregation and chromium deposition on $La_{0.6}Sr_{0.4}Co_{0.2}Fe_{0.8}O_{3-\delta}$ cathodes of solid oxide fuel cells, J. Mater. Chem. A. 2 (2014) 11114–11123. doi:10.1039/C4TA01426J.

[162] C.C. Wang, T. Becker, K. Chen, L. Zhao, B. Wei, S.P. Jiang, Effect of temperature on the chromium deposition and poisoning of $La_{0.6}Sr_{0.4}Co_{0.2}Fe_{0.8}O_{3-\delta}$ cathodes of solid oxide fuel cells, Electrochim. Acta. 139 (2014) 173–179. doi:10.1016/j.electacta.2014.07.028.

[163] X. Chen, C. Jin, L. Zhao, L. Zhang, C. Guan, L. Wang, Y.F. Song, C.C. Wang, J.Q. Wang, S.P. Jiang, Study on the Cr deposition and poisoning phenomenon at $(La_{0.6}Sr_{0.4})(Co_{0.2}Fe_{0.8})O_{3-\delta}$ electrode of solid oxide fuel cells by transmission X-ray microscopy, Int. J. Hydrogen Energy. 39 (2014) 15728–15734. doi:10.1016/j.ijhydene.2014.07.112.

[164] N.H. Menzler, D. Sebold, E. Wessel, Interaction of $La_{0.58}Sr_{0.40}Co_{0.20}Fe_{0.80}O_{3-\delta}$ cathode with volatile Cr in a stack test - Scanning electron microscopy and transmission electron microscopy investigations, J. Power Sources. 254 (2014) 148–152. doi:10.1016/j.jpowsour.2013.12.066.

[165] C. Xiong, J.A. Taillon, C. Pellegrinelli, Y.-L. Huang, L.G. Salamanca-Riba, B. Chi, L. Jian, J. Pu, E.D.. Wachsman, Long-Term Cr Poisoning Effect on LSCF-GDC Composite Cathodes Sintered at Different Temperatures, J. Electrochem. Soc. 163 (2016) F1091–F1099. doi:10.1149/2.0841609jes.

[166] E.Y. Konysheva, Effect of current density on poisoning rate of Co-containing fuel cell cathodes by chromium, Russ. J. Electrochem. 50 (2014) 630–637. doi:10.1134/S1023193514070076.

[167] D. Oh, E. Armstrong, D. Jung, C. Kan, E. Wachsman, Mechanistic Understanding of Cr Poisoning on $La_{0.6}Sr_{0.4}Co_{0.2}Fe_{0.8}O_{3-\delta}$ (LSCF), ECS Trans. 25 (2009) 2871–2879. doi:10.1149/1.3205852.

[168] B. Wei, K. Chen, C.C. Wang, Z. Lü, S.P. Jiang, Cr deposition on porous $La_{0.6}Sr_{0.4}Co_{0.2}Fe_{0.8}O_{3-\delta}$ electrodes of solid oxide cells under open circuit condition, Solid State Ionics. 281 (2015) 29–

37. doi:10.1016/j.ssi.2015.08.018.

[169] J.J. Bentzen, J.V.T. Hogh, R. Barfod, A. Hagen, Chromium poisoning of LSM/YSZ and LSCF/CGO composite cathodes, Fuel Cells. 9 (2009) 823–832. doi:10.1002/fuce.200800143.

[170] E. Park, S. Taniguchi, J.-T. Chou, Y. Tachikawa, Y. Shiratori, K. Sasaki, Influence of Cathode Polarization on the Chromium Poisoning of SOFC Cathodes Consisting of LSM, LSCF and LNF, ECS Trans. 50 (2013) 21–25. doi:10.1149/05030.0021ecst.

[171] G.Y. Lau, M.C. Tucker, C.P. Jacobson, S.J. Visco, S.H. Gleixner, L.C. DeJonghe, Chromium transport by solid state diffusion on solid oxide fuel cell cathode, J. Power Sources. 195 (2010) 7540–7547. doi:10.1016/J.JPOWSOUR.2010.06.017.

[172] E. Bucher, M. Yang, W. Sitte, In Situ Investigations of the Chromium-Induced Degradation of the Oxygen Surface Exchange Kinetics of IT-SOFC Cathode Materials $La_{0.6}Sr_{0.4}CoO_{3-\delta}$ and $La_{0.58}Sr_{0.4}Co_{0.2}Fe_{0.8}O_{3-\delta}$, J. Electrochem. Soc. 159 (2012) B592–B596. doi:10.1149/2.027206jes.

[173] K. Schiemann, V. Vibhu, S. Yildiz, J. Mertens, I.C. Vinke, R.-A. Eichel, L.G.J. De Haart, Chrome poisoning of non-manganiferous cathode materials for solid oxide fuel cells (SOFCs), ECS Trans. 78 (2017) 1027–1034. doi:10.1149/07801.1027ecst.

[174] H. Ding, A. V. Virkar, M. Liu, F. Liu, Suppression of Sr surface segregation in $La_{1-x}Sr_xCo_{1-y}Fe_yO_{3-\delta}$: a first principles study, Phys. Chem. Chem. Phys. 15 (2013) 489–496. doi:10.1039/C2CP43148C.

[175] Y. Yu, K.F. Ludwig, J.C. Woicik, S. Gopalan, U.B. Pal, T.C. Kaspar, S.N. Basu, Effect of Sr Content and Strain on Sr Surface Segregation of $La_{1-x}Sr_xCo_{0.2}Fe_{0.8}O_{3-\delta}$ as Cathode Material for Solid Oxide Fuel Cells, ACS Appl. Mater. Interfaces. 8 (2016) 26704–26711. doi:10.1021/acsami.6b07118.

[176] W. Li, K. Lu, Z. Xia, Interaction of $(La_{1-x}Sr_x)_nCo_{1-y}Fe_yO_{3-\delta}$ cathodes and AISI 441 interconnect for solid oxide fuel cells, J. Power Sources. 237 (2013) 119–127. doi:10.1016/j.jpowsour.2013.03.012.

[177] L. Zhao, S. Amarasinghe, S.P. Jiang, Enhanced chromium tolerance of $La_{0.6}Sr_{0.4}Co_{0.2}Fe_{0.8}O_{3-\delta}$ electrode of solid oxide fuel cells by $Gd_{0.1}Ce_{0.9}O_{1.95}$ impregnation, Electrochem. Commun. 37 (2013) 84–87. doi:10.1016/J.ELECOM.2013.10.019.

[178] F. Shen, K. Lu, $La_{0.6}Sr_{0.4}Co_{0.2}Fe_{0.8}O_3$ cathodes incorporated with $Sm_{0.2}Ce_{0.8}O_2$ by three different methods for solid oxide fuel cells, J. Power Sources. 296 (2015) 318–326. doi:10.1016/j.jpowsour.2015.07.060.

[179] K. Chen, N. Ai, K.M. O'Donnell, S.P. Jiang, Highly chromium contaminant tolerant BaO infiltrated $La_{0.6}Sr_{0.4}Co_{0.2}Fe_{0.8}O_{3-\delta}$ cathodes for solid oxide fuel cells, Phys. Chem. Chem. Phys. 17 (2015) 4870–4874. doi:10.1039/C4CP04172K.

[180] M. Kubicek, A. Limbeck, T. Frömling, H. Hutter, J. Fleig, Relationship between Cation Segregation and the Electrochemical Oxygen Reduction Kinetics of $La_{0.6}Sr_{0.4}CoO_{3-\delta}$ Thin Film Electrodes, J. Electrochem. Soc. 158 (2011) B727. doi:10.1149/1.3581114.

[181] G.M. Rupp, H. Téllez, J. Druce, A. Limbeck, T. Ishihara, J. Kilner, J. Fleig, Surface chemistry of $La_{0.6}Sr_{0.4}CoO_{3-\delta}$ thin films and its impact on the oxygen surface exchange resistance, J. Mater. Chem. A. 3 (2015) 22759–22769. doi:10.1039/C5TA05279C.

[182] X. Chen, L. Zhang, E. Liu, S.P. Jiang, A fundamental study of chromium deposition and poisoning at $(La_{0.8}Sr_{0.2})_{0.95}(Mn_{1-x}Co_x)O_{3\pm\delta}$ ($0.0 \leq x \leq 1.0$) cathodes of solid oxide fuel cells, Int. J. Hydrogen Energy. 36 (2011) 805–821. doi:10.1016/J.IJHYDENE.2010.09.087.

[183] N. Schrödl, E. Bucher, C. Gspan, A. Egger, C. Ganser, C. Teichert, F. Hofer, W. Sitte, Phase decomposition in the chromium- and silicon-poisoned IT-SOFC cathode materials $La_{0.6}Sr_{0.4}CoO_{3-\delta}$ and $La_2NiO_{4+\delta}$, Solid State Ionics. 288 (2016) 14–21. doi:10.1016/j.ssi.2016.01.006.

[184] M. Yang, E. Bucher, W. Sitte, Effects of chromium poisoning on the long-term oxygen exchange kinetics of the solid oxide fuel cell cathode materials $La_{0.6}Sr_{0.4}CoO_3$ and Nd_2NiO_4, J. Power Sources. 196 (2011) 7313–7317. doi:10.1016/j.jpowsour.2010.10.064.

[185] N. Schrödl, E. Bucher, A. Egger, P. Kreiml, C. Teichert, T. Höschen, W. Sitte, Long-term stability of the IT-SOFC cathode materials $La_{0.6}Sr_{0.4}CoO_{3-\delta}$ and $La_2NiO_{4+\delta}$ against combined chromium and silicon poisoning, Solid State Ionics. 276 (2015) 62–71. doi:10.1016/j.ssi.2015.03.035.

[186] S. Kageyama, Y. Shindo, Y. Fujimaki, K. Mizuno, Y. Kimura, T. Nakamura, F. Iguchi, K. Yashiro, H. Yugami, T. Kawada, K. Amezawa, Correlation between electrode reaction and chromium deposition in SOFC cathodes, ECS Trans. 91 (2019) 1231–1237. doi:10.1149/09101.1231ecst.

[187] T. Horita, Y. Xiong, M. Yoshinaga, H. Kishimoto, K. Yamaji, M.E. Brito, H. Yokokawa, Determination of Chromium Concentration in Solid Oxide Fuel Cell Cathodes: (La,Sr)MnO_3 and (La,Sr)FeO_3, Electrochem. Solid-State Lett. 12 (2009) B146–B149. doi:10.1149/1.3193701.

[188] T. Horita, Y. Xiong, H. Kishimoto, K. Yamaji, M.E. Brito, H. Yokokawa, Chromium Poisoning and Degradation at (La,Sr)MnO_3 and (La,Sr)FeO_3 Cathodes for Solid Oxide Fuel Cells, J. Electrochem. Soc. 157 (2010) B614–B620. doi:10.1149/1.3322103.

[189] N. Shaigan, W. Qu, D.G. Ivey, W. Chen, A review of recent progress in coatings, surface modifications and alloy developments for solid oxide fuel cell ferritic stainless steel interconnects, J. Power Sources. 195 (2010) 1529–1542. doi:10.1016/J.JPOWSOUR.2009.09.069.

[190] J.A. Schuler, C. Gehrig, Z. Wuillemin, A.J. Schuler, J. Wochele, C. Ludwig, A. Hessler-Wyser, J. Van herle, Air side contamination in Solid Oxide Fuel Cell stack testing, J. Power Sources. 196 (2011) 7225–7231. doi:10.1016/J.JPOWSOUR.2010.10.058.

[191] K. Wang, J.W. Fergus, The Effect of Manganese Doping on Chromium Deposition at Pt/YSZ Cathode Interfaces, Electrochem. Solid-State Lett. 11 (2008) B156–B160. doi:10.1149/1.2938019.

[192] K. Wang, J.W. Fergus, The Effect of Transition-Metal Doping on Chromium Deposition at Pt/YSZ Cathode Interfaces, J. Electrochem. Soc. 157 (2010) B1008. doi:10.1149/1.3428384.

[193] S.P. Jiang, Y. Zhen, Mechanism of Cr deposition and its application in the development of Cr-tolerant cathodes of solid oxide fuel cells, Solid State Ionics. 179 (2008) 1459–1464. doi:10.1016/j.ssi.2008.01.006.

[194] T.. Komatsu, H.. Arai, R.. Chiba, K.. Nozawa, M.. Arakawa, K.. Sato, Cr poisoning suppression in solid oxide fuel cells using LaNi(Fe)O_3 electrodes, Electrochem. Solid-State Lett. 9 (2006) A9–A12. doi:10.1149/1.2130309.

[195] H. Orui, K. Watanabe, R. Chiba, M. Arakawa, Application of LaNi(Fe)O_3 as SOFC Cathode, J. Electrochem. Soc. 151 (2004) A1412. doi:10.1149/1.1779628.

[196] B. Huang, X.J. Zhu, Y. Lv, H. Liu, High-performance $Gd_{0.2}Ce_{0.8}O_2$-impregnated $LaNi_{0.6}Fe_{0.4}O_{3-\delta}$ cathodes for intermediate temperature solid oxide fuel cell, J. Power Sources. 209 (2012) 209–219. doi:10.1016/j.jpowsour.2012.02.103.

[197] Y.D. Zhen, A.I.Y. Tok, S.P. Jiang, F.Y.C. Boey, La(Ni,Fe)O_3 as a cathode material with high tolerance to chromium poisoning for solid oxide fuel cells, J. Power Sources. 170 (2007) 61–66. doi:10.1016/j.jpowsour.2007.03.079.

[198] Y. Zhen, A.I.Y. Tok, F.Y.C. Boey, S.P. Jiang, Development of Cr-Tolerant Cathodes of Solid Oxide Fuel Cells, Electrochem. Solid-State Lett. 11 (2008) B42–B46. doi:10.1149/1.2828212.

[199] T. Komatsu, Y. Yoshida, K. Watanabe, R. Chiba, H. Taguchi, H. Orui, H. Arai, Degradation behavior of anode-supported solid oxide fuel cell using LNF cathode as function of current load, J. Power Sources. 195 (2010) 5601–5605. doi:10.1016/J.JPOWSOUR.2010.03.078.

[200] M. Stodolny, F.P.. van Berkel, B.A. Boukamp, La(Ni,Fe)O_3 Stability in the Presence of Cr Species - Solid State Reactivity Study, ECS Trans. 25 (2009) 2915–2922. doi:10.1149/1.3205857.

[201] M.K. Stodolny, B.A. Boukamp, D.H.A. Blank, F.P.F. van Berkel, Impact of Cr-poisoning on the conductivity of $LaNi_{0.6}Fe_{0.4}O_3$, J. Power Sources. 196 (2011) 9290–9298. doi:10.1016/J.JPOWSOUR.2011.07.070.

[202] M.K. Stodolny, B.A. Boukamp, D.H.A. Blank, F.P.F. van Berkel, Cr-poisoning of a $LaNi_{0.6}Fe_{0.4}O_3$ cathode under current load, J. Power Sources. 209 (2012) 120–129. doi:10.1016/J.JPOWSOUR.2012.02.083.

[203] M.K. Stodolny, B.A. Boukamp, D.H.A. Blank, F.P.F. van Berkel, Impact of Cr-poisoning on the conductivity of different $LaNi_{0.6}Fe_{0.4}O_3$ cathode microstructures, Solid State Ionics. 225 (2012) 136–140. doi:10.1016/J.SSI.2012.04.004.

[204] Y.-J. Choe, J.-U. Seo, K.-J. Lee, M.-J. Lee, H.-J. Hwang, Cr-poisoning under open-circuit condition in $LaNi_{0.6}Fe_{0.4}O_{3-\delta}$-based nano composite cathodes for solid oxide fuel cells prepared by infiltration process, Trans. Nonferrous Met. Soc. China. 26 (2016) 1367–1372. doi:10.1016/S1003-6326(16)64240-1.

[205] B. Huang, X. Zhu, R. Ren, Y. Hu, X. Ding, Y. Liu, Z. Liu, Chromium poisoning and degradation at $Gd_{0.2}Ce_{0.8}O_2$-impregnated $LaNi_{0.6}Fe_{0.4}O_{3-\delta}$ cathode for solid oxide fuel cell, J. Power Sources. 216 (2012) 89–98. doi:10.1016/J.JPOWSOUR.2012.05.058.

[206] B. Huang, Y. Xing, L. Xu, X. Tan, S. Xu, H. Zhang, Y. Wang, Chromium poisoning and degradation at $LaNi_{0.6}Fe_{0.4}O_3$ cathode with $LaNi_{0.6}Fe_{0.4}O_3$–$Gd_{0.2}Ce_{0.8}O_2$ functional layer for SOFC under open circuit condition, J. Solid State Electrochem. 22 (2018) 2255–2265. doi:10.1007/s10008-018-3923-1.

[207] J. Chen, S. Wang, T. Wen, J. Li, Optimization of $LaNi_{0.6}Fe_{0.4}O_{3-\delta}$ cathode for intermediate temperature solid oxide fuel cells, J. Alloys Compd. 487 (2009) 377–381. doi:10.1016/J.JALLCOM.2009.07.125.

[208] X. Chen, L. Zhang, S.P. Jiang, Chromium Deposition and Poisoning on $(La_{0.6}Sr_{0.4-x}Ba_x)(Co_{0.2}Fe_{0.8})O_3$ ($0 \le x \le 0.4$) Cathodes of Solid Oxide Fuel Cells, J. Electrochem. Soc. 155 (2008) B1093–B1101. doi:10.1149/1.2969914.

[209] Y. Zhen, S.P. Jiang, Characterization and performance of (La,Ba)(Co,Fe)O_3 cathode for solid oxide fuel cells with iron-chromium metallic interconnect, J. Power Sources. 180 (2008) 695–

703. doi:10.1016/j.jpowsour.2008.02.093.

[210] C. Setevich, F. Prado, D.Z. De Florio, A. Caneiro, Stabilization of the cubic perovskite in the system $La_{1-x}Ba_xCo_{1-y}Fe_yO_{3-\delta}$ ($0.7 \leq x \leq 0.9$) and its electrochemical performance as cathode materials for intermediate-temperature solid oxide fuel cells, J. Power Sources. 247 (2014) 264–272. doi:10.1016/j.jpowsour.2013.08.091.

[211] X. Chen, S.P. Jiang, Highly active and stable $(La_{0.24}Sr_{0.16}Ba_{0.6})(Co_{0.5}Fe_{0.44}Nb_{0.06})O_{3-\delta}$ (LSBCFN) cathodes for solid oxide fuel cells prepared by a novel mixing synthesis method, J. Mater. Chem. A. 1 (2013) 4871. doi:10.1039/c3ta10230k.

[212] L. Lin, Q. Xu, Y.P. Wang, M. Chen, J. Xiao, D.P. Huang, F. Zhang, Property optimization for strontium-rich lanthanum chromium ferrite cathodes: A demonstration of lanthanide replacement effect, Mater. Res. Bull. 106 (2018) 263–270. doi:10.1016/j.materresbull.2018.05.031.

[213] M. Chen, S. Paulson, V. Thangadurai, V. Birss, Sr-rich chromium ferrites as symmetrical solid oxide fuel cell electrodes, J. Power Sources. 236 (2013) 68–79. doi:10.1016/j.jpowsour.2013.02.024.

[214] A.J. Fernández-Ropero, J.M. Porras-Vázquez, A. Cabeza, P.R. Slater, D. Marrero-López, E.R. Losilla, High valence transition metal doped strontium ferrites for electrode materials in symmetrical SOFCs, J. Power Sources. 249 (2014) 405–413. doi:10.1016/j.jpowsour.2013.10.118.

[215] J.M. Serra, V.B. Vert, M. Betz, V.A.C. Haanappel, W.A. Meulenberg, F. Tietz, Screening of A-substitution in the system $A_{0.68}Sr_{0.3}Fe_{0.8}Co_{0.2}O_{3-\delta}$ for SOFC cathodes, J. Electrochem. Soc. 155 (2008). doi:10.1149/1.2818766.

[216] Z. Shao, S.M. Haile, A high-performance cathode for the next generation of solid-oxide fuel cells, Nature. 431 (2004) 170–173. doi:10.1038/nature02863.

[217] C. Niedrig, S. Taufall, M. Burriel, W. Menesklou, S.F. Wagner, S. Baumann, E. Ivers-Tiffée, Thermal stability of the cubic phase in $Ba_{0.5}Sr_{0.5}Co_{0.8}Fe_{0.2}O_{3-\delta}$ (BSCF)1, Solid State Ionics. 197 (2011) 25–31. doi:10.1016/J.SSI.2011.06.010.

[218] A. Yan, M. Cheng, Y. Dong, W. Yang, V. Maragou, S. Song, P. Tsiakaras, Investigation of a $Ba_{0.5}Sr_{0.5}Co_{0.8}Fe_{0.2}O_{3-\delta}$ based cathode IT-SOFC: I. The effect of CO_2 on the cell performance, Appl. Catal. B Environ. 66 (2006) 64–71. doi:10.1016/J.APCATB.2006.02.021.

[219] A. Yan, V. Maragou, A. Arico, M. Cheng, P. Tsiakaras, Investigation of a $Ba_{0.5}Sr_{0.5}Co_{0.8}Fe_{0.2}O_{3-\delta}$

based cathode SOFC: II. The effect of CO_2 on the chemical stability, Appl. Catal. B Environ. 76 (2007) 320–327. doi:10.1016/J.APCATB.2007.06.010.

[220] H. Patra, S.K. Rout, S.K. Pratihar, S. Bhattacharya, Thermal, electrical and electrochemical characteristics of $Ba_{1-x}Sr_xCo_{0.8}Fe_{0.2}O_{3-\delta}$ cathode material for intermediate temperature solid oxide fuel cells, Int. J. Hydrogen Energy. 36 (2011) 11904–11913. doi:10.1016/j.ijhydene.2011.06.021.

[221] Y. Kim, X. Chen, S.P. Jiang, J. Bae, Chromium Deposition and Poisoning at $Ba_{0.5}Sr_{0.5}Co_{0.8}Fe_{0.2}O_{3-\delta}$ Cathode of Solid Oxide Fuel Cells, Electrochem. Solid-State Lett. 14 (2011) B41–B45. doi:10.1149/1.3549169.

[222] E. Park, S. Taniguchi, T. Daio, J.T. Chou, K. Sasaki, Comparison of chromium poisoning among solid oxide fuel cell cathode materials, Solid State Ionics. 262 (2014) 421–427. doi:10.1016/j.ssi.2014.01.047.

[223] Y.-M. Kim, X. Chen, S.P. Jiang, J. Bae, Effect of Strontium Content on Chromium Deposition and Poisoning in $Ba_{1-x}Sr_xCo_{0.8}Fe_{0.2}O_{3-\delta}$ ($0.3 \le x \le 0.7$) Cathodes of Solid Oxide Fuel Cells, J. Electrochem. Soc. 159 (2012) B185–B194. doi:10.1149/2.092202jes.

[224] E. Magnone, M.J. Seo, H.J. Kim, J.H. Park, Thermal characterization and compatibility studies of perovskite-type $Ba_{0.5}Sr_{0.5}Co_{0.8}Fe_{0.2}O_{3-\delta}$ (BSCF) oxide with Cr_2O_3 at high temperature, J. Therm. Anal. Calorim. 116 (2014) 215–218. doi:10.1007/s10973-013-3496-2.

[225] M. Lumeij, M. Gilleßen, H. Bouwmeester, T. Markus, J. Barthel, S. Roitsch, J. Mayer, R. Dronskowski, Influence of the Ba^{2+} /Sr^{2+} content and oxygen vacancies on the stability of cubic $Ba_xSr_{1-x}Co_{0.75}Fe_{0.25}O_{3-\delta}$, Phys. Chem. Chem. Phys. 16 (2014) 1333–1338. doi:10.1039/C3CP53958J.

[226] P. Qiu, J. Li, L. Jia, B. Chi, J. Pu, J. Li, F. Chen, $LaCoO_{3-\delta}$ coated $Ba_{0.5}Sr_{0.5}Co_{0.8}Fe_{0.2}O_{3-\delta}$ cathode for intermediate temperature solid oxide fuel cells, Electrochim. Acta. 319 (2019) 981–989. doi:10.1016/j.electacta.2019.07.054.

[227] Y. Chen, S. Yoo, X. Li, D. Ding, K. Pei, D. Chen, Y. Ding, B. Zhao, R. Murphy, B. deGlee, J. Liu, M. Liu, An effective strategy to enhancing tolerance to contaminants poisoning of solid oxide fuel cell cathodes, Nano Energy. 47 (2018) 474–480. doi:10.1016/J.NANOEN.2018.03.043.

[228] J. Li, J. Li, D. Yan, J. Pu, B. Chi, L. Jian, Promoted Cr-poisoning tolerance of $La_2NiO_{4+\delta}$-coated $PrBa_{0.5}Sr_{0.5}Co_{1.5}Fe_{0.5}O_{5+\delta}$ cathode for intermediate temperature solid oxide fuel cells, Electrochim. Acta. 270 (2018) 294–301. doi:10.1016/J.ELECTACTA.2018.03.053.

[229] L. Zhao, Y. Cheng, S.P. Jiang, A new, high electrochemical activity and chromium tolerant cathode for solid oxide fuel cells, Int. J. Hydrogen Energy. 40 (2015) 15622–15631. doi:10.1016/J.IJHYDENE.2015.09.091.

[230] Y. Cheng, H. Zhao, D. Teng, F. Li, X. Lu, W. Ding, Investigation of Ba fully occupied A-site $BaCo_{0.7}Fe_{0.3-x}Nb_xO_{3-\delta}$ perovskite stabilized by low concentration of Nb for oxygen permeation membrane, J. Memb. Sci. 322 (2008) 484–490. doi:10.1016/J.MEMSCI.2008.05.065.

[231] J. Wang, Z. Yang, K. Yang, Y. Chen, X. Xiong, S. Peng, Chromium deposition and poisoning on $Ba_{0.9}Co_{0.7}Fe_{0.2}Nb_{0.1}O_{3-\delta}$ cathode of solid oxide fuel cells, Electrochim. Acta. 289 (2018) 503–515. doi:10.1016/J.ELECTACTA.2018.08.092.

[232] C. Xiong, W. Li, D. Ding, J. Pu, B. Chi, J. Li, Chromium poisoning effect on strontium-doped samarium manganite for solid oxide fuel cell, Int. J. Hydrogen Energy. 41 (2016) 20660–20669. doi:10.1016/j.ijhydene.2016.07.061.

[233] H. Zhao, Q. Li, L. Sun, Ln_2MO_4 cathode materials for solid oxide fuel cells, Sci. China Chem. 54 (2011) 898–910. doi:10.1007/s11426-011-4290-2.

[234] G. Amow, S.J. Skinner, Recent developments in Ruddlesden-Popper nickelate systems for solid oxide fuel cell cathodes, J. Solid State Electrochem. 10 (2006) 538–546. doi:10.1007/s10008-006-0127-x.

[235] D. Lee, H.N. Lee, Controlling oxygen mobility in ruddlesden-popper oxides, Materials (Basel). 10 (2017) 1–22. doi:10.3390/ma10040368.

[236] B. Hou, C.C. Wang, X. Cui, Y. Chen, Chromium deposition and poisoning of La_2NiO_4 cathode of solid oxide fuel cell, R. Soc. Open Sci. 5 (2018). doi:10.1098/rsos.180634.

[237] A. Egger, N. Schrödl, C. Gspan, W. Sitte, $La_2NiO_{4+\delta}$ as electrode material for solid oxide fuel cells and electrolyzer cells, Solid State Ionics. 299 (2017) 18–25. doi:10.1016/J.SSI.2016.10.002.

[238] N. Schrödl, A. Egger, C. Gspan, T. Höschen, F. Hofer, W. Sitte, Phase decomposition of $La_2NiO_{4+\delta}$ under Cr- and Si-poisoning conditions, Solid State Ionics. 322 (2018) 44–53. doi:10.1016/j.ssi.2018.05.002.

[239] Y. Gong, R. Wang, J. Banner, S.N. Basu, U.B. Pal, S. Gopalan, Improved Tolerance of Lanthanum Nickelate ($La_2NiO_{4+\delta}$) Cathodes to Chromium Poisoning Under Current Load in Solid Oxide Fuel Cells, Jom. 71 (2019) 3848–3858. doi:10.1007/s11837-019-03724-0.

[240] S.-N. Lee, A. Atkinson, J.A. Kilner, Chromium Poisoning of $La_2NiO_{4+\delta}$ Cathodes, ECS Trans. 57 (2013) 605–613. doi:10.1149/05701.0605ecst.

[241] Y. Ling, H. Xie, Z. Liu, X. Du, H. Chen, X. Ou, L. Zhao, R.A. Budiman, Enhanced Electrochemical Activity and Chromium Tolerance of the Nucleation-Agent-Free $La_2Ni_{0.9}Fe_{0.1}O_{4+\delta}$ Cathode by $Gd_{0.1}Ce_{0.9}O_{1.95}$ Incorporation, Electron. Mater. Lett. 14 (2018) 432–439. doi:10.1007/s13391-018-0045-y.

[242] K.J. Lee, J.H. Chung, M.J. Lee, H.J. Hwang, Chromium poisoning of neodymium nickelate (Nd_2NiO_4) cathodes for solid oxide fuel cells, J. Korean Ceram. Soc. 56 (2019) 160–166. doi:10.4191/kcers.2019.56.2.07.

[243] J. Andreas Schuler, H. Lübbe, A. Hessler-Wyser, J. Van herle, Nd-nickelate solid oxide fuel cell cathode sensitivity to Cr and Si contamination, J. Power Sources. 213 (2012) 223–228. doi:10.1016/J.JPOWSOUR.2012.03.112.

[244] Y.-J. Choe, K.-J. Lee, H.-J. Hwang, Cr Poisoning On $Nd_2Ni_{0.95}Cu_{0.05}O_{4+\delta}$ Cathode for Solid Oxide Fuel Cells, Arch. Metall. Mater. 61 (2016) 629–634. doi:10.1515/amm-2016-0107.

[245] R.H. Mitchell, Perovskites: Modern and Ancient, Almaz Press Inc, Ontario, 2002.

[246] B. Wei, K. Chen, C.C. Wang, Z. Lü, S.P. Jiang, Performance degradation of $SmBaCo_2O_{5+\delta}$ cathode induced by chromium deposition for solid oxide fuel cells, Electrochim. Acta. 174 (2015) 327–331. doi:10.1016/j.electacta.2015.06.019.

[247] B. Wei, M. Schroeder, M. Martin, Surface Cation Segregation and Chromium Deposition on the Double-Perovskite Oxide $PrBaCo_2O_{5+\delta}$, ACS Appl. Mater. Interfaces. 10 (2018) 8621–8629. doi:10.1021/acsami.7b17881.

[248] H. Gu, H. Chen, Y. Zheng, L. Guo, Effect of chromium poisoning on the electrochemical properties of $NdBaCo_2O_{5+\delta}$ cathode for IT-SOFCs, Int. J. Hydrogen Energy. 35 (2010) 2457–2462. doi:10.1016/J.IJHYDENE.2010.01.023.

[249] G. Amow, I. Davidson, S. Skinner, A comparative study of the Ruddlesden-Popper series, $La_{n+1}Ni_nO_{3n+1}$ (n=1, 2 and 3), for solid-oxide fuel-cell cathode applications, Solid State Ionics. 177 (2006) 1205–1210. doi:10.1016/j.ssi.2006.05.005.

[250] T. Inprasit, S. Wongkasemjit, S.J. Skinner, M. Burriel, P. Limthongkul, Effect of Sr substituted $La_{2-x}Sr_xNiO_{4+d}$ (x=0, 0.2, 0.4, 0.6 and 0.8) on oxygen stoichiometry and oxygen transport properties, (2015) 2486–2492. doi:10.1039/c4ra11672k

[251] W. Li, B. Guan, J. Yan, N. Zhang, X. Zhang, X. Liu, Enhanced surface exchange activity and electrode performance of $(La_{2-2x}Sr_{2x})(Ni_{1-x}Mn_x)O_{4+\delta}$ cathode for intermediate temperature solid oxide fuel cells, J. Power Sources. 318 (2016) 178–183. doi:10.1016/j.jpowsour.2016.04.022.

[252] X. Zhao, Y. Yan, M. Li, X. Ding, In-situ strategy to suppress chromium poisoning on $La_{0.6}Sr_{0.4}Co_{0.2}Fe_{0.8}O_{3-\delta}$ cathodes of solid oxide fuel cells, Int. J. Hydrogen Energy. 44 (2019) 30401–30408. doi:10.1016/j.ijhydene.2019.09.198.

[253] D.R. Ou, M. Cheng, Stability of manganese-oxide-modified lanthanum strontium cobaltite in the presence of chromia, J. Power Sources. 272 (2014) 513–517. doi:10.1016/j.jpowsour.2014.08.077.

[254] K. Lu, F. Shen, Long term behaviors of $La_{0.8}Sr_{0.2}MnO_3$ and $La_{0.6}Sr_{0.4}Co_{0.2}Fe_{0.8}O_3$ as cathodes for solid oxide fuel cells, Int. J. Hydrogen Energy. 39 (2014) 7963–7971. doi:10.1016/j.ijhydene.2014.03.046.

[255] W.C. Hagel, A.U. Seybolt, Cation Diffusion in Cr_2O_3, J. Electrochem. Soc. 108 (1961) 1146–1152. doi:10.1149/1.2427973.

[256] E.A. Payzant, J. Zhu, Electrical Conductivity of the Manganese Chromite Spinel Solid Solution, J. Am. Ceram. Soc. 88 (2005) 1050–1053. doi:10.1111/j.1551-2916.2005.00205.x.

[257] A. Petric, H. Ling, Electrical Conductivity and Thermal Expansion of Spinels at Elevated Temperatures, J. Am. Ceram. Soc. 90 (2007) 1515–1520. doi:10.1111/j.1551-2916.2007.01522.x.

[258] W. Liu, E.Y. Konysheva, Conductivity of $SrCrO_4$ and its Influence on Deterioration of Electrochemical Performance of Cathodes in Solid Oxide Fuel Cells, ECS Trans. 59 (2014) 327–332. doi:10.1149/05901.0327.

[259] K. Chen, N. Ai, K.M. O'Donnell, S.P. Jiang, Highly chromium contaminant tolerant BaO infiltrated $La_{0.6}Sr_{0.4}Co_{0.2}Fe_{0.8}O_{3-\delta}$ cathodes for solid oxide fuel cells, Phys. Chem. Chem. Phys. 17 (2015) 4870–4874. doi:10.1039/C4CP04172K.

[260] H.E. Höfer, R. Schmidberger, Electronic Conductivity in the La(Cr, Ni)O_3 Perovskite System, J. Electrochem. Soc. 141 (1994) 782–786. doi:10.1149/1.2054811.

[261] W. Rativa-Parada, J.A. Gomez-Cuaspud, E. Vera-Lopez, J.B. Carda, Structural and electrical study of $LaCrO_3$ modified with Fe and Co, J. Phys. Conf. Ser. 786 (2017) 1–6. doi:10.1088/1742-6596/755/1/011001.